

**Charge transport in strongly
disordered solids**
Towards the Anderson metal-insulator transition

Jindřich Kolorenč

Ph. D. thesis supervisor: Prof. RNDr. Václav Janiš, DrSc.

Results from the thesis published:

- ▶ V. Janiš and J. Koloreň. *Conservation laws in disordered electron systems: Thermodynamic limit and configurational averaging.* phys. stat. sol. (b) **241**, 2032 (2004).
- ▶ V. Janiš, J. Koloreň and V. Špička. *Density and current response functions in strongly disordered electron systems: Diffusion, electrical conductivity and Einstein relation.* Eur. Phys. J. B **35**, 77 (2003).
- ▶ J. Koloreň and V. Janiš. *Towards mean-field theory of Anderson localization.* In *Proceedings of Weak of Doctoral Students 2003*, pp. 550–555 (Charles University in Prague, Faculty of Mathematics and Physics, 2003).

Submitted for publication:

- ▶ V. Janiš and J. Koloreň. *A mean-field theory of Anderson localization.* cond-mat/0402471.
- ▶ V. Janiš and J. Koloreň. *Causality vs. Ward identity in disordered electron systems.* cond-mat/0307455.

Author's address: Institute of Physics,
Academy of Sciences of the Czech Republic
Na Slovance 2
CZ-182 21 Prague 8
Czech Republic

e-mail: kolorenc@fzu.cz

Acknowledgements

This dissertation came into existence in the Institute of Physics of the Academy of Sciences of the Czech Republic under the guidance of Prof. Václav Janiš.

First of all, I wish to thank Prof. Václav Janiš for his friendly support in the last four years. I am very grateful for his effort, which was at least as intensive as mine, to resolve every complication that we encountered on the way towards the results presented in this thesis.

I would like to mention also other people who contribute, either directly or indirectly, to broadening of my knowledge of solid state physics and physics in general. Numerous discussions with Dr. Václav Špička, mainly in early stages of my postgraduate studies, helped me quickly assimilate the phenomenology of particle motion in random media. I should not forget to name here Dr. Ludvík Smrčka and Dr. Pavel Středa who guided my diploma thesis several years ago. I still benefit from the insight into tricky parts of the linear response theory that I gained in their group.

Research on this problem was supported by the Grant Agency of the Czech Republic under Grants No. 202/01/0764 and No. 202/04/1055.

Contents	5
List of Figures	7
1 Introduction	9
1.1 Transport in disordered solids	9
1.2 Mobility edges	11
1.3 Critical exponents	12
1.4 Models of disorder	14
1.5 Outline of the thesis	15
2 Linear response of disordered media	17
2.1 Response to inhomogeneous electric field	17
2.2 Configurational averaging	18
2.3 Density response	23
2.4 Diffusion	24
2.5 Conductivity	26
2.6 Einstein relation	28
<i>Chapter summary</i>	30
3 Classical conductivity and quantum corrections	31
3.1 Local approximations	31
3.1.1 Conductivity	33
3.1.2 Diffusion pole	34
3.2 Coherent backscattering	35
3.3 A self-consistent theory of localization in low dimensions	40
<i>Chapter summary</i>	42
4 Parquet construction of vertex functions	43
4.1 Two-particle irreducibility revisited	43
4.2 Parquet equation	45
4.3 Time-reversal invariance	47
<i>Chapter summary</i>	50
5 High spatial dimensions and mean-field solution	51
5.1 Solution in infinite spatial dimensions	51
5.2 Self-consistent solution in the asymptotics $d \rightarrow \infty$	53

5.3	Diffusion pole	56
5.4	Mean-field theory of the Landau type	59
	<i>Chapter summary</i>	63
6	Physics of suppression of diffusion	65
6.1	Ward identities vs. analyticity of the selfenergy	66
6.1.1	Diffusive phase	66
6.1.2	Localized phase	69
6.2	Too distinct electron eigenstates	70
6.2.1	One particular configuration of disorder	70
6.2.2	Averaging over impurity configurations	73
	<i>Chapter summary</i>	75
	Conclusions	77
A	Relation between density response and conductivity	79
B	CPA for two-particle functions	83
C	Convolutions in high spatial dimensions	87
D	Self-consistent asymptotic solution for two-particle vertices in the strict limit $d=\infty$	93
E	Born approximation in the semi-elliptic band	97
	Bibliography	101

List of Figures

1.1	Motion of a classical particle in a random potential.	9
1.2	Lifshitz tails and the mobility edges for a two-component alloy.	11
1.3	Conductivity at the mobility edge	12
1.4	Compensated and uncompensated semiconductor materials	13
3.1	Closed trajectories and the coherent backscattering	37
5.1	Disorder driven evolution of the weight of the diffusion pole	61
5.2	Phase diagram of the mean-field theory, Born selfenergy	61
5.3	Phase diagrams of the mean-field theory, CPA selfenergy (binary alloy) .	62
6.1	Leak of the diffusive and localized states out of a finite sample	71
6.2	Configurational averaging mixes diffusive and localized states	74
D.1	Mobility edges in $d = \infty$ — strongly asymmetric binary alloy	94
D.2	Mobility edges in $d = \infty$ — box disorder	95

1.1 Transport in disordered solids

Among thermodynamic and kinetic characteristics of solids the electrical conductivity plays an important role. Virtually everyone knows Ohm's law which is relatively easy to observe experimentally. On the other hand, theoretical insight into transport properties meets a fundamental difficulty already at first stages of the investigation. The notion of non-interacting electrons in a perfect, translationally invariant lattice, so helpful in other areas of solid state physics, is not appropriate here as it yields unphysical zero value of resistivity. Therefore, in order to achieve meaningful results, some processes slowing down the electron motion have to be taken into account. This thesis focuses on an electron gas in impure metals where scatterings of electrons on lattice imperfections (impurities) represent an important contribution to nonzero resistivity. In particular, this mechanism is the dominant one at low temperatures where the effects of lattice vibrations (phonons) become negligible. Being concerned with conductivity hence essentially demands to face imperfections and disorder even in materials that are not inherently disordered, such as e. g. amorphous solids are.

The simplest theoretical description of electronic transport was proposed by Drude. It is built on the concept schematically drawn in Figure 1.1, according to which charge carriers (electrons) are supposed to move freely between successive collisions with randomly distributed scattering centers, τ being the average time separating these events. Such a picture yields a static electrical conductivity of the well known form

$$\sigma = \frac{ne^2}{m} \tau, \quad (1.1)$$

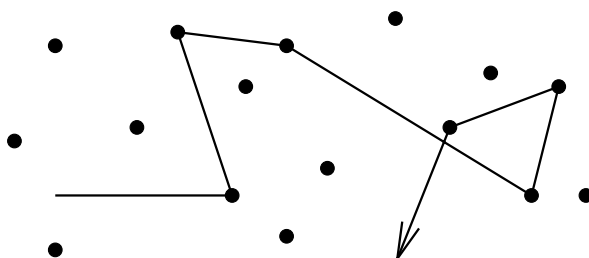


Figure 1.1: Piecewise motion of a classical particle in a random potential. The average time between individual scatterings is τ .

where n , e and m stand for concentration, charge and mass of conduction electrons, respectively. For additional technical details see any textbook on solid state physics, for example [1].

The Drude formula (1.1) can be re-derived even when the electron motion obeys quantum-mechanical laws and not classical ones that were assumed by Drude. The verbal interpretation of the underlying physics then is that due to scatterings on impurities the eigenstates of an ideal lattice, i. e. the Bloch waves that are extended through the whole sample, have a finite lifetime, τ , instead of infinite one that would correspond to a perfect crystal. We briefly touch approximations of this type in a more formal fashion in Chapter 3, Section 3.1.

The Drude theory works quite well at high temperatures. If a disordered system is cooled down, quantum coherence causes the disorder to influence the electron motion more dramatically. Anderson discovered [2] that a sufficiently strong disorder may give rise to such a destructive interference of scattered electron waves that they become *localized*, i. e., the envelope of the corresponding wavefunction decays exponentially from some point \mathbf{r}_0 in space,

$$|\psi(\mathbf{r})| \sim \exp(-|\mathbf{r} - \mathbf{r}_0|/\xi). \quad (1.2)$$

The parameter ξ that controls the spatial extension of the wavefunction is called *localization length*. The localization effects substantially depend on dimensionality of the system under investigation. They are most pronounced in one dimension where it can be rigorously shown that *all* electron eigenstates are localized for arbitrarily small degree of disorder [3]. Such a property makes impossible any charge transport in infinitely long one-dimensional wires at absolute zero of temperature, i. e., quantum wires are insulators. The Anderson insulator substantially differs from the usual one. Its insulating behavior originates from the fact that all quantum states in the vicinity of the Fermi level are localized that makes the charge carriers immobile. In the case of the conventional insulator the conductivity is zero because the Fermi energy lies inside the band gap and hence the externally applied weak electric field cannot induce current-carrying excitations.

In higher dimensions almost no rigorous results are known. Some evidence has been amassed, based on a scaling hypothesis [4] or on self-consistent diagrammatic methods [5], indicating that even in two dimensions all electron states are localized, no matter how weak the disorder is. In the same time, experimental data for both metallic and insulating behavior in 2D samples very close to $T = 0$ K were presented [6]. Attempts to explain such results suggest possible insufficiency of one-particle theories, whereto References 4 and 5 belong, and maintain importance of electron-electron interactions in *realistic* situations [7]. Of course, no such experiment can decide whether the theoretical approximation schemes do or do not treat the chosen models appropriately.

At low but nonzero temperatures quantum modifications of the Drude conductivity formula (1.1) are well described within perturbation theories. The resulting *weak localization* correction, which we discuss to some extent in Chapter 3, Section 3.2, has received a lot of both theoretical and experimental attention. The notion of weak localization and underlying quantum interference of conduction electrons at lattice defects allowed to explain logarithmic temperature dependence of conductivity [8, 9, 10]¹ and anomalous positive magnetoresistance [13, 12]. A large amount of experimental results that

¹Interpretation of this logarithmic temperature dependence is not straightforward, however. It was shown that the same correction is caused by electron-electron interactions as well [11]. To resolve which

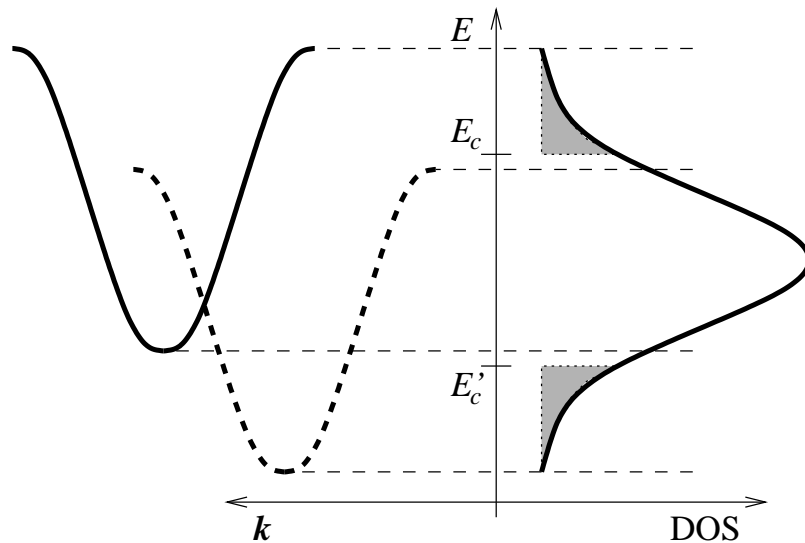


Figure 1.2: Two-component substitutional alloy. In the left part, the dispersion relations for the corresponding two *clean* components are sketched, in the right part, the alloy density of electronic states is drawn. In three dimensions it is expected that near the center of the band the wavefunctions are extended, whereas at band-edges, in the so-called Lifshitz tails (filled regions in the graph), the electron eigenstates are localized.

were obtained on a wide variety of (nearly) two-dimensional samples such as MOS inversion layers², thin metallic films or layered semiconductor heterostructures is reviewed in a comprehensive article by Bergmann [14].

1.2 Mobility edges

In three-dimensional lattices the electronic density of states (DOS) has a structure as depicted in Figure 1.2. Usually, the electron eigenstates located close to the band edges, in the so-called Lifshitz tails, are localized, whereas those belonging to the energy region around the band center are extended. The energies where the character of wavefunctions changes are referred to as *mobility edges*. In Figure 1.2 we denote them E_c , respectively E'_c . At these points the transport behavior goes over from metallic to insulating, i. e., the *metal-insulator transition* (MIT)³ takes place there. As the disorder strength grows, the mobility edges E_c and E'_c move towards the band center where they eventually meet and the whole band becomes localized. Such a scenario, originally based on more or less intuitive arguments, was later rigorously confirmed [15].

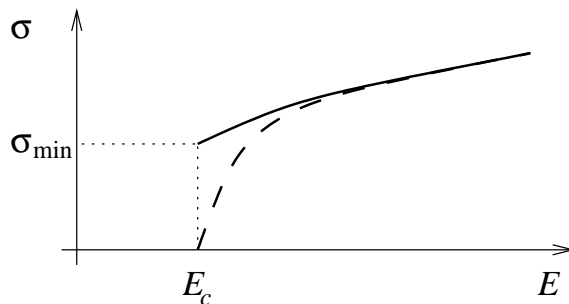
An insight into localized states in the Lifshitz tails may be won on a simple example of a binary alloy [16]. It can be shown that the density of states of such an alloy is nonzero

of the phenomena is dominant in a given sample one has to investigate also the behavior in the presence of the magnetic field [12].

²MOS = a structure consisting of three layers — metal, oxide (e. g. SiO_2) and semiconductor (e. g. silicon crystal).

³Several types of metal-insulator transitions are distinguished in the literature. Here we discuss the Anderson MIT which is caused by disorder. Mott demonstrated that a transition from metallic to insulating regime can also be driven by electron-electron interactions. Such a phenomenon is called Mott MIT.

Figure 1.3: Schematic illustration of the mobility edge E_c . The two possibilities of a continuous or discontinuous transition with minimal metallic conductivity σ_{\min} are shown. The picture is taken from Reference 22.



for all energies where either one of the densities of states corresponding to respective clean crystals is nonzero, Figure 1.2. However, outside the intersection of the two clean spectra the alloy density of states is rather small in magnitude. The electron wavefunctions contributing to these tails come from such disorder configurations, where large islands of one component exist that are immersed, far one from another, into a typical configuration of atoms in the lattice. In this way we are led to the conclusion that the Lifshitz tails are built up of states *bound* to rare fluctuations of the spatial distribution of alloy components. The closer to the alloy band edge the eigenenergy of such a bound state lies, the larger, and thus less probable, is the corresponding fluctuation.

The transition from extended to localized states is not the only change that occurs in the electronic spectrum as the disorder increases. When the alloy constituents are different enough, the respective clean bands do not overlap and the alloy band is split into two subbands. If additionally the situation is such that the concentrations of components are substantially different, i. e., one of them is almost one and the other is close to zero, we talk about the host and impurity bands, respectively. Considering this fact we may ask whether the whole band becomes localized first and only then splits or if the inverse situations occurs when the degree of disorder in the sample is increased.

Understanding the electron dynamics in three-dimensional disordered lattices is only qualitative at present. There exists no reliable theory providing *quantitative* estimates for positions of mobility edges etc. Several approximation schemes, both analytical [17] and numerical [18, 19], were developed to calculate quasi-particle spectra in disordered crystals. The numerical approaches lie outside the scope of this thesis and will not be discussed. Out of the analytical methods, the coherent-potential approximation (CPA) turned out to be the most successful. For a binary alloy model it predicts the anticipated opening of a band gap for large differences between constituents [20]. On the other hand, it is not able to reproduce the correct bandwidth. Moreover, when the CPA is applied to transport properties [21], it corresponds more or less to the simple Drude concept and contains no signs of quantum corrections originating from phase coherence. It is the aim of this thesis to extend the CPA so that the effects of quantum coherence (weak localization and beyond) would be incorporated.

1.3 Critical exponents

Once the notion of mobility edges is established a question arises, whether the transition from the conducting to the insulating regime occurring at these points of the electronic spectrum is continuous or not. Although this subject does not belong to the objectives of the thesis we include a short summary here as it nicely illustrates the present state of

the art of understanding the physics of strongly disordered electronic systems.

Historically the first proposal about the character of the MIT was given by Mott [23] who claimed that the conductivity jumps to zero discontinuously from some *minimal metallic conductivity* σ_{\min} , Figure 1.3. Later, arguments were given that the Anderson metal-insulator transition is a second order phase transition analogous to e. g. magnetism [24]. It means that the conductivity on the metallic side and the inverse of the localization length on the insulating side should go to zero continuously,

$$\sigma \sim |E - E_c|^s \quad \text{and} \quad \xi^{-1} \sim |E - E_c|^\nu. \quad (1.3)$$

Nowadays it is agreed that the second scenario is the correct one, as it is widely supported by both theory and experiment. The issue that remains open concerns the numerical values of the *critical exponents* s and ν . The analytic theory relies on mapping the problem of non-interacting disordered electrons onto a non-linear σ -model, which is known from quantum field theory. Such a connection was suggested by Wegner [25] and later demonstrated in detail by Wegner and Schäfer [26] and others. Particularly effective proved to be Efetov's approach utilizing supersymmetric fermion-boson representation [27]. The non-linear σ -model cannot be applied in three dimensions directly. Instead, the ϵ -expansion from dimension two has to be utilized. It means that the actual calculation is performed in dimension $d = 2 + \epsilon$ and a three-dimensional estimate is consequently obtained via setting $\epsilon = 1$. The values for the conductivity exponent s achieved within the non-linear σ -model read $s = 1 + O(\epsilon^3)$ [28] for purely non-interacting electrons (spin-independent time-reversal-invariant Hamiltonian) and $s = 1/2 - 3\epsilon/4 + O(\epsilon^2)$ [29] when an additional spin-flip mechanism is present. Evidently, the non-linear σ -model is rather unreliable in the spin-dependent case as the exponent s has to be positive.

Another theoretical method developed for evaluation of critical exponents is based on numerical simulations. These approaches provide the value $s \approx 1.5$ for non-interacting samples [30, 31], which disagrees with findings of the non-linear σ -model referred above. This discrepancy demonstrates that despite decades of studies only partial understanding of the Anderson metal-insulator transition has been reached.

The results of experimental investigations of the metal-insulator transition in disordered systems have evolved as follows. In the eighties of the last century, two groups of materials were found. Some solids showed the exponent $s \approx 0.5$ (*uncompensated* samples, a popular example of which is silicon doped with phosphorus, Si:P, [32]), in others the value $s \approx 1$ was measured (*compensated* samples, e. g. $\text{Ga}_x\text{Al}_{1-x}\text{As}$, [33]). The difference

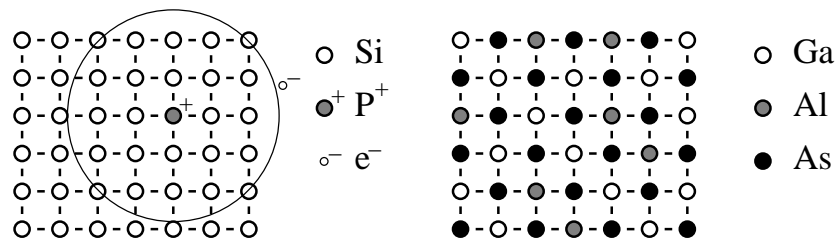


Figure 1.4: Examples of an uncompensated (left) and a compensated (right) sample. In Si:P the phosphorus acts as a donor as it has one more valence electron than silicon. In the case of $\text{Ga}_x\text{Al}_{1-x}\text{As}$ no additional electrons or holes are brought into the sample when the degree of disorder changes, because gallium and aluminium have the same number of valence electrons.

between compensated and uncompensated semiconductors is explained in Figure 1.4. At present, however, the experimental situation concerning uncompensated samples is rather unclear since both values $s \approx 0.5$ and $s \approx 1$ were reported even for the same material. Table 1.1 provides an incomplete summary of this issue. Recent papers suggest [34] that the correct critical exponent is $s \approx 1$ as this value is obtained when a very small vicinity of the critical point is taken into account, whereas s tends to 0.5 only if also data farther from the critical point are considered. The same seems to apply to new measurements as well as to reanalyzed old experimental results.

Semiconductor system	s
Si:P	0.5 [32], 1.0, 1.2
Si:As	0.5, 1.0
Si:B	0.65, 1.6
Ge:As	0.5, 1.2
Ge:Sb	0.9
Ge:Ga	0.5, 1.2

Table 1.1: Conductivity critical exponent s reported for a wide variety of uncompensated samples. Table is adopted from Reference 34.

1.4 Models of disorder

In order to be prepared for the formal development presented in the subsequent chapters we need to specify what will exactly be meant by disordered electrons. The model we use throughout the thesis is the original Anderson model [2], the Hamiltonian of which reads

$$\hat{H} = \hat{H}_0 + \hat{V} = \sum_{i,j} t_{ij} \hat{c}_i^\dagger \hat{c}_j + \sum_i V_i \hat{c}_i^\dagger \hat{c}_i, \quad (1.4)$$

where \hat{c}_i^\dagger and \hat{c}_i create and annihilate, respectively, an electron on lattice site i . The matrix t_{ij} describes probability of a particle hopping from site j to site i . In the simplest version only hoppings between nearest neighbors are allowed, $t_{ij} = t\delta_{|i-j|,1}$. The local energies V_i are random, characterized by a probability distribution $P(V_i)$. The distribution $P(V_i)$ is site-independent, i. e. the same for all lattice sites without any correlations between them. A wide range of more or less realistic choices for $P(V_i)$ can be found in the literature. In particular, Anderson [2] used a box distribution

$$P(V_i) = \frac{1}{2\delta} \theta(\delta^2 - V_i^2) = \begin{cases} \frac{1}{2\delta} & \text{for } |V_i| < \delta, \\ 0 & \text{elsewhere,} \end{cases} \quad (1.5)$$

where θ denotes the Heaviside step function. The rigorous results by Fröhlich and Spencer [15] mentioned in Section 1.2 were obtained for a Gaussian disorder

$$P(V_i) = \frac{1}{\sqrt{2\pi}\delta} \exp\left(-\frac{V_i^2}{2\delta^2}\right). \quad (1.6)$$

The non-linear σ -model also assumes the random potential to have the form of the Gaussian white noise (1.6). Another widely used model with clear physical content is defined by the distribution function of the form

$$P(V_i) = c \delta(V_i - V_A) + (1 - c) \delta(V_i - V_B). \quad (1.7)$$

It corresponds to a substitutional alloy consisting of two compounds that we labelled A and B . Every lattice site can be occupied by an atom A with probability c and by an atom B with probability $1 - c$.

1.5 Outline of the thesis

The objective of the thesis is to construct an approximation scheme that would inherit the properties of the CPA and, in the same time, contain nontrivial quantum corrections to the semi-classical values of transport coefficients. These corrections, which are absent in the coherent-potential approximation, originate in the inter-site phase coherence that enhances backward scatterings. Predictions of the demanded theory should comply with the phenomenological expectations listed in Section 1.2, i. e., the quantum phenomena should be most pronounced at the band edges and in the contingent impurity band. It will be demonstrated that the mean-field-like approximation constructed in Chapter 5 really behaves in that way. Furthermore, since the approximation is self-consistent, it allows us to access not only corrections of a perturbative character, but non-perturbative effects as well. The non-perturbative phenomenon that we are heading for is the Anderson metal-insulator transition.

To study directly the Anderson Hamiltonian (1.4) is possible only numerically since it has too many parameters (the on-site potentials V_i) and it lacks any apparent symmetry that would help with their reduction. As we want to tackle the problem analytically we perform averaging over all possible disorder configurations that restores the translational invariance obeyed by a clean (non-disordered) lattice. This simplification has its price — the averaging procedure transforms the original system of non-interacting electrons to a correlated one. However, we gain more than we lose as the effective interacting system can be studied with the aid of standard many-body diagrammatic techniques, which is the method we utilize in the following chapters.

The steps towards our goal are organized as follows. In Chapter 2 we review relevant parts of linear response theory with emphasis on first-principle quantum-mechanical description of electron diffusion in disordered materials. The need for studying two-particle Green functions is made obvious. A diagrammatic perturbation expansion in powers of the random potential is constructed and a concept of averaging over disorder configurations is introduced. Chapter 3 describes selected methods and approximations presently available to deal with transport in non-interacting disordered electrons. The single-site approximations (CPA) and the weak localization correction are covered. Finally, assumptions and results of the Vollhardt and Wölfle self-consistent theory of localization [5] are summarized.

The rest of the thesis is devoted to our own approach. In Chapter 4 two-particle diagrams are examined in detail. Classification into topologically distinct scattering channels is used to formulate self-consistent equations for two-particle Green functions (parquet scheme). In the following Chapter 5 an asymptotic limit to high spatial dimensions, i. e.

the standard “generator” of mean-field theories, is utilized for a systematic construction of approximate solutions of the parquet equations. In the strict limit $d = \infty$ only terms of the order $O((1/d)^0)$ contribute and a simple sum of the CPA and the weak localization is obtained. A further self-consistent inclusion of $O(1/d)$ terms leads to an advanced approximation scheme that predicts vanishing of diffusion, and therefore zero value of conductivity, above a certain critical disorder strength in any finite dimension.

In the course of developing our mean-field-like solution a crucial difficulty is encountered when a selfenergy, which would match the two-particle functions found from parquet equations, is searched for. The scheme proposed in Chapter 5 does not comply with the particle number conservation, in other words, Ward identities for averaged Green functions are not fulfilled to the extent that is nowadays widely assumed. Chapter 6 elucidates this issue. At first it is demonstrated that the violation of Ward identities is not an artifact of our approximations. On the contrary, it is inevitable in principle. Finally, arguments are given that the particle number non-conservation is only virtual and can be understood if configurational averaging is reexamined. It turns out that only extended states can survive the averaging procedure and that localized states are lost already during this very early step of the theoretical description of electrons subject to a random potential.

Notation and conventions

The Planck constant \hbar is set to 1 throughout the thesis. Exemptions are several equations that are adopted directly from literature — Kubo formulae for the density-density and the current-current response functions, equations (2.3) and (2.43), and definition of the velocity operator, equation (2.41). In first appearances of these expressions the Planck constant is written explicitly. The elementary electric charge is denoted e , electron charge then is $-e$.

2

Linear response of disordered media

A universal method of investigating physical systems is to drive them out of equilibrium and observe their reactions. For example, an external electric field generates currents flowing through a conducting sample. A description of non-equilibrium phenomena is, in general, rather involved. However, when the external field is weak enough, the responses of the system are proportional to the magnitude of the field. In such a regime, the non-equilibrium properties, like electrical conductivity, can be calculated by means of equilibrium statistical mechanics. This fundamental feature of the so-called Kubo linear response theory [35] obviously greatly simplifies the treatment of weakly non-equilibrium situations.

In this chapter we use the Kubo formalism to deal with the response of disordered electron systems to electromagnetic perturbations. We start with externally induced changes of spatial particle density and their subsequent relaxation back to equilibrium. When we become familiar with the formalism explained on the density response, we turn our attention to a current response and to the corresponding response function — conductivity. The electrical conductivity is in a sense more interesting property of a system than the density response as it is better experimentally accessible. On the other hand, the theoretical description appears to be considerably more involved in the case of currents when compared to the particle density. Motivated by this fact, a close relationship between the density and current responses is demonstrated at the end of this chapter, which allows for a simplified indirect evaluation of the conductivity via the density response function.

2.1 Response to inhomogeneous electric field

Starting with the simplest case of a response, we subject our system to an external electric field $\mathbf{E}(t, \mathbf{r})$. We use a gauge in which the field is generated by a scalar potential $\varphi(t, \mathbf{r})$, i. e. $\mathbf{E}(t, \mathbf{r}) = -\text{grad } \varphi(t, \mathbf{r})$. In such a description the electric field interacts with electrons via their number density $\hat{n}(\mathbf{r})$, giving rise to a Hamiltonian term

$$\hat{H}_{\text{ext}}(t) = -e \int d^3r \hat{n}(\mathbf{r}) \varphi(t, \mathbf{r}) \quad (2.1)$$

where $-e$ stands for the electron charge. The quantity of our interest is the induced electron density variation $\delta n(t, \mathbf{r})$, which is the difference between the non-equilibrium

and the equilibrium values of the particle density, $\delta n(t, \mathbf{r}) = n(t, \mathbf{r}) - n_0(\mathbf{r})$.¹ The linear part of the deviation $\delta n(t, \mathbf{r})$ can generally be written in a form

$$\delta n(t, \mathbf{r}) = \int_{-\infty}^{\infty} dt' \int d^3 r' \chi(t - t'; \mathbf{r}, \mathbf{r}') e\varphi(t, \mathbf{r}') \quad (2.2)$$

where the retarded density-density *response function* $\chi(t; \mathbf{r}, \mathbf{r}')$ is introduced. To evaluate this response function we use the Kubo formalism [35] that is based on the first order perturbation expansion of the statistical density matrix. It is thus comparable to the Fermi golden rule well known from quantum mechanics. The Kubo formula for the present case reads

$$\chi(t - t'; \mathbf{r}, \mathbf{r}') = \frac{i}{\hbar} \theta(t - t') \text{Tr} \left(f(\hat{H}) [\hat{n}(t, \mathbf{r}), \hat{n}(t', \mathbf{r}')] \right) \quad (2.3)$$

with $f(\hat{H})$ being the Fermi-Dirac distribution function. For the time evolution of the density operators $\hat{n}(t, \mathbf{r})$ the Heisenberg picture is used. Introducing Green functions in a standard way we end up with an expression (detailed derivation can be found in e. g. [36])

$$\begin{aligned} \chi(\omega + i0; \mathbf{r}, \mathbf{r}') &= \int_{-\infty}^{\infty} dt e^{i(\omega + i0)t} \chi(t; \mathbf{r}, \mathbf{r}') \\ &= \int_{-\infty}^{\infty} \frac{dE}{2\pi i} \{ [f(E + \omega) - f(E)] \mathcal{G}^A(E; \mathbf{r}', \mathbf{r}) \mathcal{G}^R(E + \omega; \mathbf{r}, \mathbf{r}') \\ &\quad + f(E) \mathcal{G}^R(E; \mathbf{r}', \mathbf{r}) \mathcal{G}^R(E + \omega; \mathbf{r}, \mathbf{r}') \\ &\quad - f(E + \omega) \mathcal{G}^A(E; \mathbf{r}', \mathbf{r}) \mathcal{G}^A(E + \omega; \mathbf{r}, \mathbf{r}') \} \end{aligned} \quad (2.4)$$

where $\mathcal{G}^R(E; \mathbf{r}', \mathbf{r})$ and $\mathcal{G}^A(E; \mathbf{r}', \mathbf{r})$ are matrix elements of the retarded and the advanced resolvent operators,

$$\mathcal{G}^R(E; \mathbf{r}', \mathbf{r}) = \langle \mathbf{r}' | (E + i0 - \hat{H})^{-1} | \mathbf{r} \rangle, \quad (2.5a)$$

$$\mathcal{G}^A(E; \mathbf{r}', \mathbf{r}) = \langle \mathbf{r}' | (E - i0 - \hat{H})^{-1} | \mathbf{r} \rangle. \quad (2.5b)$$

Equation (2.4) refers to one particular configuration of impurities. Due to the lack of symmetry in a disordered system, the Green functions involved are quite complex quantities and we can hardly proceed much further with any kind of calculation. It is therefore very convenient to find a physically justifiable method of restoring the (discrete) translational invariance of a perfect crystal. Such a procedure is the averaging over disorder configurations that is discussed in the following paragraph.

2.2 Configurational averaging

We have argued that averaging over all impurity configurations with the same macroscopic properties (like the impurity concentration) is technically desirable. However, to be

¹The equilibrium density $n_0(\mathbf{r})$ depends on the position vector \mathbf{r} , since the system we are dealing with, defined by the Anderson Hamiltonian (1.4), is generally inhomogeneous.

allowed to proceed with this step we need a proper physical justification. Considering transport properties at finite temperatures the following picture can be used.

An electron moves coherently only between inelastic scattering events, e.g. collisions with phonons, and thus the purely quantum mechanical description (Kubo formula) holds only in a piecewise sense. This means that at a time only a (small) part of the whole system is relevant. Therefore, as the electron travels through the sample it is effectively averaging over local disorder configurations that it feels. Presence of localized states, however, invalidates this notion as the electron can be confined to a finite region in space. In such a case it does not have the opportunity to move in other than just the one specific disorder pattern. We will see later that under such conditions the configurationally averaged quantities behave somewhat differently than the same quantities related to one particular sample. Nevertheless, even when the localized states are important, the averages still contain valuable physical information.

As could be expected, simplifications are not the only effect that the averaging brings in. Besides a symmetry enhancement it changes the system of uncorrelated electrons to a correlated one. This feature is demonstrated on low orders of perturbation theory as follows. Let the Anderson Hamiltonian (1.4) be quite simple with only two distinct values of the local potential V_i , $V_i = v$ on impurity sites and $V_i = 0$ elsewhere. Concentration of impurities is denoted c . According to the time-independent perturbation theory the resolvent is given by

$$\hat{\mathcal{G}}(z) = \hat{G}^{(0)}(z) + \hat{G}^{(0)}(z)\hat{V}\hat{\mathcal{G}}(z) \quad (2.6)$$

where $\hat{G}^{(0)}(z)$ corresponds to the pure host lattice with the Hamiltonian \hat{H}_0 . We average the perturbation expansion (2.6) term by term and take a closer look at the third-order contribution. Feynman diagrams are found to be the most convenient tool for this purpose. The averaged third-order term can be represented as

$$\begin{aligned} \left\langle \sum_{ijk} \begin{array}{c} \vdots \\ \vdots \\ \vdots \\ \longrightarrow \\ \vdots \\ \vdots \\ \vdots \end{array} \right\rangle_{\text{av.}} &= \sum'_{ijk} \begin{array}{c} \times \\ \vdots \\ \times \\ \longrightarrow \\ \times \\ \vdots \\ \times \end{array} \\ &+ \sum'_{ik} \begin{array}{c} \times \\ \vdots \\ \times \\ \longrightarrow \\ \times \\ \vdots \\ \times \end{array} + \sum'_{ik} \begin{array}{c} \times \\ \vdots \\ \times \\ \longrightarrow \\ \times \\ \vdots \\ \times \end{array} \\ &+ \sum'_{ij} \begin{array}{c} \times \\ \vdots \\ \times \\ \longrightarrow \\ \times \\ \vdots \\ \times \end{array} + \sum_i \begin{array}{c} \times \\ \vdots \\ \times \\ \longrightarrow \\ \times \\ \vdots \\ \times \end{array} \end{aligned} \quad (2.7)$$

where the solid line visualizes $G_{ij}^{(0)}(z)$ and the dotted line is the potential at a given site, V_i . On the right-hand side the dashed line represents v and the cross stands for the concentration c . The quite large number of different diagrams generated by configurational averaging is caused by the fact that distinct contributions are obtained depending on how many potentials V_i sits on the same site. For the same reason the sums on the right-hand side carry a prime which means that all the site indices have to be different.

Summing up only a finite part of a perturbation series (a few low order terms) cannot lead to emergence of any qualitatively new phenomena in comparison to the unperturbed

system. To investigate, whether or not a given perturbation is able to induce such a new quality, we need to take into account an infinite subset of the corresponding perturbation expansion. A convenient way to sum an infinite number of one particle diagrams is to express the averaged resolvent $\hat{G}(z) = \langle \hat{G}(z) \rangle_{\text{av}}$. (thick fermion line in diagrams) via a Dyson equation

$$i \xrightarrow{\text{thick}} j = i \xrightarrow{\text{thin}} j + \sum_{i'j'} i \xrightarrow{\text{thin}} i' \textcircled{\Sigma} j' \xrightarrow{\text{thick}} j, \quad (2.8a)$$

$$G_{ij}(z) = G_{ij}^{(0)}(z) + \sum_{i'j'} G_{ii'}^{(0)}(z) \Sigma_{i'j'}(z) G_{j'j}(z), \quad (2.8b)$$

an expanded form of which reads

$$\begin{aligned} i \xrightarrow{\text{thick}} j &= i \xrightarrow{\text{thin}} j + \sum_{i'j'} i \xrightarrow{\text{thin}} i' \textcircled{\Sigma} j' \xrightarrow{\text{thin}} j \\ &+ \sum_{i'j'k'l'} i \xrightarrow{\text{thin}} i' \textcircled{\Sigma} j' \xrightarrow{\text{thin}} k' \textcircled{\Sigma} l' \xrightarrow{\text{thin}} j + \dots \end{aligned} \quad (2.9)$$

The introduced selfenergy $\Sigma_{ij}(z)$ is a sum of all one-particle irreducible diagrams, i. e. diagrams that do not split into two pieces if one of their fermion lines is cut.

Reading out the selfenergy expression from the perturbation expansion given above, e. g. from formula (2.7), is not quite straightforward. Difficulties originate from the fact that for the formulation of the Dyson equation it is essential that summations over site indices are unrestricted. We therefore need to remove the primes from the sums in formula (2.7) to become compatible with representation (2.9). Such a problem resembles that of a self-avoided random walk. In our case it can be solved if a new type of one-particle irreducible diagrams, so-called *multiple-occupancy corrections*, is introduced. This procedure is best explained on an example, in the place of which we use the second term from the right-hand side of equation (2.7). The cumbersome restriction $i \neq k$ is eliminated as follows,

$$\sum_{ik} \text{diag}_{ik}^{\text{prime}} = \sum_{ik} \text{diag}_{ik}^{\text{unprime}} - c \sum_i \text{diag}_i^{\text{unprime}}. \quad (2.10)$$

Note the extra concentration factor at the correcting term. Repeating analogous steps for all other parts of expression (2.7) we end up with a diagrammatic expansion of the selfenergy up to third order in the impurity strength v . It reads

$$\begin{aligned} \Sigma_{ii}(z) &= \text{diag}_i^{\text{prime}} + (1-c) \text{diag}_i^{\text{unprime}} + (1-c) \sum_j \text{diag}_{ij}^{\text{unprime}} \\ &+ (1-3c+2c^2) \text{diag}_i^{\text{unprime}} + \dots \end{aligned} \quad (2.11)$$

with the additional concentration factors being just the multiple-occupancy corrections. All drawn low order terms are local but it is clear that among higher orders there are nonlocal contributions as well.

Due to translational invariance the selfenergy depends only on the difference of the two positions that it connects. This property allows us to carry out the Fourier transform. Doing so, we come to a momentum representation in which the selfenergy operator is diagonal. Therefore, the Dyson equation (2.8) is easily solved and we get the averaged Green function $G(z, \mathbf{k})$ in the form

$$G(z, \mathbf{k}) = \frac{1}{N} \sum_{ij} e^{i\mathbf{k}\cdot\mathbf{R}_i} e^{-i\mathbf{k}\cdot\mathbf{R}_j} G_{ij}(z) = \frac{1}{z - \epsilon(\mathbf{k}) - \Sigma(z, \mathbf{k})}. \quad (2.12)$$

The Fourier transform is normalized using the number of the lattice sites that we denote N . The vector \mathbf{R}_i points to the position of the lattice site i .

A very similar analysis can be applied to the average of a product of two resolvents. Such products are substantial for linear response calculations as they appear in Kubo formulae, e. g. in equation (2.4). The third order term, analogous to the one examined above in the case of the averaged one-particle Green function G , is visualized as

$$\left\langle \sum_{ijk} \begin{array}{c} \xrightarrow{k} \\ \vdots \\ \xleftarrow{j} \end{array} \right\rangle_{\text{av.}} = \sum'_{ijk} \begin{array}{c} \xrightarrow{k} \\ \times \\ \times \\ \times \\ \xleftarrow{j} \end{array} + \sum'_{ik} \begin{array}{c} \xrightarrow{i} \\ \times \\ \times \\ \xleftarrow{j} \end{array} + \sum'_{ik} \begin{array}{c} \xrightarrow{j} \\ \times \\ \times \\ \xleftarrow{i} \end{array} + \sum'_{ij} \begin{array}{c} \xrightarrow{k} \\ \times \\ \times \\ \xleftarrow{i} \end{array} + \begin{array}{c} \xrightarrow{i} \\ \times \\ \times \\ \xleftarrow{i} \end{array} \quad (2.13)$$

where every element has its counterpart in the diagrammatic equation (2.7). We can find here the selfenergy contributions as well as new diagrams connecting both electron lines. The latter represent pairwise correlations in the motion of the electrons. After removing primes from the sums we can again divide the involved diagrams into two classes. One of them contains reducible and the other comprises irreducible graphs. The so-called two-particle irreducibility means that a diagram cannot be split into two parts by cutting two fermion lines.² All the two-particle irreducible diagrams build up the two-particle irreducible vertex $\Lambda_{ij,kl}(z_1, z_2)$. The two-particle Green function $G_{ij,kl}^{(2)}(z_1, z_2) = \langle \mathcal{G}_{ik}(z_1) \mathcal{G}_{jl}(z_2) \rangle_{\text{av.}}$ is then generated with the aid of a Bethe-Salpeter equation,

$$\begin{array}{c} \xrightarrow{i} \\ \parallel \\ \xleftarrow{j} \end{array} \begin{array}{c} \xrightarrow{k} \\ \parallel \\ \xleftarrow{l} \end{array} G^{(2)} = \begin{array}{c} \xrightarrow{i} \\ \parallel \\ \xleftarrow{j} \end{array} \begin{array}{c} \xrightarrow{k} \\ \parallel \\ \xleftarrow{l} \end{array} + \begin{array}{c} \xrightarrow{i} \\ \parallel \\ \xleftarrow{j} \end{array} \begin{array}{c} \xrightarrow{i'} \\ \parallel \\ \xleftarrow{j'} \end{array} \Lambda \begin{array}{c} \xrightarrow{k'} \\ \parallel \\ \xleftarrow{l'} \end{array} \begin{array}{c} \xrightarrow{k} \\ \parallel \\ \xleftarrow{l} \end{array} G^{(2)}, \quad (2.14a)$$

$$G_{ij,kl}^{(2)}(z_1, z_2) = G_{ik}(z_1) G_{jl}(z_2) + \sum_{i'j'k'l'} G_{ii'}(z_1) G_{jj'}(z_2) \Lambda_{i'j',k'l'}(z_1, z_2) G_{k'l',kl}^{(2)}(z_1, z_2). \quad (2.14b)$$

²This definition of the two-particle irreducibility is in fact ambiguous. We postpone this issue to the beginning of Chapter 4, since at this moment it is not needed to enter such details.

The selfenergy insertions are absorbed in the full averaged one-particle Green functions $G_{ij}(z)$ appearing in this formula. The low order contributions to the irreducible vertex are local

$$\Lambda_{ii,ii}(z_1, z_2) = (1-c) \begin{array}{c} i \\ \vdots \\ \times \\ \vdots \\ i \end{array} + (1-3c+2c^2) \begin{array}{c} i \\ \diagup \quad \diagdown \\ \leftarrow \quad \rightarrow \\ i \quad i \end{array} + (1-3c+2c^2) \begin{array}{c} i \\ \diagdown \quad \diagup \\ \rightarrow \quad \leftarrow \\ i \quad i \\ \vdots \\ i \end{array} + \dots, \quad (2.15)$$

non-locality comes from the fourth and higher orders in the impurity strength v .

By virtue of translational invariance of the averaged quantities, the irreducible vertex $\Lambda_{ij,kl}$, as well as the full two-particle Green function $G_{ij,kl}^{(2)}$, actually do not depend on all four indicated positions but rather on their three respective differences. This suggests a threefold Fourier transform to momentum space. The notation for the Fourier transformed two-particle functions used throughout the thesis is

$$G_{\mathbf{k}\mathbf{k}'}^{(2)}(z_1, z_2; \mathbf{q}) = \frac{1}{N^2} \sum_{ijkl} e^{i(\mathbf{k}+\mathbf{q})\cdot\mathbf{R}_i} e^{-i\mathbf{k}\cdot\mathbf{R}_j} e^{-i(\mathbf{k}'+\mathbf{q})\cdot\mathbf{R}_k} e^{i\mathbf{k}'\cdot\mathbf{R}_l} G_{ij,kl}^{(2)}(z_1, z_2) \quad (2.16)$$

that in the diagrammatic representation reads

$$G_{\mathbf{k}\mathbf{k}'}^{(2)}(z_1, z_2; \mathbf{q}) = \begin{array}{ccc} z_1, \mathbf{k} + \mathbf{q} & \xrightarrow{\quad} & z_1, \mathbf{k}' + \mathbf{q} \\ \left[\begin{array}{c} \xrightarrow{\quad} \\ G^{(2)} \\ \xleftarrow{\quad} \end{array} \right] & & \\ z_2, \mathbf{k} & \xleftarrow{\quad} & z_2, \mathbf{k}' \end{array} . \quad (2.17)$$

The Bethe-Salpeter equation (2.14) is, within the just introduced convention, written as

$$\begin{array}{ccc} \mathbf{k} + \mathbf{q} & \xrightarrow{\quad} & \mathbf{k}' + \mathbf{q} \\ \left[\begin{array}{c} \xrightarrow{\quad} \\ G^{(2)} \\ \xleftarrow{\quad} \end{array} \right] & = & \begin{array}{c} \xrightarrow{\quad} \\ \xleftarrow{\quad} \\ \mathbf{k} \end{array} + \begin{array}{c} \mathbf{k} + \mathbf{q} \quad \mathbf{k}'' + \mathbf{q} \quad \mathbf{k}' + \mathbf{q} \\ \left[\begin{array}{c} \xrightarrow{\quad} \\ \Lambda \\ \xleftarrow{\quad} \end{array} \right] \left[\begin{array}{c} \xrightarrow{\quad} \\ G^{(2)} \\ \xleftarrow{\quad} \end{array} \right] \\ \mathbf{k} \quad \mathbf{k}'' \quad \mathbf{k}' \end{array} , \end{array} \quad (2.18a)$$

$$G_{\mathbf{k}\mathbf{k}'}^{(2)}(z_1, z_2; \mathbf{q}) = G(z_1, \mathbf{k} + \mathbf{q})G(z_2, \mathbf{k}) \times \left[\delta(\mathbf{k} - \mathbf{k}') + \frac{1}{N} \sum_{\mathbf{k}''} \Lambda_{\mathbf{k}\mathbf{k}''}(z_1, z_2; \mathbf{q}) G_{\mathbf{k}''\mathbf{k}'}^{(2)}(z_1, z_2; \mathbf{q}) \right]. \quad (2.18b)$$

The presented introduction into diagrammatic methods in the (averaged) disordered-electron problem is sufficient for understanding the subsequent chapters. A deeper treatment of multiple-occupancy corrections and constructions of various approximations for the selfenergy can be found in e. g. [17, 36, 37].

2.3 Density response

At this point we have enough knowledge to return back and average the density-density response function χ given by formula (2.4). Using the momentum representation we have

$$\chi(\omega + i0, \mathbf{q}) = \int_{-\infty}^{\infty} \frac{dE}{2\pi i} \left\{ [f(E + \omega) - f(E)] \Phi^{AR}(E, E + \omega; \mathbf{q}) + f(E) \Phi^{RR}(E, E + \omega; \mathbf{q}) - f(E + \omega) \Phi^{AA}(E, E + \omega; \mathbf{q}) \right\}. \quad (2.19)$$

We introduced three *correlation functions* that are defined as traces of the two-particle Green functions,

$$\Phi^{AR}(E, E + \omega; \mathbf{q}) = \frac{1}{N^2} \sum_{\mathbf{k}\mathbf{k}'} G_{\mathbf{k}\mathbf{k}'}^{AR}(E, E + \omega; \mathbf{q}). \quad (2.20)$$

Very similar definitions hold for the other combinations of superscripts R and A , which carry information about signs of infinitesimal imaginary parts of the corresponding energy variables.

To evaluate the response function χ we generally need to know the whole two-particle Green function. However, certain specific limits can be directly related to one-particle functions. This is done with the aid of the Ward identity

$$\frac{1}{N} \sum_{\mathbf{k}'} G_{\mathbf{k}\mathbf{k}'}^{(2)}(z_1, z_2; \mathbf{0}) = \frac{1}{z_2 - z_1} [G(\mathbf{k}, z_1) - G(\mathbf{k}, z_2)] \quad (2.21)$$

that was for the first time used by Velický within the coherent-potential approximation (CPA) [21]. We discuss some aspects of this approximation in Section 3.1. Identity (2.21) results from configurational averaging of the expression

$$\hat{\mathcal{G}}(z_2) = \hat{\mathcal{G}}(z_1) + (z_1 - z_2) \hat{\mathcal{G}}(z_1) \hat{\mathcal{G}}(z_2) \quad (2.22)$$

that is just the perturbation expansion (2.6) with the choice $\hat{V} = (z_1 - z_2)\hat{1}$. Ward identity (2.21) can thus be viewed as a consequence of invariance to a very specific gauge transformation, namely to adding a constant to the scalar potential φ .

Using formula (2.21) in expression (2.19) we find that the density response to a homogeneous perturbation vanishes,

$$\chi(\omega + i0, \mathbf{0}) = \frac{1}{\omega} \int_{-\infty}^{\infty} \frac{dE}{2\pi i} \left\{ f(E + \omega) [G^A(E + \omega) - G^R(E + \omega)] - f(E) [G^A(E) - G^R(E)] \right\} = 0. \quad (2.23)$$

In particular, we therefore know the limit

$$\lim_{\omega \rightarrow 0} \lim_{\mathbf{q} \rightarrow \mathbf{0}} \chi(\omega + i0, \mathbf{q}) = 0. \quad (2.24)$$

We denoted the local element of the averaged one-particle Green function as $G(z)$, $G(z) = N^{-1} \sum_{\mathbf{k}} G(z, \mathbf{k})$. Result (2.23) expresses the particle number conservation law that requires the total density variation to be zero,

$$\int d^3r \delta n(t, \mathbf{r}) = 0. \quad (2.25)$$

Similarly, we can evaluate the response function χ in the limit $\omega \rightarrow 0$, $\mathbf{q} \rightarrow \mathbf{0}$ with order of limits reversed compared to the case (2.24). Letting $\omega = 0$ in expression (2.19) we get the static density response,

$$\chi(\mathbf{q}, 0) = \int_{-\infty}^{\infty} \frac{dE}{\pi} f(E) \Im \Phi^{RR}(E, E; \mathbf{q}). \quad (2.26)$$

Further on, for $\mathbf{q} = \mathbf{0}$, the Ward identity (2.21) provides a formula

$$\Phi^{RR}(E, E; \mathbf{0}) = -\frac{\partial G^R(E)}{\partial E} \quad (2.27)$$

with the help of which we express the desired limit as

$$\begin{aligned} \lim_{\mathbf{q} \rightarrow \mathbf{0}} \lim_{\omega \rightarrow 0} \chi(\omega + i0, \mathbf{q}) &= \int_{-\infty}^{\infty} \frac{dE}{\pi} \frac{\partial f(E)}{\partial E} \Im G^R(E) \\ &= -\int_{-\infty}^{\infty} \frac{dE}{\pi} \frac{\partial f(E)}{\partial \mu} \Im G^R(E) = \frac{\partial n}{\partial \mu}. \end{aligned} \quad (2.28)$$

We see that at the point $\omega = 0$, $\mathbf{q} = \mathbf{0}$ the response function χ is non-analytic as the order of limits is found to be substantial. Actually, based on results (2.24) and (2.28), we can write the small frequency and small momentum asymptotics of the density-density response function in a form³

$$\chi(\omega + i0, \mathbf{q}) = \frac{\frac{\partial n}{\partial \mu} D q^2}{-i\omega + D q^2}. \quad (2.29)$$

The constant D remains unevaluated within the above reasoning. The following section shows that it is just the diffusion constant.

2.4 Diffusion

The next physical process we are going to discuss is relaxation of a non-equilibrium particle density distribution. In many classical systems, approaching the equilibrium state has a diffusive character. In such a case the density variation evolves according to the law

$$\left(\frac{\partial}{\partial t} - D \Delta \right) \delta n(t, \mathbf{r}) = 0, \quad (2.30)$$

³To be precise, the asymptotic form of the response function χ , allowed by formulae (2.24) and (2.28), generally reads

$$\chi(\omega + i0, \mathbf{q}) = \frac{\frac{\partial n}{\partial \mu} D q^\beta}{-i\omega^\alpha + D q^\beta},$$

where $\alpha \geq 1$ and β is an even number due to the apparent symmetry $\chi(\omega + i0, -\mathbf{q}) = \chi(\omega + i0, \mathbf{q})$. It will be shown in Section 2.6 that only the case with $\alpha = 1$ and $\beta = 2$ is compatible with a nonzero conductivity σ . Namely, it is the generalized Einstein relation, equation (2.56), that is responsible for this final restriction.

the solution of which reads ($t > 0$)

$$\delta n(t, \mathbf{q}) = \delta n(t = 0, \mathbf{q}) \theta(t) e^{-Dq^2 t}, \quad \delta n(\omega + i0, \mathbf{q}) = \frac{\delta n(t = 0, \mathbf{q})}{i\omega - Dq^2}. \quad (2.31)$$

In the following we show how the density relaxation can be treated in quantum mechanical systems. Unlike Section 2.1, the now considered non-equilibrium behavior of the electronic system is induced by a spatial variation of the chemical potential μ and not by a Hamiltonian perturbation of any kind. To study the diffusion phenomena we should therefore use methods developed in References 38 and 39, which deal with the so-called thermal perturbations. However, if we restrict the initial non-equilibrium state so that it can be generated with the aid of an external force, we are allowed to stay within the framework of Hamiltonian perturbations.

We describe the relaxation of the particle density variation that arose as a response to a weak inhomogeneous electric field.⁴ For this purpose the perturbation is first slowly (adiabatically) switched on during the time interval $(-\infty, 0)$ and then suddenly turned off at $t = 0$. The scalar potential φ corresponding to the given scenario is $\varphi(t, \mathbf{q}) = \theta(-t) \exp(\varepsilon t) \varphi(\mathbf{q})$. The induced non-equilibrium density variation evolves according to formula (2.2). For the period of positive times, $t > 0$,⁵ when relaxation takes place, the time evolution is given by an expression

$$\delta n_{\text{relax}}(t, \mathbf{q}) = e\varphi(\mathbf{q}) \theta(t) \int_{-\infty}^0 dt' e^{\varepsilon t'} \chi(t - t', \mathbf{q}) = e\varphi(\mathbf{q}) \phi(t, \mathbf{q}). \quad (2.32)$$

We introduced a *relaxation function* $\phi(t, \mathbf{q})$. Its Fourier transform with respect to time reads

$$\phi(\omega + i0, \mathbf{q}) = \frac{1}{i} \frac{\chi(\omega + i0, \mathbf{q}) - \chi(i0, \mathbf{q})}{\omega - i0}. \quad (2.33)$$

Being interested only in slow dynamics of weakly spatially varying particle densities, we can continue with the asymptotic form of the density-density response function χ , equation (2.29). Then, in the limit of small frequency ω and small momentum \mathbf{q} , the relaxation function ϕ becomes

$$\phi(\omega + i0, \mathbf{q}) = \frac{(\partial n / \partial \mu)}{-i\omega + Dq^2}. \quad (2.34)$$

This equation has the same form as a solution of the diffusion equation, formula (2.31). Therefore, the relaxation of a disordered electron system is diffusive, starting from the zero-time density variation $\delta n(t = 0, \mathbf{q}) = \delta \mu (\partial n / \partial \mu) = -e\varphi(\mathbf{q}) (\partial n / \partial \mu)$. Consequently, the non-analyticity that the relaxation function ϕ displays at point $\omega = 0$, $\mathbf{q} = \mathbf{0}$ will be referred to as the *diffusion pole*.

A final observation of this section is that the diffusion pole in the relaxation function ϕ is entirely determined by the correlation function Φ^{AR} , whereas the other two, Φ^{RR} and Φ^{AA} , play no role in this asymptotics. As a consequence of the Ward identity (2.21) the correlation functions Φ^{RR} and Φ^{AA} are finite in the limit $\omega \rightarrow 0$, $\mathbf{q} \rightarrow \mathbf{0}$ and given

⁴The method of introduction the electron diffusion that we use here is analogous to the approach adopted in Reference 40.

⁵Note the presence of Heaviside function $\theta(t)$ in formula (2.32).

by expression (2.27). On the other hand, the asymptotic behavior of the correlation function Φ^{AR} is substantially different as an appropriate replacement of equation (2.27) reads

$$\Phi^{AR}(E, E + \omega; \mathbf{0}) = \frac{2\pi i \Im G^A(E)}{\omega}. \quad (2.35)$$

Using the above properties of the correlation functions, the expansion of the response function χ in powers of frequency ω has a form

$$\chi(\omega + i0, \mathbf{q}) = \chi(i0, \mathbf{q}) + \frac{i\omega}{2\pi} \Phi^{AR}(E_F, E_F + \omega; \mathbf{q}) + O(\omega). \quad (2.36)$$

This leads to the following expression for the relaxation function,

$$\phi(\omega + i0, \mathbf{q}) = \frac{1}{2\pi} \Phi^{AR}(E_F, E_F + \omega; \mathbf{q}), \quad (2.37)$$

that is valid as far as the diffusion pole is concerned. Note that the last two formulae apply in the presented simple form only in the limit of zero temperature, $T \rightarrow 0$.

2.5 Conductivity

In this section, currents generated by an external electric field are examined and a formula for electrical conductivity is derived. As already noted at the beginning of this chapter, dealing with conductivity instead of density response gets us closer to experimental probes of transport properties of solids. When dealing with the conductivity it is technically favorable to describe the electric field with the aid of a time-dependent vector potential⁶ $\mathbf{A}(t, \mathbf{r})$, $\mathbf{E}(t, \mathbf{r}) = -\partial\mathbf{A}(t, \mathbf{r})/\partial t$. The interaction of the electric field with electrons is given by the Hamiltonian term

$$\hat{H}_{\text{ext}}(t) = - \int d^3r \hat{\mathbf{j}}(\mathbf{r}) \cdot \mathbf{A}(t, \mathbf{r}) \quad (2.38)$$

where $\hat{\mathbf{j}}$ stands for the charged current density. The operator $\hat{\mathbf{j}}$ itself depends on the applied field \mathbf{A} . However, as long as we stay within the linear response, the full current $\hat{\mathbf{j}}$ can be replaced with its \mathbf{A} -independent part, which we denote $\hat{\mathbf{j}}^{(0)}$. The difference $\hat{\mathbf{j}} - \hat{\mathbf{j}}^{(0)}$ is linear in the vector potential \mathbf{A} , and therefore generates Hamiltonian contributions that are quadratic in the external field. From now on we thus use the reduced form of the interaction Hamiltonian (2.38),

$$\hat{H}_{\text{ext}}(t) \approx - \int d^3r \hat{\mathbf{j}}^{(0)}(\mathbf{r}) \cdot \mathbf{A}(t, \mathbf{r}). \quad (2.39)$$

The current in the absence of the vector potential has an anti-commutator form

$$\hat{\mathbf{j}}^{(0)}(\mathbf{r}) = -\frac{e}{2} \{ \hat{\mathbf{v}}, \hat{n}(\mathbf{r}) \} \quad (2.40)$$

with the velocity operator given by (see any textbook on quantum theory of solids, e. g. [1])

$$\hat{\mathbf{v}} = \frac{i}{\hbar} [\hat{H}, \hat{\mathbf{r}}] = \sum_{\mathbf{k}} |\mathbf{k}\rangle \mathbf{v}(\mathbf{k}) \langle \mathbf{k}|, \quad v_{\alpha}(\mathbf{k}) = \frac{1}{\hbar} \frac{\partial \epsilon(\mathbf{k})}{\partial k_{\alpha}}. \quad (2.41)$$

⁶It is possible but rather tedious to use a scalar potential as well, see e.g. [37].

Vectors $|\mathbf{k}\rangle$, i. e. Bloch waves, are eigenstates of the Hamiltonian \hat{H}_0 and energies $\epsilon(\mathbf{k})$ are their corresponding eigenvalues. The local part of the Hamiltonian, \hat{V} , does not contribute to the velocity because it commutes with the position operator $\hat{\mathbf{r}}$.

Our aim is to calculate the current response that means to find an expectation value for the current operator $\hat{\mathbf{j}} = \hat{\mathbf{j}}^{(0)} + \hat{\mathbf{j}}^{(A)}$. This procedure would not need any additional comments if we were studying continuous models (free electrons). In that case we could proceed in a straightforward way as it would be easy to write down the explicit expression for the gauge current $\hat{\mathbf{j}}^{(A)}$. However, the problem of finding the current $\hat{\mathbf{j}}^{(A)}$ within the tight-binding lattice models represents a rather difficult task. We show that it is possible to derive the total current response using just the zero field operator $\hat{\mathbf{j}}^{(0)}$ and the requirement of gauge invariance of the result.

The current $\mathbf{j}^{(0)}(t, \mathbf{r})$ due to perturbation (2.39) is given by an expression

$$j_\alpha^{(0)}(t, \mathbf{r}) = \sum_\beta \int_{-\infty}^{\infty} dt' \int d^3 r' \Pi_{\alpha\beta}(t - t'; \mathbf{r}, \mathbf{r}') A_\beta(t', \mathbf{r}') \quad (2.42)$$

and the Kubo formula for the current-current response function $\Pi_{\alpha\beta}(t - t'; \mathbf{r}, \mathbf{r}')$ reads

$$\Pi_{\alpha\beta}(t - t'; \mathbf{r}, \mathbf{r}') = \frac{i}{\hbar} \theta(t - t') \text{Tr} \left(f(\hat{H}) [\hat{j}_\alpha^{(0)}(t, \mathbf{r}), \hat{j}_\beta^{(0)}(t', \mathbf{r}')] \right). \quad (2.43)$$

After coming over to the frequency representation and after introducing Green functions we have

$$\begin{aligned} \Pi_{\alpha\beta}(\omega + i0; \mathbf{r}, \mathbf{r}') = \int_{-\infty}^{\infty} \frac{dE}{2\pi i} \left\{ [f(E + \omega) - f(E)] \tilde{\Pi}_{\alpha\beta}^{AR}(E, E + \omega; \mathbf{r}, \mathbf{r}') \right. \\ \left. + f(E) \tilde{\Pi}_{\alpha\beta}^{RR}(E, E + \omega; \mathbf{r}, \mathbf{r}') - f(E + \omega) \tilde{\Pi}_{\alpha\beta}^{AA}(E, E + \omega; \mathbf{r}, \mathbf{r}') \right\} \quad (2.44) \end{aligned}$$

with the correlation functions $\tilde{\Pi}_{\alpha\beta}^{ab}$ defined as

$$\tilde{\Pi}_{\alpha\beta}^{ab}(E, E + \omega; \mathbf{r}, \mathbf{r}') = \text{Tr} \left[\hat{\mathcal{G}}^a(E) \hat{j}_\alpha^{(0)}(\mathbf{r}) \hat{\mathcal{G}}^b(E + \omega) \hat{j}_\beta^{(0)}(\mathbf{r}') \right]. \quad (2.45)$$

In the last step we carry out the configurational averaging that allows for a Fourier transform to momentum space. Using the equations defining the current operator, (2.40) and (2.41), we end up with an expression for the correlation functions (2.45),

$$\begin{aligned} \tilde{\Pi}_{\alpha\beta}^{ab}(E, E + \omega; \mathbf{q}) = \frac{e^2}{4N^2} \sum_{\mathbf{k}\mathbf{k}'} [v_\alpha(\mathbf{k}) + v_\alpha(\mathbf{k} + \mathbf{q})] \\ \times [v_\beta(\mathbf{k}') + v_\beta(\mathbf{k}' + \mathbf{q})] G_{\mathbf{k}\mathbf{k}'}^{ab}(E, E + \omega; \mathbf{q}). \quad (2.46) \end{aligned}$$

The induced total current, averaged over disorder configurations, can be given in the ω, \mathbf{q} -representation by a formula

$$j_\alpha(\omega, \mathbf{q}) = \sum_\beta K_{\alpha\beta}(\omega, \mathbf{q}) A_\beta(\omega, \mathbf{q}). \quad (2.47)$$

The complete response function $K_{\alpha\beta}(\omega, \mathbf{q})$ combines the previously calculated contribution $\Pi_{\alpha\beta}(\omega, \mathbf{q})$ with a gauge fixing term that we find as follows. The pure gauge field

$\mathbf{A}(t, \mathbf{r}) = \text{grad } \lambda(\mathbf{r})$ does not generate any physical fields, i. e. $\mathbf{E}(t, \mathbf{r}) = \mathbf{0}$ and $\mathbf{B}(t, \mathbf{r}) = \mathbf{0}$. Such a vector potential therefore cannot induce any currents in the sample. With a single Fourier component, $\lambda(\mathbf{r}) = \lambda_{\mathbf{q}} \exp(i\mathbf{q} \cdot \mathbf{r})$, inserted into formula (2.47) the latter becomes

$$j_{\alpha}(0, \mathbf{q}) = \sum_{\beta} -iK_{\alpha\beta}(0, \mathbf{q}) q_{\beta} \lambda_{\mathbf{q}}. \quad (2.48)$$

The current component on the left hand side of this equation is zero which imposes the condition $K_{\alpha\beta}(0, \mathbf{q}) = 0$. We are thus forced to set $K_{\alpha\beta}(\omega, \mathbf{q}) = \Pi_{\alpha\beta}(\omega, \mathbf{q}) - \Pi_{\alpha\beta}(0, \mathbf{q})$.

The tensor of the electrical conductivity $\sigma_{\alpha\beta}$ is defined as the coefficient of proportionality between the current and the electric field. With the aid of the relation $\mathbf{E}(\omega, \mathbf{q}) = i\omega \mathbf{A}(\omega, \mathbf{q})$ the conductivity is written as

$$\sigma_{\alpha\beta}(\omega, \mathbf{q}) = \frac{1}{i\omega} K_{\alpha\beta}(\omega, \mathbf{q}) = \frac{1}{i\omega} [\Pi_{\alpha\beta}(\omega, \mathbf{q}) - \Pi_{\alpha\beta}(0, \mathbf{q})]. \quad (2.49)$$

Inserting the explicit expression for the current-current response function we arrive at the final formula

$$\begin{aligned} \sigma_{\alpha\beta}(\omega, \mathbf{q}) = & -\frac{e^2}{4N^2} \sum_{\mathbf{k}\mathbf{k}'} [v_{\alpha}(\mathbf{k}) + v_{\alpha}(\mathbf{k} + \mathbf{q})] [v_{\beta}(\mathbf{k}') + v_{\beta}(\mathbf{k}' + \mathbf{q})] \\ & \times \int_{-\infty}^{\infty} \frac{dE}{2\pi\omega} \left\{ [f(E + \omega) - f(E)] G_{\mathbf{k}\mathbf{k}'}^{AR}(E, E + \omega; \mathbf{q}) \right. \\ & \quad + f(E) G_{\mathbf{k}\mathbf{k}'}^{RR}(E, E + \omega; \mathbf{q}) - f(E + \omega) G_{\mathbf{k}\mathbf{k}'}^{AA}(E, E + \omega; \mathbf{q}) \\ & \quad \left. - f(E) [G_{\mathbf{k}\mathbf{k}'}^{RR}(E, E; \mathbf{q}) - G_{\mathbf{k}\mathbf{k}'}^{AA}(E, E; \mathbf{q})] \right\}. \quad (2.50) \end{aligned}$$

The obtained result is precisely the same as the usually derived conductivity of continuous models. The only difference is the replacement of the velocity components $\hbar k_{\alpha}/m \rightarrow \hbar^{-1} \partial \epsilon(\mathbf{k}) / \partial k_{\alpha}$.

2.6 Einstein relation

The electrical conductivity derived in the previous section is significantly more complicated than expressions concerning responses or relaxation of the particle density. It is a rather difficult problem to work with the conductivity formula (2.50) when quantum coherence becomes important. A mean-field-like treatment of this task was recently proposed [41]. However, such an approach seems to over-simplify the problem and a more sophisticated procedure is generally needed.

It is very desirable to find a relation between density and current responses that would allow us to calculate conductivity indirectly. An example of such a formula is the Einstein relation,

$$\sigma = e^2 D \frac{\partial n}{\partial \mu}, \quad (2.51)$$

according to which the homogeneous static conductivity σ is given solely by the diffusion constant D . Formula (2.51) was derived in the framework of linear response theory

already by Kubo [35]. Here we present a more general relation between the conductivity σ and the density-density response function χ that reduces to the original Einstein relation (2.51) in a certain limit.

We start with a simple motivation, in the literature widely presented as a proof (see e. g. Reference 36). The operators for particle and current densities obey the continuity equation

$$-e \frac{\partial \hat{n}(t, \mathbf{r})}{\partial t} + \text{div } \hat{\mathbf{j}}(t, \mathbf{r}) = 0 \quad (2.52)$$

that is a consequence of Heisenberg equations of motion. Written in terms of expectation values the continuity equation reads

$$i\omega e \delta n(\omega, \mathbf{q}) + i \mathbf{q} \cdot \mathbf{j}(\omega, \mathbf{q}) = 0 \quad (2.53)$$

where the variation $\delta n(\omega, \mathbf{q}) = n(\omega, \mathbf{q}) - n_0$ replaces the full value $n(\omega, \mathbf{q})$ itself as the equilibrium particle density n_0 is time-independent.⁷ Within the linear response to the external electric field \mathbf{E} , $\mathbf{E} = -\text{grad } \varphi$, we have

$$\delta n(\omega, \mathbf{q}) = e \chi(\omega, \mathbf{q}) \varphi(\omega, \mathbf{q}) \quad (2.54)$$

and

$$\mathbf{j}(\omega, \mathbf{q}) = \boldsymbol{\sigma}(\omega, \mathbf{q}) \cdot \mathbf{E}(\omega, \mathbf{q}) = -i \boldsymbol{\sigma}(\omega, \mathbf{q}) \cdot \mathbf{q} \varphi(\omega, \mathbf{q}) \quad (2.55)$$

where $\boldsymbol{\sigma}(\mathbf{q}, \omega)$ denotes the tensor of electrical conductivity. Inserting these two expectation values into equation (2.53) we obtain, in the isotropic case, a generalization of the Einstein relation,

$$\sigma(\omega, \mathbf{q}) = \frac{-ie^2 \omega}{q^2} \chi(\omega, \mathbf{q}). \quad (2.56)$$

We should explain why we do not regard the above reasoning as a proof of relation (2.56). First, the continuity equation in the form (2.52) applies only to cases with quadratic dispersion relation and it needs to be modified to hold also within the lattice models. Second, the time-dependence of Kubo formulae (2.3) and (2.43) is not directly related to the evolution of Heisenberg operators. This fact makes the step from equation (2.52) to formula (2.53) unjustified.

In Appendix A we provide a proof that does not suffer the mentioned flaws. In order to construct such a proof the validity of relation (2.56) has to be restricted to (infinitesimally) small momenta \mathbf{q} . The approach presented in the appendix is based on the Ward identity

$$\Sigma(z_1, \mathbf{k} + \mathbf{q}) - \Sigma(z_2, \mathbf{k}) = \frac{1}{N} \sum_{\mathbf{k}'} \Lambda_{\mathbf{k}\mathbf{k}'}(z_1, z_2; \mathbf{q}) [G(z_1, \mathbf{k}' + \mathbf{q}) - G(z_2, \mathbf{k}')] \quad (2.57)$$

proved by Vollhardt and Wölfle in [42].⁸ This identity directly shows which property of the irreducible vertex functions has to be fulfilled for relation (2.56) to hold. Such

⁷Unlike Section 2.1, the quantity n_0 is homogeneous here, since we now work with configurational averages and not with individual disorder realizations.

⁸In a less general form the Ward identity (2.57) was used already in an earlier paper on quantum diffusion [43].

a knowledge is very useful for constructing approximate calculational schemes because irreducible vertices are their basic building blocks.

At this point we return to the question how the Einstein relation (2.51) emerges from formula (2.56). To proceed with this goal we insert the asymptotic form (2.29) of the density-density response function χ into equation (2.56). This gives the conductivity in the vicinity of point $\omega = 0$, $\mathbf{q} = \mathbf{0}$,

$$\sigma(\omega, \mathbf{q}) = \frac{-i\omega e^2 D \frac{\partial n}{\partial \mu}}{-i\omega + Dq^2}. \quad (2.58)$$

Finally, the static limit of the homogeneous conductivity,

$$\sigma = \lim_{\omega \rightarrow 0} \lim_{\mathbf{q} \rightarrow \mathbf{0}} \sigma(\omega, \mathbf{q}) = e^2 D \frac{\partial n}{\partial \mu}, \quad (2.59)$$

is given just by the original Einstein relation (2.51).

Chapter summary

With the aid of the Kubo linear response theory we showed how disordered electronic systems respond to weak externally applied electric fields. We derived formulae for the density response function χ , describing the non-equilibrium charge redistribution, and for the electrical conductivity σ , allowing to calculate induced currents. Both responses were expressed in terms of configurationally averaged Green functions. Namely, the two-particle Green function was shown to be essential when calculating characteristics of weakly non-equilibrium states. The averaging over disorder configurations was introduced to provide for translationally invariant description even in the case of disordered, and thus irregular, lattices, which are the subject of our study.

Relaxation of small non-equilibrium particle density variations back to the equilibrium state was observed to have the diffusive character. The corresponding diffusion constant D was found to be accessible from the density response function χ in the limit of slowly varying, both in space and time, particle densities.

Moreover, a close relationship between the density response χ and the electrical conductivity σ was uncovered, allowing to calculate σ from χ and vice versa. Such an option is very convenient as the conductivity formula represents a rather complicated expression. In the time-independent case, the relation between χ and σ reduces to the well known Einstein relation linking the static conductivity directly with the diffusion constant.

3

Classical conductivity and quantum corrections

In this chapter we describe some methods available for approximate evaluation of linear response formulae. Our starting point is a theory with momentum-independent two-particle irreducible vertex Λ . Such an approximation completely disregards any inter-site quantum effects, which makes it compatible with classical considerations (Drude formula). In the next step we perturbatively include the so-called coherent backscattering process and show how it lowers conductivity. For low-dimensional systems, $d \leq 2$, the corresponding conductivity correction diverges. This effect, known as weak localization, indicates that a perturbative treatment of quantum corrections is generally insufficient. Finally, we briefly summarize results of a self-consistent (non-perturbative) approach to transport properties of disordered electronic systems proposed by Vollhardt and Wölfle, [5].

3.1 Local approximations

The simplest approximation with local, i. e. momentum-independent, two-particle irreducible vertex Λ is the Born approximation. This vertex is given by the lowest order of the perturbation expansion,

$$\lambda_B = (1 - c) \begin{array}{c} | \\ \times \\ | \end{array} = c(1 - c)v^2, \quad (3.1a)$$

which limits its applicability to weak disorder situations. The corresponding selfenergy reads

$$\Sigma_B(z) = (1 - c) \begin{array}{c} \times \\ \swarrow \quad \searrow \\ \hline \end{array} = c(1 - c)v^2 G(z), \quad (3.1b)$$

where the fermion line represents the full one-particle Green function.¹ The theory defined by equations (3.1) is easily shown to comply with the Ward identities (2.21) and (2.57).²

¹From now on the fermion lines in Feynman diagrams will always denote the full averaged Green function G and hence there will be no need to distinguish thin lines ($G^{(0)}$) and thick lines (G).

²These two identities are completely equivalent when both the selfenergy Σ and the irreducible vertex Λ are local quantities.

Note that the selfenergy Σ_B must contain infinitely many diagrams to be consistent with the vertex λ_B , although the latter is completely trivial — being just a single diagram.

Within the Born approximation, the Bethe-Salpeter equation (2.18) generates the two-particle Green function as a sum of ladder diagrams, an example of which is

Due to momentum independence of the vertex λ_B , the momentum summations in the Bethe-Salpeter equation decouple and we are able to write the two-particle Green function in a closed form,

$$G_{\mathbf{k}\mathbf{k}'}^{(2)}(z_1, z_2; \mathbf{q}) = G(z_1, \mathbf{k} + \mathbf{q})G(z_2, \mathbf{k}) \left[N\delta_{\mathbf{k},\mathbf{k}'} + \frac{\lambda_B G(z_1, \mathbf{k}' + \mathbf{q})G(z_2, \mathbf{k}')}{1 - \lambda_B \chi(\mathbf{q})} \right], \quad (3.3)$$

where $\chi(\mathbf{q})$ denotes a convolution of two one-particle Green functions,³

$$\chi(\mathbf{q}) = \frac{1}{N} \sum_{\mathbf{k}} G(z_1, \mathbf{k} + \mathbf{q})G(z_2, \mathbf{k}).$$

The energy variables of the “bubble” χ were dropped for the sake of simplicity. The particularly simple form of the two-particle Green function (3.3) results entirely from locality of the irreducible vertex λ_B , limitation to a weak scattering does not play any role here. All single-site, i. e. local, approximations provide the two-particle Green function $G^{(2)}$ of the same form as the Born approximation does, the only modification is a replacement of the vertex λ_B with another value, possibly dependent on the energy variables z_1 and z_2 .

In the later development we use the best single-site theory available — the coherent-potential approximation (CPA, [20]). The selfenergy calculated within the CPA was shown to be the exact solution of the Anderson Hamiltonian (1.4) in the limit of infinite spatial dimensions (see [44]). It is thus considered as the mean-field approximation for the non-interacting disordered electron problem. The CPA selfenergy is the solution of the Soven equation

$$\left\langle \frac{1}{1 + (\Sigma(z) - V)G(z)} \right\rangle_{\text{av.}} = 1 \quad (3.4)$$

where V is the random local potential and $G(z)$ stands for the local element of the averaged Green function, $G(z) = N^{-1} \sum_{\mathbf{k}} G(z, \mathbf{k})$. The physical content of approximation (3.4) is elucidated within the multiple-scattering formalism in Reference 45. Formula (3.4) is obtained by summing up all scatterings on a single impurity whereas quantum coherence between different scattering centers is neglected.⁴ The same method can be used to derive the CPA two-particle irreducible vertex λ ,

$$\lambda(z_1, z_2) = \frac{1}{G(z_1)G(z_2)} \left[1 - \left\langle \frac{1}{1 + (\Sigma(z_1) - V)G(z_1)} \frac{1}{1 + (\Sigma(z_2) - V)G(z_2)} \right\rangle_{\text{av.}}^{-1} \right], \quad (3.5)$$

³Avoid confusion with similar notation used for the density-density response function.

⁴A diagrammatic approach to deduce Soven equation was developed as well, but it is rather tedious. See [17] for details.

needed for calculations of transport properties, [21]. In Appendix B we offer an alternative construction of the irreducible vertex λ based on the scheme of Baym and Kadanoff, [46]. In this approach a two-particle function corresponding to a given selfenergy is found in such a way that the resulting approximation obeys conservation laws, i. e. the Ward identities, formulae (2.21) and (2.57), are satisfied.

3.1.1 Conductivity

Now we use the two-particle Green function (3.3)⁵ to calculate the conductivity σ from equation (2.50). Only the first term in the square brackets (Kronecker delta) in expression (3.3) contributes to the homogeneous conductivity $\sigma(\omega) = \sigma(\omega, \mathbf{0})$. The second term, the so-called *vertex correction*, vanishes due to odd symmetry of the velocity, $\mathbf{v}(-\mathbf{k}) = -\mathbf{v}(\mathbf{k})$, that stems from the simplicity of our model (only a single band) and from the time-reversal invariance. In the case of multi-band calculations or in the presence of the magnetic field the CPA vertex correction generally plays a role (for an example see e. g. [47]). However, even in such situations, the contribution coming from vertex corrections is not primarily caused by disorder. Therefore, the effect of impurity scatterings in the framework of a single-site approximation reduces to a shift in eigenenergies, $\Re\Sigma$, and to a finite lifetime of current-carrying Bloch states, $\tau = 1/(2\Im\Sigma)$. This is equivalent to the physics behind the Drude conductivity formula (1.1).

Insertion of expression (3.3) into formula (2.50) leads to the following form of the homogeneous dynamical conductivity,

$$\sigma_{\alpha\alpha}(\omega) = \frac{e^2}{N} \sum_{\mathbf{k}} v_{\alpha}^2(\mathbf{k}) \int_{-\infty}^{\infty} \frac{dE}{2\pi} f(E) \left\{ [G^A(E, \mathbf{k}) - G^R(E, \mathbf{k})] \times \left[\frac{G^R(E + \omega, \mathbf{k}) - G^R(E, \mathbf{k})}{\omega} - \frac{G^A(E, \mathbf{k}) - G^A(E - \omega, \mathbf{k})}{\omega} \right] \right\}. \quad (3.6)$$

Particularly, if we limit our investigation only to the response to a static external field at zero temperature, $T = 0$, we come to a simple representation of the static conductivity in the isotropic system,

$$\sigma_0 = -\frac{e^2}{4\pi N} \sum_{\mathbf{k}} v_{\alpha}^2(\mathbf{k}) [G^A(E_F, \mathbf{k}) - G^R(E_F, \mathbf{k})]^2. \quad (3.7)$$

The notation was changed from σ to σ_0 in order to distinguish the single-site conductivity (3.7) from results of more sophisticated approximations that include non-trivial vertex corrections. Such theories are introduced in the following sections where the conductivity σ_0 serves as a reference value. For the same reason, the diffusion constant calculated within local approximations will be denoted D_0 .

At the end of this paragraph we explicitly demonstrate that equation (3.7) is more or less equivalent to the Drude formula (1.1) as anticipated above. To do so quickly we resort to the effective mass approximation for the electron dispersion relation $\epsilon(\mathbf{k})$, i. e. $\epsilon(\mathbf{k}) = k^2/(2m^*)$ and $v_{\alpha} = k_{\alpha}/m^*$. The

⁵The Born vertex λ_B is from now on replaced with the CPA value λ .

replacement of momentum summation with integration, $\sum_{\mathbf{k}} \rightarrow 1/(2\pi)^3 \int d^3k$, and the consequent change of the integration variable from momenta \mathbf{k} to energy ϵ yield

$$\sigma_0 = \frac{1}{3} \frac{e^2}{(2\pi)^3} 2^{3/2} (m^*)^{1/2} \int_0^\infty d\epsilon \epsilon^{3/2} \frac{4(\Im\Sigma)^2}{[(E_F - \epsilon)^2 + (\Im\Sigma)^2]^2}. \quad (3.8)$$

The real part of the selfenergy, $\Re\Sigma$, is not important and was neglected. In the limit of weak scatterings, the fraction in the integrand can be approximated by a δ -function,

$$\frac{4(\Im\Sigma)^2}{[(E_F - \epsilon)^2 + (\Im\Sigma)^2]^2} = \frac{2\pi}{\Im\Sigma} \delta(E_F - \epsilon) + o\left(\frac{1}{\Im\Sigma}\right). \quad (3.9)$$

Doing so, the integral in equation (3.8) is easily evaluated and we obtain

$$\sigma_0 = \frac{1}{3} \frac{e^2}{(2\pi)^2} 2^{3/2} (m^*)^{1/2} \frac{1}{\Im\Sigma} E_F^{3/2}. \quad (3.10)$$

Recalling the density of states of the ideal electron gas, $g(E) = (2m^*)^{3/2} E^{1/2}/(2\pi)^2$, we identify a large part of expression (3.10) as the electron density n ,

$$n = \int_0^{E_F} g(E) dE = \frac{2}{3} \frac{1}{(2\pi)^2} (2m^* E_F)^{3/2}. \quad (3.11)$$

Finally, equation (3.10) can be rewritten to the form

$$\sigma_0 = \frac{n e^2}{m^*} \frac{1}{2 \Im\Sigma} \quad (3.12)$$

that is just the Drude formula (1.1) with the scattering time given by $\tau = 1/(2 \Im\Sigma)$.

3.1.2 Diffusion pole

Within the CPA, the diffusion pole in the correlation function Φ reads

$$\Phi(z_1, z_2; \mathbf{q}) = \frac{\chi(\mathbf{q})}{1 - \lambda(z_1, z_2)\chi(\mathbf{q})}. \quad (3.13)$$

We are interested only in the small momentum behavior, so we expand the ‘‘bubble’’ $\chi(\mathbf{q})$ in powers of q^2 ,

$$\chi(\mathbf{q}) = \frac{\langle \Delta G \rangle}{-\Delta z + \Delta \Sigma} + \frac{1}{6} q^2 \text{grad}_{\mathbf{q}}^2 \chi(\mathbf{q}) \Big|_{\mathbf{q}=\mathbf{0}} + O(q^4). \quad (3.14)$$

To simplify this and subsequent formulae we use angular brackets to indicate momentum summations, $\langle F \rangle = N^{-1} \sum_{\mathbf{k}} F(\mathbf{k})$. The rearrangement in the first term on the right-hand side of expression (3.14) was done using the identity $G_1 G_2 = (G_2 - G_1)/(G_1^{-1} - G_2^{-1})$. The notation for the introduced differences is $\Delta G = G(z_2, \mathbf{k}) - G(z_1, \mathbf{k})$ and similarly for Δz and $\Delta \Sigma$. The gradient in equation (3.14) is easily evaluated as only one of the involved Green functions depends on momentum \mathbf{q} . We successively derive

$$\begin{aligned} \text{grad}_{\mathbf{q}}^2 \chi(\mathbf{q}) \Big|_{\mathbf{q}=\mathbf{0}} &= \frac{1}{N} \sum_{\mathbf{k}} G(z_2, \mathbf{k}) \text{grad}_{\mathbf{k}}^2 G(z_1, \mathbf{k}) \\ &= -\frac{1}{N} \sum_{\mathbf{k}} \text{grad}_{\mathbf{k}} G(z_1, \mathbf{k}) \cdot \text{grad}_{\mathbf{k}} G(z_2, \mathbf{k}) \\ &= -\frac{1}{N} \sum_{\mathbf{k}} v^2(\mathbf{k}) G^2(z_1, \mathbf{k}) G^2(z_2, \mathbf{k}) = -\frac{\langle v^2(\mathbf{k}) (\Delta G)^2 \rangle}{(-\Delta z + \Delta \Sigma)^2} \end{aligned} \quad (3.15)$$

where the integration by parts was used in the second equality.

To analyze the singular part of the correlation function Φ we insert the expansion of the “bubble” $\chi(\mathbf{q})$, equation (3.14), into expression (3.13). In the numerator the momentum-independent term is sufficient, whereas in the denominator it is essential to include also the $O(q^2)$ contribution. Doing so we obtain an expression

$$\begin{aligned}\Phi_{\text{sing}}(z_1, z_2; \mathbf{q}) &= \frac{\langle \Delta G \rangle}{-\Delta z + \Delta \Sigma - \lambda(z_1, z_2) \left(\langle \Delta G \rangle - \frac{1}{2} q^2 \frac{\langle v_\alpha^2(\mathbf{k}) (\Delta G)^2 \rangle}{-\Delta z + \Delta \Sigma} \right)} \\ &= \frac{\langle \Delta G \rangle}{-\Delta z + \frac{1}{2} q^2 \frac{\Delta \Sigma}{-\Delta z + \Delta \Sigma} \frac{\langle v_\alpha^2(\mathbf{k}) (\Delta G)^2 \rangle}{\langle \Delta G \rangle}}\end{aligned}\quad (3.16)$$

where the Vollhardt-Wölfle identity (2.57) was utilized in the second step. Specifying the energy variables, $z_1 = E_F - i0$ and $z_2 = E_F + \omega + i0$, and comparing with the conductivity formula (3.7) we come to the final representation of the diffusion pole

$$\Phi_{\text{sing}}^{AR}(E, E + \omega; \mathbf{q}) = \frac{2\pi g_F}{-i\omega + \frac{\sigma_0}{e^2 g_F} q^2}\quad (3.17)$$

where g_F denotes the density of electron states at the Fermi energy E_F , $g_F = g(E_F)$. The achieved result, $D_0 = \sigma_0/(e^2 g_F)$, is in agreement with the Einstein relation (2.51) because the derivative $\partial n/\partial \mu$ approaches the value g_F in the limit of zero temperature.

Up to equation (3.16) we used only expansion in small momenta \mathbf{q} but no assumptions has been made about frequency ω . It is tempting to generalize the diffusion constant D to a dynamical quantity $D(\omega)$ via

$$\Phi_{\text{sing}}^{AR}(E, E + \omega; \mathbf{q}) = \frac{2\pi g_F}{-i\omega + D(\omega)q^2}.\quad (3.18)$$

We know, however, only little about the physical content of such a dynamical diffusion “constant” $D(\omega)$. It obviously cannot be related to the dynamical conductivity $\sigma(\omega)$ with the aid of the Einstein relation, since

$$e^2 g_F D(\omega) = -\frac{e^2}{4\pi} \frac{\Delta \Sigma}{\Delta \Sigma - \omega} \langle v_{\alpha\alpha}^2(\mathbf{k}) (\Delta G)^2 \rangle \neq \sigma(\omega).\quad (3.19)$$

This inequality is not surprising because the diffusion is calculated using Green functions of only two energy arguments E_F and $E_F + \omega$, whereas in the conductivity formula all energy arguments between values $E_F - \omega$ and $E_F + \omega$ are involved (at $T = 0$). The above reasoning is not confined only to the CPA which indicates that nonequivalence (3.19) is a generally valid property.

3.2 Coherent backscattering

We have demonstrated that ladder diagrams (3.2) generate a quasi-classical theory of electron transport. To describe purely quantum effects we have to seek for another class

of diagrams. A quite natural extension of the ladder approximation is inclusion of the so-called *maximally crossed diagrams*, i. e. diagrams in which every interaction line crosses all others. An example of such a contribution to the two-particle Green function is

Diagrams of this type were for the first time considered by Langer and Neal, [48]. With all the maximally crossed diagrams taken into account the two-particle Green function has a form

$$G_{\mathbf{k}\mathbf{k}'}^{(2)}(z_1, z_2; \mathbf{q}) = G(z_1, \mathbf{k} + \mathbf{q})G(z_2, \mathbf{k}) \left[N\delta_{\mathbf{k},\mathbf{k}'} + \frac{\lambda_B G(z_1, \mathbf{k}' + \mathbf{q})G(z_2, \mathbf{k}')}{1 - \lambda_B \chi(\mathbf{q})} + \frac{\lambda_B G(z_1, \mathbf{k}' + \mathbf{q})G(z_2, \mathbf{k}')}{1 - \lambda_B \chi(\mathbf{k} + \mathbf{k}' + \mathbf{q})} - \lambda_B G(z_1, \mathbf{k}' + \mathbf{q})G(z_2, \mathbf{k}') \right] \quad (3.21)$$

where the last term in the square brackets compensates for the doubly-counted diagram with one interaction line. Actually, there are even more diagrams that are included twice in expression (3.21). These are the terms built up of only local elements of one-particle Green functions G . As the multiple counting of local contributions is not crucial for present considerations, we postpone its analysis to later chapters, where quite powerful methods will be developed to deal with such complications.

There are, however, several shortcomings in the two-particle Green function (3.21) that should be discussed right now. First, it cannot be written in a form of a Bethe-Salpeter equation and thus some formulae involving the two-particle irreducible function Λ , such as the Vollhardt-Wölfle identity (2.57), do not make sense. This is only a formal difficulty as it is the full two-particle Green function that we need to evaluate in physical quantities.

Second, it is not clear what selfenergy should be chosen to complete the one-particle sector of the approximation. The literature concerning the maximally crossed diagrams and related phenomena generally lacks a proper discussion of this issue. In order to guarantee compatibility of approximate one- and two-particle Green functions with conservation laws, Ward identities have to be fulfilled. Out of the two identities discussed in Chapter 2, formulae (2.21) and (2.57), only the Velický identity (2.21) is applicable in the present case. As noted above, the Vollhardt-Wölfle identity (2.57) cannot be formulated when the two-particle Green function $G^{(2)}$ is of form (3.21). Unfortunately, we do not know any calculational scheme that would provide the selfenergy to a given two-particle Green function so that the Velický identity (2.21) would be fulfilled. Moreover, it is unlikely to be possible to find such a procedure for an arbitrary functional $G^{(2)}[G]$ and some restrictions on the form of the Green function $G^{(2)}$ are to be expected.

Despite of all these inconveniences we still can obtain reasonable physical results quite easily if we take the same selfenergy as in the preceding section. In such a case, *and in such a case only*, the second term in the Green function (3.21) contains the diffusion

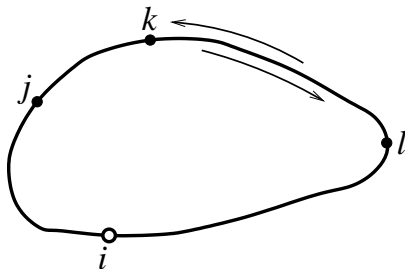


Figure 3.1: Two oppositely oriented trajectories contributing to the return probability P_{ii} . Quantum interference of the corresponding probability amplitudes gives rise to the so-called coherent backscattering.

pole, i. e., its denominator is zero for $\mathbf{q} = \mathbf{0}$ and $z_2 = \bar{z}_1$. The corresponding diffusion constant D equals to the single-site result D_0 . This holds due to the fact that all other contributions in expression (3.21) remain finite at the diffusion pole and hence the non-analyticity at $\mathbf{q} = \mathbf{0}$ and $z_2 = \bar{z}_1$ is just the same as in the CPA. On the other hand, if we use the Kubo formula (2.50) to calculate the electrical conductivity, we obtain a non-trivial correction to the value σ_0 , equation (3.6), acquired within a local approximation. The form of this additional contribution is governed by a pole that is present in the third term on the right-hand side of equation (3.21). This divergency, referred to as *Cooper pole*, takes place for $\mathbf{k}' = -\mathbf{k} - \mathbf{q}$ when $z_2 = \bar{z}_1$.

Before we evaluate the conductivity correction generated by the maximally crossed diagrams we first take a closer look at the physics described by this type of two-particle contributions. Let us discuss the probability that a diffusing particle travels along a trajectory $i \rightarrow j \rightarrow k \rightarrow l \rightarrow i$, i. e., it returns to its starting point i after encountering three scattering events at lattice sites j , k and l . The quantum mechanical probability amplitude corresponding to this path we denote A_{ijkli} . Obviously, also the reversed path exists with an amplitude A_{ilkji} , see Figure 3.1. Taking into account only these two trajectories the return probability P_{ii} is given by the expression

$$P_{ii} = |A_{ijkli} + A_{ilkji}|^2 = |A_{ijkli}|^2 + |A_{ilkji}|^2 + A_{ijkli}A_{ilkji}^* + A_{ilkji}^*A_{ijkli}. \quad (3.22)$$

The first two terms are classical contributions whereas the other two are due to quantum interference. If the system is invariant with respect to time reversal the amplitudes A_{ijkli} and A_{ilkji} are the same. As a result, the quantum value of the return probability P_{ii} is twice as large as its classical counterpart. Quantum interference therefore slows down the electron propagation through random media. This phenomenon is known as *coherent backscattering*.

Now we inspect a diagrammatic representation of probability (3.22). The proper graphs are those that build up the correlation function Φ^{AR} , i. e. those that have one fermionic line advanced and the other retarded. We use a notation according to which a fermion line pointing from site index i to index j represents the retarded one-particle propagator G_{ij}^R , whereas an opposite line, oriented from j to i , stands for the advanced propagator G_{ij}^A . Such identification is possible due to an identity $G_{ij}(\bar{z}) = \langle i|\hat{G}(\bar{z})|j\rangle = \langle j|\hat{G}(z)|i\rangle = G_{ji}(z)$ arising from definitions (2.5). The upper line in the ladder diagram

depicts the amplitude A_{ijkli} and the lower line corresponds to its complex conjugate, A_{ijkli}^* . Ladder diagrams thus describe the classical type of contribution that is in agreement with the analysis given in the previous section. The lower line in the maximally crossed diagram

(3.24)

denotes the complex conjugate of the reversed amplitude, A_{ilkji}^* . Therefore, these diagrams correspond to the quantum coherence contributions that are found in equation (3.22). A very similar explanation, using the behavior in k -space, is given in [49, 14]. Another arguments, bringing to light the importance of real-space trajectories with closed loops, were presented by Larkin and Khmel'nitskii in [50, 51]. Their ideas were later reformulated by Chakravarty and Schmid in terms of quasi-classical approximation of the Feynman path integral formalism [52].

Finally, we proceed with the evaluation of the conductivity σ . The contribution from the first two terms in the formula (3.21) is already known — it is the value σ_0 , equation (3.7).⁶ Out of the remaining terms the most significant is the one that involves the Cooper pole. Its contribution to the homogeneous conductivity reads

$$\delta\sigma(\omega) = \delta\sigma_{\alpha\alpha}(\omega) = \frac{e^2}{2\pi} \frac{1}{N^2} \sum'_{\mathbf{k}\mathbf{k}'} v_{\alpha}(\mathbf{k}) v_{\alpha}(\mathbf{k}') G_{\mathbf{k}\mathbf{k}'}^{AR}{}_{\text{Cooper}}(E_F, E_F + \omega; \mathbf{0}) \quad (3.25)$$

where the prime at the sum indicates the restriction of summation to a vicinity of the pole. The magnitude of a suitable cut-off is not particularly important, a natural choice is seen to be the inverse of the *electronic mean free path* l . The length l is defined as the average distance traveled by an electron between individual collisions with scattering centers, recall Figure 1.1.⁷ Inserting the relevant part of the Green function (3.21) into expression (3.25) and making the substitution $\mathbf{k}' = \mathbf{Q} - \mathbf{k}$ we come to an approximate formula

$$\delta\sigma(\omega) \approx \frac{e^2}{2\pi} \frac{1}{N} \sum_{\mathbf{k}} v_{\alpha}(\mathbf{k}) v_{\alpha}(-\mathbf{k}) \lambda_B [G^A(E_F, \mathbf{k}) G^R(E_F, \mathbf{k})]^2 \times \frac{1}{N} \sum'_{\mathbf{Q}} \frac{1}{1 - \lambda_B \chi^{AR}(\mathbf{Q})}. \quad (3.26)$$

Momentum \mathbf{Q} was disregarded (set equal to zero) everywhere except in the denominator that vanishes for $\mathbf{Q} = \mathbf{0}$. The summation over momentum \mathbf{k} is easily performed

⁶In fact, the value σ_0 is given just by the first term in the square brackets in equation (3.21) as the second term does not contribute to the conductivity σ at all.

⁷Note that the introduction of the mean free path l does not bring in any of concepts known from a weak disorder limit. In the present case, l is just an easily calculated number.

proceeding along the following steps,

$$\begin{aligned} & \frac{1}{N} \sum_{\mathbf{k}} v_{\alpha}(\mathbf{k}) v_{\alpha}(-\mathbf{k}) \lambda_B [G^A(E_F, \mathbf{k}) G^R(E_F, \mathbf{k})]^2 \\ &= -\frac{1}{N} \sum_{\mathbf{k}} v_{\alpha}^2(\mathbf{k}) \lambda_B \frac{(\Delta G)^2}{(\Delta \Sigma)^2} = \frac{1}{\Delta \Sigma} \frac{1}{\langle \Delta G \rangle} \frac{1}{N} \sum_{\mathbf{k}} v_{\alpha}^2(\mathbf{k}) (\Delta G)^2 = \frac{2i}{\Delta \Sigma} D_0. \end{aligned} \quad (3.27)$$

In the first equality the product of the two Green functions was rewritten with the aid of the identity introduced earlier (see the paragraph after formula (3.14) where the differences ΔG and $\Delta \Sigma$ are introduced as well). Consequently, the Vollhardt-Wölfle identity in the form $\lambda_B = \Delta \Sigma / \langle \Delta G \rangle$ was utilized. Finally, the conductivity σ_0 was expressed in terms of the diffusion constant D_0 via the Einstein relation (2.51). A simple expression for the trace of the difference of two one-particle Green functions, $\langle \Delta G \rangle = -2\pi i g_F$, was used in the last step of the calculation.

In order to simplify the denominator in equation (3.26) we expand the quantity χ^{AR} in small momentum \mathbf{Q} and small frequency ω ,⁸

$$\chi^{AR}(\mathbf{Q}) = \frac{\langle \Delta G \rangle}{\Delta \Sigma} + \frac{\langle \Delta G \rangle}{(\Delta \Sigma)^2} \omega + 2\pi \frac{g_F D_0}{(\Delta \Sigma)^2} Q^2 + O(\omega^2, Q^4, \omega Q^2). \quad (3.28)$$

Inserting this formula together with the above result (3.27) into expression (3.26) we arrive at the final form of the so-called weak localization correction,

$$\delta\sigma(\omega) \approx -\frac{e^2}{\pi} D_0 \frac{1}{N} \sum'_{\mathbf{Q}} \frac{1}{-i\omega + D_0 Q^2}. \quad (3.29)$$

In two dimensions, for instance, the small frequency asymptotics reads⁹

$$\delta\sigma(\omega) \approx -\frac{e^2}{4\pi^2} \ln \frac{1}{\omega\tau}, \quad (3.30)$$

where τ denotes the scattering time that can be calculated from the mean free path l as $\tau = l^2 / (2D_0)$. We explicitly see that the coherent backscattering lowers the conductivity being thus a precursor of the eventual strong Anderson localization. On the other hand, the result (3.30) can hardly be used for anything else than for recognition of the trends as the whole conductivity $\sigma = \sigma_0 + \delta\sigma$ becomes negative (and thus unphysical) for sufficiently small frequency ω . A more comprehensive approach that removes the just mentioned weakness will be briefly touched in the next section.

Before we turn to that subject we examine formula (3.29) in a general spatial dimension d . In such a case, the full momentum summation is a rather involved task. The non-analytic part of the frequency dependence, being the direct consequence of the Cooper pole, is, however, obtained quite easily and can be written as

$$\delta\sigma_{\text{sing}}(\omega) = -e^2 K_d D_0^{1-d/2} \times \begin{cases} \omega^{d/2-1} & \text{if } d \text{ is odd,} \\ \omega^{d/2-1} \ln \frac{1}{\omega\tau} & \text{if } d \text{ is even.} \end{cases} \quad (3.31)$$

⁸Compare with the analogous expansion (3.14) where the magnitude of $\Delta z = \omega$ is unrestricted.

⁹Our result (3.30) is of a factor 2 smaller than corresponding formulae in the literature, [5, 36]. This discrepancy is due to the fact that we work with spinless fermions.

We introduced the dimensionless d -dependent constant K_d . In one- and two-dimensional cases the conductivity itself diverges, in higher dimensions it is its $(d/2 - 1)$ -th derivative that becomes infinite at the point $\omega = 0$. Note also that besides the displayed singular part (3.31) there always exists a regular one that governs the small frequency asymptotics in dimensions $d > 2$.

3.3 A self-consistent theory of localization in low dimensions

We saw in the last section that the Kubo formula (2.50) is not appropriate for the evaluation of the conductivity when the quantum effects become important. In such situations we are barely able to control positiveness of the result as it is a sum of terms with both negative and positive signs. Moreover, the eventual value $\sigma = 0$, being a consequence of the fully localized electron eigenfunctions, is reached only when all orders of perturbation series are summed up. Much more favorable would be an analogous diagrammatic expansion but for the *inverse* of the conductivity, $1/\sigma$, or for the inverse of the diffusion constant, $1/D$. The absence of diffusion in a system is signaled by a divergence of these quantities and thus only the largest contributions are significant. An approximate formula that allows for the suggested alternative expansion was derived by Vollhardt and Wölfle in [53] and reads

$$\frac{D_0}{D(\omega, \mathbf{q})} = 1 + \frac{\tau}{\pi m^* c} \frac{1}{N^2} \sum_{\mathbf{k}\mathbf{k}'} (\mathbf{k} \cdot \hat{\mathbf{q}}) \Delta G_{\mathbf{k}} [\Lambda_{\mathbf{k}\mathbf{k}'}(E_F, E_F + \omega; \mathbf{q}) - \lambda_B] \Delta G_{\mathbf{k}'}(\mathbf{k}' \cdot \hat{\mathbf{q}}). \quad (3.32)$$

This equation forms one of the key steps towards the Vollhardt-Wölfle theory of Anderson localization, construction of which was presented in [42, 53, 5]. The notation used here is $\Delta G_{\mathbf{k}} = G^R(E_F + \omega, \mathbf{k} + \mathbf{q}) - G^A(E_F, \mathbf{k}')$ for the Green functions difference and $\hat{\mathbf{q}}$ for the unit vector pointing in the direction of momentum \mathbf{q} . Besides these quantities, also the effective electron mass m^* and the impurity concentration c enter the fundamental formula (3.32).

The usage of equation (3.32) is limited to certain special cases as it is not an exact identity. In the course of its derivation the limit to a weak scattering was used and directional dependencies in k -space were simplified as well. To demonstrate the approximation technique more closely we look at one of the steps that lead to formula (3.32),

$$\frac{1}{N} \sum_{\mathbf{k}'} G_{\mathbf{k}\mathbf{k}'}^{AR}(E_F, E_F + \omega; \mathbf{q}) \approx \Delta G_{\mathbf{k}} [f_1(E_F, \omega, q) + f_2(E_F, \omega, q) (\mathbf{k} \cdot \hat{\mathbf{q}})]. \quad (3.33)$$

Here it is assumed that the dependence of the two-particle Green function G^{AR} on the magnitude of the wave vectors is dominated by the peaked structure of the difference $\Delta G_{\mathbf{k}}$. This is the better approximation the weaker the disorder is. The remaining angular dependence in G^{AR} is then reduced only to the first two terms ($l = 0$ and $l = 1$) of a Legendre expansion.

In the Vollhardt-Wölfle theory, the frequency and momentum dependent diffusivity $D(\omega, \mathbf{q})$ is extracted from the diffusion pole in the correlation function Φ^{AR} . We argued at the end of Section 3.1 that such a quantity has not a straightforward physical interpretation, e. g. it is not easily related to the conductivity $\sigma(\omega, \mathbf{q})$. Nevertheless, it

certainly carries some information about a diffusive transport in a system under investigation.

In the preceding section it was shown that in one and two dimensions the backscattering processes dominate over the quasi-classical terms in the conductivity formula as the static limit is approached. Therefore, the sum of maximally crossed diagrams is a reasonable candidate for inclusion into the two-particle irreducible vertex Λ on the right-hand side of formula (3.32). Doing so we come to the following representation of the homogeneous diffusivity,

$$\frac{D_0}{D(\omega)} = 1 + \frac{1}{\pi g_F} \frac{1}{N} \sum_{\mathbf{Q}} \frac{1}{-i\omega + D_0 Q^2}. \quad (3.34)$$

For not too small frequencies, i. e. $\omega\tau \gtrsim 1$, the ratio $D_0/D(\omega)$ is close to one and the weak localization correction (3.29) is recovered. In the limit $\omega \rightarrow 0$ the right-hand side of equation (3.34) diverges implying that in two dimensions the diffusivity $D(\omega)$ goes to zero as $-1/\ln(\omega\tau)$. This conclusion is, however, unreliable because it exceeds the validity range of the perturbation expansion it is based on.

A suitable extension of the perturbation theory is the approach of self-consistency. To proceed in this way we have to find a functional equation of the form

$$D(\omega) = \mathcal{F}[D(\omega)] \quad (3.35)$$

so that it is compatible with the weak disorder limit, which is accessible by the perturbation expansion. The equation that has the required properties was shown to be

$$\frac{D_0}{D(\omega)} = 1 + \frac{1}{\pi g_F} \frac{1}{N} \sum_{\mathbf{Q}} \frac{1}{-i\omega + D(\omega)Q^2}. \quad (3.36)$$

The transformation of formula (3.34) to equation (3.36) based on diagrammatic arguments is presented in Reference 5.

In low spatial dimensions, $d \leq 2$, the diffusivity $D(\omega)$ has to behave so that $D(0) = 0$, otherwise the pole in formula (3.36) is not integrable. The small frequency asymptotics that is found from equation (3.36) in these dimensions reads $D(\omega) = -i\omega\xi^2$. Such a result corresponds to the diffusion pole in the electron-hole correlation function of the form

$$\Phi^{AR}(E, E + \omega; \mathbf{q}) = \frac{1}{-i\omega} \frac{2\pi g_F}{1 + (\xi q)^2}, \quad (3.37)$$

which can be identified with a regime where all electron eigenstates are localized, ξ being their localization length, see [42, 53]. This considerably differs from predictions of the simple perturbation theory (weak localization). It confirms the conjecture that there are no extended states in two dimensions no matter how weak the disorder is. The same applies to the one-dimensional case. This result is in agreement with conclusions drawn from the scaling approach to disordered systems, [4].

Chapter summary

The main goal of this chapter was to analyze certain, particularly simple, classes of two-particle diagrams from the viewpoint of their contributions to electrical conductivity. It was shown that ladder diagrams such as (3.2) correspond to the classical value of conductivity (Drude formula). Later on, the coherent backscattering was introduced. It is a process that originates in quantum interference of electrons traveling in forward and backward directions along closed loop trajectories. Using simple arguments, this purely quantum effect was demonstrated to slow down the electron motion in random media. In the diagrammatic language, the coherent backscattering was identified with the so-called maximally crossed diagrams, an example of which is (3.20). The explicit calculation taking into account this class of diagrams leads to a negative correction to the Drude conductivity. In low dimensions, $d \leq 2$, the effects of quantum coherence are so strong that they cause a breakdown of the perturbation expansion of the conductivity in powers of disorder strength. In these dimensions the conductivity correction due to the coherent backscattering diverges to $-\infty$ in the static limit.

To achieve physically meaningful results one has to resort to non-perturbative treatments, such as the self-consistent theory of Vollhardt and Wölfle is (Section 3.3). Their approach predicts vanishing of the zero-temperature conductivity in dimensions $d = 1$ and $d = 2$ for arbitrarily weak disorder, which is in agreement with scaling theories of electronic transport in disordered solids. In three and more dimensions the properties of disordered materials are substantially different. To reach a non-diffusive transport regime a certain minimal disorder strength is needed to be exceeded. Below this critical value the usual diffusion process takes place. The Vollhardt-Wölfle theory, defined by equation (3.36), follows this widely accepted picture (see Reference 54), but there are several drawbacks as well. Formula (3.32) that allowed the subsequent progress in building-up the theory is limited to the weak scattering limit. We thus cannot safely go up to large disorder strengths that are necessary for diffusion to be absent. This leaves understanding of Anderson localization above two dimensions as an open problem that we are going to address our way in subsequent chapters.

4

Parquet construction of vertex functions

The material presented in preceding chapters was either introductory, specifying the physical questions we are asking (Chapter 2), or summarizing, partly, the state of the art in the description of disordered electronic systems with averaged Green functions (Chapter 3). In the rest of the thesis we present our own concepts that allow us to describe and understand how quantum coherence effects influence the electron diffusion in these systems. We start with a closer examination of two-particle irreducibility that helps systematically classify two-particle diagrams. Consequently, self-consistent equations for two-particle vertex functions are constructed using the so-called parquet scheme. These nonlinear integral equations reduce to just a single equation when time-reversal invariant systems are considered. Finally, in Chapter 5, a mean field solution for two-particle vertices is found with the aid of a limit to high spatial dimensions.

The parquet scheme for summation of two-particle diagrams was developed in the particle physics [55, 56] and later utilized in the theory of quantum liquids [57] and in the description of strongly correlated electron systems [58]. The construction presented in this chapter builds on and further extends a recent paper, Reference 59, where the parquet approach is applied to the problem of disordered non-interacting electrons.

4.1 Two-particle irreducibility revisited

The notion of two-particle irreducibility, allowing for classification of diagrams that involve a correlated propagation of two electrons, was introduced already in Section 2.2 where the Bethe-Salpeter equation was formulated. The definition used there was quite naive but adequate for constructions made so far. However, to be able to proceed further in a systematic way, it is essential to examine two-particle functions more carefully.

A diagram that has been up to now referred to as a two-particle reducible one has

a general form

$$(4.1)$$

Such a graph can be divided into two pieces by cutting two fermion lines, $G_{k'i'}$ and $G_{j'l'}$. These lines point in opposite directions, which is the origin of the label *electron-hole* reducibility. The diagrams that cannot be decomposed into the form (4.1) are called *electron-hole irreducible*. As already anticipated in Section 2.2, there exist diagrams that are *electron-hole irreducible* but still divisible into two parts with only two cuts. Such graphs can generically be drawn as

$$(4.2)$$

The lines to be cut for their decomposition have the same direction after which the reducibility (4.2) is given the attribute *electron-electron*.

Based on the observations just made we have two options how to write down the Bethe-Salpeter equation. We have already become familiar with the one of them,

$$(4.3a)$$

$$\Gamma_{\mathbf{k}\mathbf{k}'}(z_1, z_2; \mathbf{q}) = \Lambda_{\mathbf{k}\mathbf{k}'}^{eh}(z_1, z_2; \mathbf{q}) + \frac{1}{N} \sum_{\mathbf{k}''} \Lambda_{\mathbf{k}\mathbf{k}''}^{eh}(z_1, z_2; \mathbf{q}) \times G(z_1, \mathbf{k}'' + \mathbf{q})G(z_2, \mathbf{k}'')\Gamma_{\mathbf{k}''\mathbf{k}'}(z_1, z_2; \mathbf{q}), \quad (4.3b)$$

which we have used since Section 2.2. In this way, reducible diagrams are generated as ladders in the *electron-hole* scattering channel. The two-particle vertex function Γ , which we use instead of the full two-particle Green function $G^{(2)}$ to formulate the Bethe-Salpeter equation, is just the function $G^{(2)}$ with uncorrelated electron motion subtracted,

$$\Gamma_{\mathbf{k}\mathbf{k}'}(z_1, z_2; \mathbf{q}) = G^{-1}(z_1, \mathbf{k} + \mathbf{q})G^{-1}(z_2, \mathbf{k}) \times \left[G_{\mathbf{k}\mathbf{k}'}^{(2)}(z_1, z_2; \mathbf{q}) - N\delta_{\mathbf{k},\mathbf{k}'}G(z_1, \mathbf{k} + \mathbf{q})G(z_2, \mathbf{k}) \right] \times G^{-1}(z_1, \mathbf{k}' + \mathbf{q})G^{-1}(z_2, \mathbf{k}'). \quad (4.4)$$

The second possibility to construct the vertex function Γ is to consider ladders from the electron-electron scattering channel. Such a procedure corresponds to a Bethe-Salpeter equation written in the form

$$\Gamma_{\mathbf{k}\mathbf{k}'}(z_1, z_2; \mathbf{q}) = \Lambda_{\mathbf{k}\mathbf{k}'}^{ee}(z_1, z_2; \mathbf{q}) + \int \frac{d^d k''}{N} \Lambda_{-\mathbf{k}'', \mathbf{k}'}^{ee}(z_1, z_2; \mathbf{q} + \mathbf{k} + \mathbf{k}'') \times G(z_1, \mathbf{k} + \mathbf{k}' + \mathbf{k}'' + \mathbf{q}) G(z_2, \mathbf{k}'') \Gamma_{\mathbf{k}, -\mathbf{k}''}(z_1, z_2; \mathbf{q} + \mathbf{k}' + \mathbf{k}''). \quad (4.5a)$$

$$\Gamma_{\mathbf{k}\mathbf{k}'}(z_1, z_2; \mathbf{q}) = \Lambda_{\mathbf{k}\mathbf{k}'}^{ee}(z_1, z_2; \mathbf{q}) + \frac{1}{N} \sum_{\mathbf{k}''} \Lambda_{-\mathbf{k}'', \mathbf{k}'}^{ee}(z_1, z_2; \mathbf{q} + \mathbf{k} + \mathbf{k}'') \times G(z_1, \mathbf{k} + \mathbf{k}' + \mathbf{k}'' + \mathbf{q}) G(z_2, \mathbf{k}'') \Gamma_{\mathbf{k}, -\mathbf{k}''}(z_1, z_2; \mathbf{q} + \mathbf{k}' + \mathbf{k}''). \quad (4.5b)$$

In equations (4.3) and (4.5) we introduced the two-particle irreducible vertices Λ^{eh} and Λ^{ee} that correspond to the sets of electron-hole and electron-electron irreducible diagrams, respectively.

Besides the two scattering channels discussed above there exists also a third one, the so-called *vertical* channel. We do not mention it here in any detail because the two nonequivalent Bethe-Salpeter equations, (4.3) and (4.5), are already sufficient for the construction of the parquet equation given in the next paragraph. Moreover, the vertical channel does not contain the diffusion pole, and hence it is not interesting for us. An approach that explicitly utilizes all the three channels is presented in [59].

4.2 Parquet equation

At the end of Chapter 3 we argued that a calculational method, self-consistent at the two-particle level, is needed in order to reach the strong-disorder limit. It means that we have to find self-consistent equations for the irreducible vertices Λ^{eh} and Λ^{ee} . Such equations represent a tool to sum infinite subsets of two-particle irreducible diagrams that build up these vertices. The desired set of equations is provided by means of the so-called parquet scheme that completes the Bethe-Salpeter equations (4.3) and (4.5) with a third relation involving vertices Λ^{eh} , Λ^{ee} and Γ .

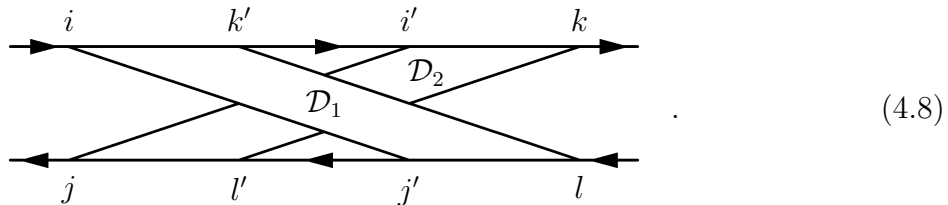
To find the parquet equation we proceed with a further inspection of two-particle diagrams. We define the completely irreducible two-particle vertex I that comprehends diagrams irreducible in both scattering channels, $I = \Lambda^{eh} \cap \Lambda^{ee}$. Any Λ^{eh} contribution that is not completely irreducible can be found among ee -reducible diagrams,

$$\Lambda^{eh} - I \subset \Gamma - \Lambda^{ee}. \quad (4.6)$$

If also inverse relation held, i. e., if every electron-electron reducible contribution belonged to the vertex Λ^{eh} ,

$$\Gamma - \Lambda^{ee} \subset \Lambda^{eh}, \quad (4.7)$$

then the equality sign could be used in relation (4.6) and the complete set of equations for quantities Λ^{eh} , Λ^{ee} and Γ would be found. Assertion (4.7) is indeed true as can be easily demonstrated if a general ee -reducible diagram (4.2) is drawn in a slightly distorted form,



Clearly, no such diagram can result from the electron-hole multiplication in the Bethe-Salpeter equation (4.3). In other words, every diagram of the generic form (4.8) is eh -irreducible. We can thus write down the so-called parquet equation¹

$$\Gamma_{\mathbf{k}\mathbf{k}'}(z_1, z_2; \mathbf{q}) = \Lambda_{\mathbf{k}\mathbf{k}'}^{eh}(z_1, z_2; \mathbf{q}) + \Lambda_{\mathbf{k}\mathbf{k}'}^{ee}(z_1, z_2; \mathbf{q}) - I_{\mathbf{k}\mathbf{k}'}(z_1, z_2; \mathbf{q}), \quad (4.9)$$

which says that *a diagram reducible in one scattering channel is irreducible in the other*. Equation (4.9) is used to eliminate the full vertex Γ from the Bethe-Salpeter equations (4.3) and (4.5) leaving two coupled integral equations for the irreducible vertices Λ^{eh} and Λ^{ee} . The input of the scheme is the completely irreducible vertex I that serves as a basic building block for the other two-particle functions.

In the next chapter we solve the parquet scheme with the aid of the asymptotic limit to high spatial dimensions, $d \rightarrow \infty$. In this limit, the behavior of local and non-local elements of the one-particle Green function G substantially differs. The local part, G_{ii} , remains finite for $d = \infty$, whereas the non-local part, G_{ij} with $i \neq j$, scales as $d^{-1/2}$. To take advantage of this diversity it is convenient to reformulate the Bethe-Salpeter equations (4.3) and (4.5) so that the differently behaved Green function elements become naturally separated. An appropriate form providing such separation reads

$$\Gamma_{\mathbf{k}\mathbf{k}'}(z_1, z_2; \mathbf{q}) = \bar{\Lambda}_{\mathbf{k}\mathbf{k}'}^{eh}(z_1, z_2; \mathbf{q}) + \frac{1}{N} \sum_{\mathbf{k}''} \bar{\Lambda}_{\mathbf{k}\mathbf{k}''}^{eh}(z_1, z_2; \mathbf{q}) \times \bar{G}(z_1, \mathbf{k}'' + \mathbf{q}) \bar{G}(z_2, \mathbf{k}'') \Gamma_{\mathbf{k}''\mathbf{k}'}(z_1, z_2; \mathbf{q}), \quad (4.10a)$$

$$\Gamma_{\mathbf{k}\mathbf{k}'}(z_1, z_2; \mathbf{q}) = \bar{\Lambda}_{\mathbf{k}\mathbf{k}'}^{ee}(z_1, z_2; \mathbf{q}) + \frac{1}{N} \sum_{\mathbf{k}''} \bar{\Lambda}_{-\mathbf{k}'', \mathbf{k}'}^{ee}(z_1, z_2; \mathbf{q} + \mathbf{k} + \mathbf{k}'') \times \bar{G}(z_1, \mathbf{k} + \mathbf{k}' + \mathbf{k}'' + \mathbf{q}) \bar{G}(z_2, \mathbf{k}'') \Gamma_{\mathbf{k}, -\mathbf{k}''}(z_1, z_2; \mathbf{q} + \mathbf{k}' + \mathbf{k}''), \quad (4.10b)$$

where the Green function \bar{G} represents the off-diagonal part of the full one-particle resolvent G , i. e. $\bar{G}_{ij}(z) = G_{ij}(z) - \delta_{ij}G_{ii}(z)$ in the direct space and $\bar{G}(z, \mathbf{k}) = G(z, \mathbf{k}) - G(z)$ in the momentum space.² The newly introduced two-particle irreducible vertices $\bar{\Lambda}^{eh}$ and $\bar{\Lambda}^{ee}$ fulfill the parquet equation

$$\Gamma_{\mathbf{k}\mathbf{k}'}(z_1, z_2; \mathbf{q}) = \bar{\Lambda}_{\mathbf{k}\mathbf{k}'}^{eh}(z_1, z_2; \mathbf{q}) + \bar{\Lambda}_{\mathbf{k}\mathbf{k}'}^{ee}(z_1, z_2; \mathbf{q}) - \bar{I}_{\mathbf{k}\mathbf{k}'}(z_1, z_2; \mathbf{q}) \quad (4.11)$$

¹The name describes the two-dimensional, area-covering character of the two-particle diagrams iteratively generated from equations (4.3), (4.5) and (4.9), if they are drawn in a certain specific way.

²Recall the expression for the local element $G(z) = N^{-1} \sum_{\mathbf{k}} G(z, \mathbf{k})$ that was used already on pages 23 and 32.

with $\bar{I} = \bar{\Lambda}^{eh} \cap \bar{\Lambda}^{ee}$. Note that the full vertex Γ cannot depend on the way how we calculate it. The concept of two-particle irreducibility now applies only to the off-diagonal elements \bar{G} . Therefore, the completely irreducible vertex \bar{I} contains *all purely local diagrams*. That is, it comprehends all diagrams of the functional form $\mathcal{D}[G_{ii}]$ regardless whether they are irreducible or reducible with respect to the original Bethe-Salpeter equations (4.3) and (4.5).

The new scheme given by formulae (4.10) and (4.11) is somewhat poorer than the approach utilizing the full Green function G , since the local two-particle contributions have to be evaluated outside the parquet scheme and then put by hand into the completely irreducible vertex \bar{I} . However, this deficiency represents only a minor problem as we already know the sum of all purely local diagrams — it is the coherent potential approximation. This conclusion follows directly from the fact that the CPA selfenergy is an exact solution for the infinite-dimensional lattice where only the local elements of the one-particle Green function G survive.

The evaluation of the purely local terms within the parquet approach is not straightforward anyway. The reason is that topological nonequivalence of the scattering channels (4.3) and (4.5) disappears when dealing with these local contributions. If two diagrams of the form $\mathcal{D}[G_{ii}]$, both involving the same site index i , are connected with two fermion lines, the same contribution is obtained regardless the scattering channel used,

$$(4.12)$$

Both sides of this equation represent the expression $\mathcal{D}_1[G_{ii}]G_{ii}G_{ii}\mathcal{D}_2[G_{ii}]$.

4.3 Time-reversal invariance

In the case of a system invariant with respect to time-reversal³ the set of equations formulated in the preceding paragraph reduces to a single equation. The time reversal invariance implies that the electron states with wave vectors \mathbf{k} and $-\mathbf{k}$ are equivalent. The consequent symmetry of the one-particle Green function, $G(z, \mathbf{k}) = G(z, -\mathbf{k})$, is easily transferred to the following identity between elements of the full two-particle vertex Γ ,

$$\Gamma_{-\mathbf{k}', -\mathbf{k}}(z_1, z_2; \mathbf{q} + \mathbf{k} + \mathbf{k}') = \Gamma_{\mathbf{k}, \mathbf{k}'}(z_1, z_2; \mathbf{q}). \quad (4.13)$$

³This restriction rules out the presence of the magnetic field or magnetic impurities. Nevertheless, it does not limit us as we do not aim to address such situations.

This equality is easily proven using diagrammatic arguments as shown bellow.

$$\begin{aligned}
 & \begin{array}{c} k+q \\ \swarrow \quad \searrow \\ \Gamma \\ \swarrow \quad \searrow \\ k \quad k' \end{array} = \begin{array}{c} \swarrow \quad \searrow \\ \searrow \quad \swarrow \\ \swarrow \quad \searrow \\ k' \quad k \end{array} \\
 & = \begin{array}{c} \swarrow \quad \searrow \\ \Gamma \\ \swarrow \quad \searrow \\ k' \quad k \end{array} = \begin{array}{c} k+q \quad k'+q \\ \swarrow \quad \searrow \\ \Gamma \\ \swarrow \quad \searrow \\ -k \quad -k' \end{array} \quad (4.14)
 \end{aligned}$$

The first transformation is twisting of the lower part of every diagram contributing to Γ , the second equality utilizes the fact that the full vertex Γ contains *all* diagrams so that the preceding twisting does not actually change anything, only reverses the direction of the lower line. Finally, the last step uses the identity $G(z, \mathbf{k}) = G(z, -\mathbf{k})$ to reverse the lower line once more.

For a better understanding the above sequence of diagrammatic transformations, expression (4.14), we repeat the steps once again for an explicitly drawn subset of low order diagrams.

$$\begin{aligned}
 & \begin{array}{c} \swarrow \quad \searrow \\ \swarrow \quad \searrow \\ k \quad k' \end{array} + \begin{array}{c} \swarrow \quad \searrow \\ \swarrow \quad \searrow \\ k \quad k' \end{array} \\
 & = \begin{array}{c} \swarrow \quad \searrow \\ \swarrow \quad \searrow \\ k' \quad k \end{array} + \begin{array}{c} \swarrow \quad \searrow \\ \swarrow \quad \searrow \\ k' \quad k \end{array} \\
 & = \begin{array}{c} \swarrow \quad \searrow \\ \swarrow \quad \searrow \\ -k' \quad -k \end{array} + \begin{array}{c} \swarrow \quad \searrow \\ \swarrow \quad \searrow \\ -k' \quad -k \end{array} \quad (4.15)
 \end{aligned}$$

Here we clearly see how the twisting of the lower line leads only to the change in its direction. Besides that, equation (4.15) indicates that the time-reversal transformation \mathcal{T} ,

$$(\mathcal{T}F)_{\mathbf{k}, \mathbf{k}'}(z_1, z_2; \mathbf{q}) = F_{-\mathbf{k}', -\mathbf{k}}(z_1, z_2; \mathbf{q} + \mathbf{k} + \mathbf{k}'), \quad (4.16)$$

converts electron-hole irreducible diagrams into electron-electron irreducible ones and vice versa,

$$\bar{\Lambda}_{-\mathbf{k}', -\mathbf{k}}^{eh}(z_1, z_2; \mathbf{q} + \mathbf{k} + \mathbf{k}') = \bar{\Lambda}_{\mathbf{k}, \mathbf{k}'}^{ee}(z_1, z_2; \mathbf{q}), \quad (4.17a)$$

$$\bar{\Lambda}_{-\mathbf{k}', -\mathbf{k}}^{ee}(z_1, z_2; \mathbf{q} + \mathbf{k} + \mathbf{k}') = \bar{\Lambda}_{\mathbf{k}, \mathbf{k}'}^{eh}(z_1, z_2; \mathbf{q}). \quad (4.17b)$$

In the following we show that these formulae are generally valid as far as equation (4.13) holds. Moreover, we will see that at the same time the Bethe-Salpeter equations (4.10)

map onto each other under transformation (4.16). Applying the operation \mathcal{T} on both sides of the Bethe-Salpeter equation in the electron-hole channel, formula (4.10a), and using invariance (4.13) in the resulting equation we come to a representation

$$\begin{aligned} \Gamma_{\mathbf{k},\mathbf{k}'}(z_1, z_2; \mathbf{q}) &= \bar{\Lambda}_{-\mathbf{k}',-\mathbf{k}}^{eh}(z_1, z_2; \mathbf{q} + \mathbf{k} + \mathbf{k}') + \frac{1}{N} \sum_{\mathbf{k}''} \bar{\Lambda}_{-\mathbf{k}',\mathbf{k}''}^{eh}(z_1, z_2; \mathbf{q} + \mathbf{k} + \mathbf{k}') \\ &\quad \times \bar{G}(z_1, \mathbf{k} + \mathbf{k}' + \mathbf{k}'' + \mathbf{q}) \bar{G}(z_2, \mathbf{k}'') \Gamma_{\mathbf{k},-\mathbf{k}''}(z_1, z_2; \mathbf{q} + \mathbf{k}' + \mathbf{k}''). \end{aligned} \quad (4.18)$$

If we now identify the electron-electron irreducible vertex $\bar{\Lambda}^{ee}$ according to formula (4.17a) we obtain exactly the Bethe-Salpeter equation in the electron-electron channel (4.10b) that completes the proof of equivalence of the two scattering channels in the case of a time-reversal invariant system.

Chapter summary

The analysis of two-particle diagrams given in the present chapter can be used to formulate a single non-linear integral equation for one of the two-particle irreducible vertices. Let us choose the vertex $\bar{\Lambda}^{ee}$. The required equation is obtained from the Bethe-Salpeter equation (4.10a) by successive elimination of the vertices Γ and $\bar{\Lambda}^{eh}$ with the aid of relations (4.11) and (4.17). The resulting formula reads

$$\begin{aligned} \bar{\Lambda}_{\mathbf{k}\mathbf{k}'}^{ee}(z_1, z_2; \mathbf{q}) &= \bar{I}_{\mathbf{k}\mathbf{k}'}(z_1, z_2; \mathbf{q}) \\ &+ \frac{1}{N} \sum_{\mathbf{k}''} \bar{\Lambda}_{-\mathbf{k}'', -\mathbf{k}}^{ee}(z_1, z_2; \mathbf{q} + \mathbf{k} + \mathbf{k}'') \bar{G}(z_1, \mathbf{k}'' + \mathbf{q}) \bar{G}(z_2, \mathbf{k}'') \\ &\times [\bar{\Lambda}_{-\mathbf{k}', -\mathbf{k}''}^{ee}(z_1, z_2; \mathbf{q} + \mathbf{k}' + \mathbf{k}'') + \bar{\Lambda}_{\mathbf{k}'', \mathbf{k}'}^{ee}(z_1, z_2; \mathbf{q}) - \bar{I}_{\mathbf{k}'', \mathbf{k}'}(z_1, z_2; \mathbf{q})]. \end{aligned} \quad (4.19)$$

This equation represents a powerful tool when acting as an approximation scheme, the input of which is the completely irreducible vertex \bar{I} . Even if we choose only the Born diagram λ_B , expression (3.1a), to contribute to the vertex \bar{I} , we arrive at an approximation that is considerably richer than the one examined in Section 3.2 (coherent backscattering). To be precise, the correct approximation for the vertex \bar{I} should read

$$\bar{I}(z_1, z_2) = \gamma_B(z_1, z_2) = \frac{\lambda_B}{1 - \lambda_B G(z_1)G(z_2)} \quad (4.20)$$

instead of just $\bar{I} = \lambda_B$, because *all* local diagrams were qualified to be completely irreducible (recall Section 4.1).

The above statements about capacity of approximations based on equation (4.19) remain formal unless we are able to actually solve this equation for a chosen vertex \bar{I} . Unfortunately, equation (4.19) is too complicated to be solved exactly and we have to resort to approximate treatments. The simplest conceivable approach is to force all the irreducible vertices (\bar{I} , $\bar{\Lambda}^{ee}$ and $\bar{\Lambda}^{eh}$) to be independent on momenta. Although this is a rather crude approximation it allows for some level of introspection into what the parquet scheme offers. Such a local technique we proposed in Reference 60. We do not discuss those results here, as we preferably turn to a significantly more sophisticated and consistent approach of approximating the fundamental equation (4.19). The method we have in mind is the limit to high spatial dimensions introduced in the following chapter.

5

High spatial dimensions and mean-field solution

The investigation of the limit to high spatial dimensions, $d \rightarrow \infty$, is motivated by its close connection to mean-field approximations. For example, the Weiss solution of the Ising model of ferromagnets becomes exact when the dimensionality of the lattice, or, equivalently, the number of nearest neighbors of a given lattice site, approaches infinity, [61]. Therefore, the limit to infinite spatial dimensions is a feasible tool for a reasonable reduction of the problem complexity.

Quantum fermionic systems were first studied with this technique by Metzner and Vollhardt, [62]. They showed that although the correlated electron problem is substantially simpler in the limit $d = \infty$ than in finite dimensions, it remains nontrivial as not all correlations among electrons are suppressed in this limit. These findings played a substantial role in the development of the so-called Dynamical Mean-Field Theory (DMFT, [63]) that became a successful framework for ab-initio calculations, [64].

In our case of equation (4.19), the limit to high spatial dimensions helps simplify the momentum convolutions occurring there to a tractable form. The strategy implemented in this chapter is such that we solve the parquet equation (4.19) first in the strict limit $d = \infty$ and then include terms of the order d^{-1} in a *non-perturbative* way. Finally, the obtained solution is transferred from the asymptotics $d \rightarrow \infty$ to physical dimensions where it serves as a mean-field theory and where it can be used as an advanced calculational scheme. Once the theory is formulated, its properties and predictions are examined. Namely, it is found that the diffusive transport regime goes over to a non-diffusive one when a certain critical disorder strength is exceeded, i. e., the proposed mean-field theory displays the Anderson metal-insulator transition. The findings are demonstrated on a few model calculations.

5.1 Solution in infinite spatial dimensions

In the course of approaching the limit $d = \infty$ a proper scaling of the hopping $t \sim 1/\sqrt{d}$ is crucial to keep the dynamic balance between kinetic and potential energy, [62]. The original Hamiltonian (1.4) has to be substituted with

$$\hat{H}_d = \frac{t}{\sqrt{d}} \sum_{\langle ij \rangle} \hat{c}_i^\dagger \hat{c}_j + \sum_i V_i \hat{c}_i^\dagger \hat{c}_i, \quad (5.1)$$

which provides a finite density of states and the total energy proportional to the volume in the limit $d = \infty$. Appendix C describes methods how to calculate Green functions and their momentum convolutions in high spatial dimensions. It is shown that, in the case of a hypercubic lattice with the lattice constant $a = 1$, the non-local part of the one-particle Green function can be written in a form

$$\bar{G}(z, \mathbf{k}) \doteq t \langle G^2(z) \rangle \frac{1}{\sqrt{d}} \sum_{\nu=1}^d \cos k_{\nu} = t \langle G^2(z) \rangle x(\mathbf{k}), \quad (5.2)$$

where

$$\langle G^2(z) \rangle = \frac{1}{N} \sum_{\mathbf{k}} \frac{1}{[z - \Sigma(z) - \epsilon(\mathbf{k})]^2}. \quad (5.3)$$

The effective value (5.2) is justified as far as we are interested only in the leading order of both the d^{-1} expansion and the expansion in momentum dependence (consult Appendix C for the exact content of this statement). The selfenergy standing in formula (5.3) is the CPA value, i. e. the exact selfenergy for the infinite-dimensional disordered lattice, [44]. Analogously, the completely two-particle irreducible function \bar{I} is local in the limit $d = \infty$, see Reference 65 and Appendix B. Therefore, also the vertex \bar{I} equals its CPA value,

$$\bar{I}(z_1, z_2) = \gamma(z_1, z_2) = \frac{\lambda(z_1, z_2)}{1 - \lambda(z_1, z_2) G(z_1) G(z_2)}, \quad (5.4)$$

in this limit.

At this point we turn to a classification of (reducible) two-particle diagrams with respect to their dependence on the dimensionality d . Ladders in both electron-hole and electron-electron scattering channels are built up of only powers of the vertex γ and powers of convolutions of two off-diagonal one-particle Green functions (5.2),

$$\bar{\chi}(z_1, z_2; \mathbf{q}) = \frac{1}{N} \sum_{\mathbf{k}} \bar{G}(z_1, \mathbf{k} + \mathbf{q}) \bar{G}(z_2, \mathbf{k}) = \frac{1}{2} t^2 \langle G(z_1)^2 \rangle \langle G(z_2)^2 \rangle X(\mathbf{q}). \quad (5.5)$$

The ‘‘bubble’’ $\bar{\chi}$ is proportional to $X(\mathbf{q}) = d^{-1} \sum_{\nu=1}^d \cos k_{\nu} = d^{-1/2} x(\mathbf{q})$, which remains nonzero in the limit $d = \infty$ for specific points in momentum space such as $\mathbf{q} = \mathbf{0}$ or $\mathbf{q} = (\pi, \dots, \pi)$.¹ Therefore, the ladders survive in the high-dimensional asymptotics.

What happens if the scattering channels are crossed, i. e. if a two-particle diagram contains both *eh*- and *ee*-multiplications? Generally, every channel crossing generates a factor d^{-1} that causes such contributions to vanish in $d = \infty$. It makes the ladders to be the only diagrams contributing in infinite spatial dimensions. To demonstrate the claimed property we analyze the momentum dependence of a particular diagram, say

¹We distinguish the fermionic, x , and bosonic, X , functions despite its close relationship $X = d^{-1/2} x$. This notation helps keep the subsequent formulae easily readable.

in which two eh -ladders are connected via a single ee -multiplication. Apart from an energy dependent factor, diagram (5.6) represents the algebraic expression

$$\begin{aligned} \frac{1}{N} \sum_{\mathbf{k}''} X(\mathbf{k} + \mathbf{k}'' + \mathbf{q}) x(\mathbf{k} + \mathbf{k}' + \mathbf{k}'' + \mathbf{q}) x(\mathbf{k}'') X(\mathbf{k}' + \mathbf{k}'' + \mathbf{q}) \\ \doteq \frac{1}{4d} [X(\mathbf{k}') X(\mathbf{k}' + \mathbf{q}) + X(\mathbf{k}) X(\mathbf{k} + \mathbf{q}) + X(\mathbf{k} - \mathbf{k}') X(\mathbf{k} + \mathbf{k}' + \mathbf{q})] \end{aligned} \quad (5.7)$$

asymptotics of which behaves as $\sim d^{-1}$ for any momenta. For the method used to evaluate the momentum sum compare to formula (C.12) at the end of Appendix C.

Based on the above reasoning we can conclude that the full two-particle vertex Γ in $d = \infty$ reads²

$$\begin{aligned} \Gamma_{\mathbf{k}\mathbf{k}'}(\mathbf{q}) &= \frac{\gamma}{1 - \gamma \bar{\chi}(\mathbf{q})} + \frac{\gamma}{1 - \gamma \bar{\chi}(\mathbf{k} + \mathbf{k}' + \mathbf{q})} - \gamma \\ &= \frac{\lambda}{1 - \lambda \chi(\mathbf{q})} + \frac{\lambda}{1 - \lambda \chi(\mathbf{k} + \mathbf{k}' + \mathbf{q})} - \gamma, \end{aligned} \quad (5.8)$$

where the energy variables z_1 and z_2 were dropped for the sake of simplicity. Vertex (5.8) almost matches the Green function (3.21), the only difference is the subtraction of the local irreducible vertex λ in expression (3.21) instead of the full local vertex γ here. This discrepancy is due to double inclusion of local contributions in the former case. This mistake could have been easily overlooked in Chapter 3, where just the simplest diagrammatic methods were utilized. By contrast, the present systematic approach, which relies on the limit $d \rightarrow \infty$, leads us to the correct result quite naturally.

The two-particle vertex (5.8), unlike the CPA one (Section 3.1), complies with the time-reversal invariance of the studied system, i. e., it is electron-hole symmetric. On the other hand, as already pointed out in Section 3.2, it is not compatible with Ward identities, which substantially influences the physical interpretation of achieved quantities. The topic is thoroughly discussed in Chapter 6.

5.2 Self-consistent solution in the asymptotics $d \rightarrow \infty$

In the preceding paragraph we reached more or less the same results as those already obtained in Section 3.2. It was shown there that a two-particle resolvent of the form (5.8) describes the weak localization phenomena. This fact could seem disappointing if compared with the large number of formal steps that were performed up to this point. We first had to develop the parquet scheme in Chapter 4 and the high-dimensional calculus in Appendix C. However, it definitely was not a waste of time as we now have at hand a *systematic* means how to improve the above approximation, equation (5.8). The procedure we refer to is adding further orders from the d^{-1} expansion to the leading order term (5.8).

The simplest way how to proceed is adding series of diagrams with one, two and more channel crossings. This is the routine how to generate contributions of consecutive orders

²Note that vertex (5.8) does not represent the complete $d = \infty$ solution as we did not include the vertical scattering channel, which is not significant for our purposes. The full solution is derived in Reference 59.

in the small parameter d^{-1} , because every channel crossing costs just one factor d^{-1} as we previously argued. Nevertheless, such an approach has one substantial weakness — it is perturbative, so that it cannot provide any dramatic change of physical properties in comparison to the $d = \infty$ limit. As we are, at least in part, interested in the Anderson localization transition, we need to adopt an alternative scheme. Motivated by the findings of the preceding section we try an electron-hole symmetric ansatz for the irreducible vertices of the form

$$\bar{\Lambda}_{\mathbf{k}\mathbf{k}'}^{eh}(\mathbf{q}) = \sum_{n=0}^{\infty} \Lambda_n \bar{\chi}^n(\mathbf{q} + \mathbf{k} + \mathbf{k}') \quad \text{and} \quad \bar{\Lambda}_{\mathbf{k}\mathbf{k}'}^{ee}(\mathbf{q}) = \sum_{n=0}^{\infty} \Lambda_n \bar{\chi}^n(\mathbf{q}), \quad (5.9)$$

i. e., we enforce the same functions of momenta as those found in the strict $d = \infty$ limit, but allow for a self-consistent adjustment of their amplitudes Λ_n . From a perturbative point of view we may write $\Lambda_n = \gamma^n + o(d^{-1})$, but this is not what we want. In the following it will be demonstrated that ansatz (5.9) provides a self-consistent solution that has qualitatively different properties than those of a perturbative solution.

All the dependence on momenta enters both vertices (5.9) and the parquet equation (4.19) only through the basic one- and two-particle functions — the off-diagonal part of the one-particle Green function $\bar{G} \sim x$, equation (5.2), and the two-particle “bubble” $\bar{\chi} \sim X$, formula (5.5). Their elementary momentum convolutions in the high-dimensional limit read

$$\overline{\bar{G}_1(\mathbf{q}_1)\bar{G}_2(\mathbf{q}_2)} = \bar{\chi}_{12}(\mathbf{q}_1 - \mathbf{q}_2), \quad (5.10a)$$

$$\overline{\bar{G}_1(\mathbf{q}_1)\bar{\chi}_{23}(\mathbf{q}_2)} \doteq \frac{W_{23}}{4d} \bar{G}_1(\mathbf{q}_1 - \mathbf{q}_2), \quad (5.10b)$$

$$\overline{\bar{\chi}_{12}(\mathbf{q}_1)\bar{\chi}_{34}(\mathbf{q}_2)} \doteq \frac{W_{12}}{4d} \bar{\chi}_{34}(\mathbf{q}_1 - \mathbf{q}_2) = \frac{W_{34}}{4d} \bar{\chi}_{12}(\mathbf{q}_1 - \mathbf{q}_2), \quad (5.10c)$$

where we adopted a simplifying notation,

$$\frac{1}{N} \sum_{\mathbf{k}} F_1(\mathbf{k} + \mathbf{q}_1) F_2(\mathbf{k} + \mathbf{q}_2) = \overline{F_1(\mathbf{q}_1)F_2(\mathbf{q}_2)}. \quad (5.11)$$

We observe that the function \bar{G} behaves as a Gaussian random variable with respect to these momentum convolutions. The lower indices at \bar{G} , $\bar{\chi}$ and W in equations (5.10) indicate the corresponding energy variables. The introduced quantity W_{ij} stands for the product $t^2 \langle G^2(z_i) \rangle \langle G^2(z_j) \rangle$ (cf. Appendix C). In the following, the two involved energies appear every time in the same pair, z_1 and z_2 , and we are thus allowed to continue with just W and $\bar{\chi}$ without subscripts.

In order to proceed with the determination of the unknown coefficients Λ_n we insert our ansatz (5.9) into the right-hand side of formula (4.19), where the completely irreducible vertex \bar{I} is again set local, $\bar{I} = \gamma$. Doing so we arrive at an equation

$$\begin{aligned} \bar{\Lambda}_{\mathbf{k}\mathbf{k}'}^{ee}(\mathbf{q}) = \gamma + \frac{1}{N} \sum_{\mathbf{k}''} \left\{ \sum_{n=0}^{\infty} \Lambda_n \bar{\chi}^n(\mathbf{q} + \mathbf{k} + \mathbf{k}'') \bar{G}_1(\mathbf{k}'' + \mathbf{q}) \bar{G}_2(\mathbf{k}'') \right. \\ \left. \times \left[\sum_{m=0}^{\infty} \Lambda_m \bar{\chi}^m(\mathbf{q}) + \sum_{m=0}^{\infty} \Lambda_m \bar{\chi}^m(\mathbf{q} + \mathbf{k}' + \mathbf{k}'') - \gamma \right] \right\}. \quad (5.12) \end{aligned}$$

In the next step the momentum summations are evaluated using the facts delineated in Appendix C. Namely, we apply the property that a convolution of $2n$ elementary functions (\bar{G} or $\bar{\chi}$) decomposes into a combination of all possible pair-wise contractions (5.10), cf. equations (C.11) and (C.12). Utilizing this Wick-like theorem we obtain contributions that are compatible with the left-hand side of equation (5.12) as well as those whose momentum dependencies differ from ansatz (5.9). Our approximation is to drop the incompatible terms. Doing so we end up with a formula

$$\bar{\Lambda}_{\mathbf{k}\mathbf{k}'}^{ee}(\mathbf{q}) = \sum_{n=0}^{\infty} \Lambda_n \bar{\chi}^n(\mathbf{q}) = \gamma + \bar{\gamma} \bar{\chi}(\mathbf{q}) \left[\sum_{n=0}^{\infty} \Lambda_n \bar{\chi}^n(\mathbf{q}) + \bar{\gamma} - \gamma \right], \quad (5.13)$$

as the only allowed, i. e. compatible, elementary contractions are

$$\overbrace{\bar{\chi}(\mathbf{q} + \mathbf{k})\bar{\chi}(\mathbf{q} + \mathbf{k})}, \quad \overbrace{\bar{G}_1(\mathbf{q})\bar{G}_2(\mathbf{0})} \quad \text{and} \quad \overbrace{\bar{\chi}(\mathbf{q} + \mathbf{k}')\bar{\chi}(\mathbf{q} + \mathbf{k}')}$$

In equation (5.13) we introduced a number $\bar{\gamma} = N^{-1} \sum_{\mathbf{q}} \Lambda_{\mathbf{k}\mathbf{k}'}^{ee}(\mathbf{q})$ that will serve as the only parameter needed to determine the amplitudes Λ_n in vertices (5.9). The vertex $\bar{\gamma}$ plays within our approximation a very similar role as γ does within the CPA. Before we finish the construction of an equation for the quantity $\bar{\gamma}$, we briefly comment on the steps made so far from the viewpoint of the d^{-1} expansion.

The performed procedure is not absolutely consistent because of the following reason. Although the high-dimensional “technology” developed in Appendix C is justified for the leading order terms only, we apply it to next to leading orders as well.³ There are next to leading order terms of two distinct origins. The first of them are corrections to the effective Green function (5.2) that would improve the accuracy of momentum convolutions etc. Such contributions we do not take into account. The second type of corrections are those that come from the structure of the Bethe-Salpeter equations. These are far more important than modifications of the one-particle propagator \bar{G} and are included in equation (5.13). However, not all the next to leading order terms of purely two-particle origin are relevant for the description of diffusion in disordered materials. An example of the insignificant contributions is the $O(d^{-1})$ diagram (5.6), which is apparently incompatible with our ansatz (5.9). This means, however, that it does not renormalize the diffusion pole in the vertex $\bar{\Lambda}^{ee}$ and can thus be (and was) safely excluded from our considerations.

In order to extract expressions for the unknown quantities Λ_n we compare coefficients standing at the same powers of the “bubble” $\bar{\chi}$ on the left and right-hand sides of equation (5.13). In this way we arrive at a set of equations

$$\Lambda_0 = \gamma, \quad (5.14a)$$

$$\Lambda_1 = \bar{\gamma}(\Lambda_0 + \bar{\gamma} - \gamma) = \bar{\gamma}^2, \quad (5.14b)$$

$$\Lambda_n = \bar{\gamma}\Lambda_{n-1} = \bar{\gamma}^{n+1}, \quad \text{for } n > 1. \quad (5.14c)$$

Consequently, the irreducible vertex is expressed as a geometric series,

$$\bar{\Lambda}_{\mathbf{k}\mathbf{k}'}^{ee}(\mathbf{q}) = \gamma + \bar{\gamma} \frac{\bar{\gamma} \bar{\chi}(\mathbf{q})}{1 - \bar{\gamma} \bar{\chi}(\mathbf{q})}, \quad (5.15a)$$

³As already stated just below ansatz (5.9), the leading order term for the coefficients Λ_n is γ^n .

depending on the single parameter $\bar{\gamma}$. An equation for this quantity is easily derived by summing up equation (5.15a) over the only involved momentum \mathbf{q} . Doing so we finally obtain

$$\bar{\gamma} = \gamma + \bar{\gamma} \frac{1}{N} \sum_{\mathbf{q}} \frac{\bar{\gamma}^2 \bar{\chi}^2(\mathbf{q})}{1 - \bar{\gamma} \bar{\chi}(\mathbf{q})} \quad (5.15b)$$

that completes our construction of the two-particle vertex functions.

Although the solution given by formulae (5.15) was derived from the high-dimensional reasoning, its application is not limited to the limit $d \rightarrow \infty$. It can be, and it is intended to be, used in any spatial dimension as a mean-field-like approximation. In such a case, the $d \rightarrow \infty$ limit of the ‘‘bubble’’ $\bar{\chi}$ standing in equations (5.15) is replaced with its actual d -dimensional value. Then, of course, the convolution rules (5.10) cannot be used to simplify the determination of the vertex $\bar{\gamma}$ from equation (5.15b) and a full d -dimensional calculation has to be performed.

5.3 Diffusion pole

Having formulated the mean field solution (5.15), we turn to the question what it says about electron diffusion in disordered lattices. Is the diffusion constant D lowered in comparison to the (semi)classical Drude value D_0 ? Is the diffusive character of the particle density relaxation allowed in the whole range of disorder parameters and if not, where are located the mobility edges? We will see shortly.

The fundamental quantity for investigating diffusion is the correlation function Φ as pointed out in Section 2.4, where the diffusion process was introduced. Combining the definition of Φ , equation (2.20), with the definition of the complete two-particle vertex Γ , formula (4.4), the correlation function can be written as

$$\begin{aligned} \Phi(z_1, z_2; \mathbf{q}) &= \frac{1}{N} \sum_{\mathbf{k}} G_1(\mathbf{k} + \mathbf{q}) G_2(\mathbf{k}) \\ &+ \frac{1}{N^2} \sum_{\mathbf{k}\mathbf{k}'} G_1(\mathbf{k} + \mathbf{q}) G_2(\mathbf{k}) \Gamma_{\mathbf{k}\mathbf{k}'}(\mathbf{q}) G_1(\mathbf{k}' + \mathbf{q}) G_2(\mathbf{k}'). \end{aligned} \quad (5.16)$$

The vertex Γ to be used in this expression is, within our approximation, given by equations (4.11) and (5.15) and reads

$$\Gamma_{\mathbf{k}\mathbf{k}'}(\mathbf{q}) = \gamma + \bar{\gamma} \frac{\bar{\gamma} \bar{\chi}(\mathbf{q})}{1 - \bar{\gamma} \bar{\chi}(\mathbf{q})} + \bar{\gamma} \frac{\bar{\gamma} \bar{\chi}(\mathbf{k} + \mathbf{k}' + \mathbf{q})}{1 - \bar{\gamma} \bar{\chi}(\mathbf{k} + \mathbf{k}' + \mathbf{q})}. \quad (5.17)$$

Out of all possible combinations of the energy arguments, z_1 and z_2 , the only one important for reading out the physical quantities is $z_1 = E_F - i0$ and $z_2 = E_F + \omega + i0$. Such a choice corresponds to the electron-hole correlation function $\Phi^{AR}(\omega, \mathbf{q}) = \Phi(E_F - i0, E_F + \omega + i0; \mathbf{q})$ that displays a diffusion pole for small values of frequency ω and momentum q , recall Sections 2.3 and 2.4. A non-analytic behavior of this type can originate only from the second term on the right-hand side of equation (5.17). Leaving both other contributions as irrelevant yields

$$\Phi^{AR}(\omega, \mathbf{q}) \sim \frac{\bar{\lambda}^2(\omega) [\chi(\omega, \mathbf{q}) - \chi_0(\omega)]}{[1 - \bar{\lambda}(\omega) \chi_0(\omega)] [1 - \bar{\lambda}(\omega) \chi(\omega, \mathbf{q})]} \chi^2(\omega, \mathbf{q}), \quad (5.18)$$

where the non-local “bubble” $\bar{\chi}$ was eliminated with the aid of the formula $\bar{\chi} = \chi - G_1 G_2 = \chi - \chi_0$ that expresses the non-local part $\bar{\chi}$ as the difference between the full value χ and the local part χ_0 . Besides that we introduced $\bar{\lambda}$ as a counterpart to the CPA irreducible vertex λ ,

$$\bar{\gamma}(\omega) = \frac{\bar{\lambda}(\omega)}{1 - \bar{\lambda}(\omega) \chi_0(\omega)}, \quad \bar{\lambda}(\omega) = \frac{\bar{\gamma}(\omega)}{1 + \bar{\gamma}(\omega) \chi_0(\omega)}. \quad (5.19)$$

In a sense, the local quantity $\bar{\lambda}$ plays the role of the two-particle irreducible vertex, although there is no Bethe-Salpeter equation, with $\bar{\lambda}$ as its input, that could be used to generate the full vertex (5.17).

In order to the diffusion pole be really present in the correlation function (5.18), i. e. the constructed approximation to have physical meaning, a proper selfenergy has to be chosen. A relation that ensures the existence of the diffusion pole in the function Φ^{AR} is a form of the Ward identity (2.57),⁴

$$\bar{\lambda}(0) \chi(0, \mathbf{0}) = 1 \quad \text{or} \quad \Im \Sigma^A = \pi g_F \bar{\lambda}(0). \quad (5.20)$$

The conversion between the two forms of identity (5.20) was done using the equation $\chi(0, \mathbf{0}) = \pi g_F / \Im \Sigma^A$ that easily follows from the earlier expressions (3.14) and (3.28). The Ward identity (5.20) *defines* the imaginary part of the selfenergy consistent with the two-particle approximation derived in the preceding section. The real part of the selfenergy can be accessed via a Kramers-Kronig relation

$$\Re \Sigma^A(E) = \Sigma^A(\infty) + P \int_{-\infty}^{\infty} \frac{dE'}{\pi} \frac{\Im \Sigma^A(E')}{E' - E}. \quad (5.21)$$

The proposed mean-field description of disordered systems based on high-dimensional expansion, which we started to develop at the beginning of this chapter, is thereby completed.

Now we are ready to proceed with the analysis of the electron-hole correlation function Φ^{AR} . Using the Ward identity (5.20), the above expression (5.18) can be simplified to a form

$$\Phi^{AR}(\omega, \mathbf{q}) = \frac{\chi(0, \mathbf{0})}{\bar{\lambda}(0) \chi(0, \mathbf{0}) - \bar{\lambda}(\omega) \chi(\omega, \mathbf{q})}. \quad (5.22)$$

As we are interested only in the limit $\omega \rightarrow 0$ and $\mathbf{q} \rightarrow \mathbf{0}$, the values $\omega = 0$ and $\mathbf{q} = \mathbf{0}$ were set everywhere except in the denominator that becomes zero at this point. To access the desired asymptotics we expand the ω, \mathbf{q} -dependent quantities in the denominator to first orders in these small parameters,

$$\chi(\omega, \mathbf{q}) \approx \chi(0, \mathbf{0}) \left(1 + \frac{1}{2\Im \Sigma^A} i\omega - \frac{\sigma_0}{2e^2 g_F \Im \Sigma^A} q^2 \right), \quad (5.23a)$$

$$\bar{\lambda}(\omega) \approx \bar{\lambda}(0) + \left. \frac{\partial \bar{\lambda}(\omega)}{\partial \omega} \right|_{\omega=0} \omega. \quad (5.23b)$$

⁴The need of imposing the Ward identity (5.20) was analyzed already in Section 3.2. It was stressed that physical interpretation of an approximative theory cannot be provided when the diffusion pole is absent. Without this pole, no approximation can be matched with the perturbative result of the weak disorder limit.

Formula (5.23a) is nothing but a special case of expansion (3.28) used in the analysis of the weak localization phenomena in Section 3.2. The conductivity σ_0 , which appears in equation (5.23a), is the static value without any vertex corrections, i. e.

$$\sigma_0 = -\frac{e^2}{4\pi N} \sum_{\mathbf{k}} v_{\alpha}^2(\mathbf{k}) [G^A(E_F, \mathbf{k}) - G^R(E_F, \mathbf{k})]^2. \quad (5.24)$$

This is exactly the form of the static conductivity calculated within the coherent-potential approximation, equation (3.7). However, the one-particle Green functions standing in formula (5.24) differ from their CPA values as the selfenergy determined from equations (5.20) and (5.21) does not, in general, match the CPA selfenergy.

Inserting finally the approximate expressions (5.23) into the correlation function (5.22) we end up with the diffusion pole of the form

$$\begin{aligned} \Phi^{AR}(\omega, \mathbf{q}) &= \frac{1}{\bar{\lambda}(0) \left(-\frac{1}{2\Im\Sigma^A} i\omega + \frac{\sigma_0}{2e^2 g_F \Im\Sigma^A} q^2 - \frac{1}{\bar{\lambda}(0)} \left. \frac{\partial \bar{\lambda}(\omega)}{\partial \omega} \right|_{\omega=0} \right)} \\ &= \frac{2\pi g_F}{-i\omega \left(1 - \frac{2i\Im\Sigma^A}{\bar{\lambda}(0)} \left. \frac{\partial \bar{\lambda}(\omega)}{\partial \omega} \right|_{\omega=0} \right) + \frac{\sigma_0}{e^2 g_F} q^2}. \end{aligned} \quad (5.25)$$

To make the result more readable we introduce a new quantity A , inversion of which we call the *weight of the diffusion pole*,

$$A = 1 - \frac{2i\Im\Sigma^A}{\bar{\lambda}(0)} \left. \frac{\partial \bar{\lambda}(\omega)}{\partial \omega} \right|_{\omega=0}. \quad (5.26)$$

With the aid of this definition and the Einstein-like relation $\sigma_0 = e^2 D_0 g_F$, cf. equation (2.51), we come to the following representation of the singular part of the electron-hole correlation function,

$$\Phi^{AR}(\omega, \mathbf{q}) = \frac{2\pi g_F}{-iA\omega + D_0 q^2} = \frac{2\pi g_F/A}{-i\omega + Dq^2}, \quad (5.27)$$

where the diffusion constant D is introduced as $D = D_0/A$. The weight A^{-1} is generally smaller than 1 as will be demonstrated on explicit model calculations in the next section. Therefore, the mean-field approximation (5.15) predicts the diffusion constant D to be smaller than the (semi)classical value D_0 . Such a result agrees with our expectations.

The obtained formula (5.27) differs from the conclusions of the general analysis of the diffusive solution, Section 2.4. This discrepancy stems from the fact that we are not able to satisfy the Ward identities (2.21) and (2.57) in full, we can warrant only their limited (static, $\omega = 0$) version (5.20) instead. One could admit that we do not try hard enough as we force the selfenergy to be momentum independent. However, allowing a momentum dependence of the selfenergy cannot help because the Ward identities require a momentum independent selfenergy to a momentum independent two-particle irreducible vertex, which equals to $\bar{\lambda}$ in our case. Being unable to comply with the Ward identities, i. e. with conservation laws, can have one of the following meanings. It either says that the

approach we have chosen is somewhat wrong and cannot be used, or it indicates that demanding the Ward identities to hold in their full forms (2.21) and (2.57) is naive and needs to be reexamined. The next chapter collects strong arguments for the second option concluding that the Ward identities *cannot* be fully fulfilled in principle. Enforcing them would lead to a violation of analytic properties of the configurationally averaged Green functions. This would be a severe problem since the analyticity of Green functions is closely related to causality which simply cannot be given up.

As a consistency check we show that if we were able to find the selfenergy in such a way that the complete Ward identity is satisfied, i. e., if we could write

$$\bar{\lambda}(\omega) = \frac{\Sigma^A(E_F) - \Sigma^R(E_F + \omega)}{G^A(E_F) - G^R(E_F + \omega)}, \quad (5.28)$$

then equation (5.26) goes over to $A = 1$. Recalling once again formula (3.14), the electron-hole “bubble” χ can be, for $\mathbf{q} = \mathbf{0}$, casted to

$$\chi(\omega, \mathbf{0}) = \frac{G^A(E_F) - G^R(E_F + \omega)}{\omega + \Sigma^A(E_F) - \Sigma^R(E_F + \omega)}. \quad (5.29)$$

Combining the last two formulae yields the following expression for the two-particle vertex $\bar{\lambda}$,

$$\bar{\lambda}(\omega) = \frac{1}{\chi(\omega, \mathbf{0})} - \frac{\omega}{G^A(E_F) - G^R(E_F + \omega)}, \quad (5.30)$$

derivative of which with respect to frequency ω reads

$$\left. \frac{\partial \bar{\lambda}(\omega)}{\partial \omega} \right|_{\omega=0} = -\frac{1}{\chi^2(0, \mathbf{0})} \left. \frac{\partial \chi(\omega, \mathbf{0})}{\partial \omega} \right|_{\omega=0} - \frac{1}{G^A(E_F) - G^R(E_F)} - \omega \left. \frac{\partial}{\partial \omega} \frac{1}{G^A(E_F) - G^R(E_F + \omega)} \right|_{\omega=0} = 0. \quad (5.31)$$

This derivative is zero because the quantity $[G^A(E_F) - G^R(E_F + \omega)]^{-1}$ is a regular function of frequency ω . The first two terms on the right-hand side of equation (5.31) exactly cancel each other due to already employed identities, cf. formula (5.23a),

$$\chi(0, \mathbf{0}) = \frac{\pi g_F}{\Im \Sigma^A(E_F)}, \quad \left. \frac{\partial \chi(\omega, \mathbf{0})}{\partial \omega} \right|_{\omega=0} = -\frac{\chi(0, \mathbf{0})}{2i \Im \Sigma^A(E_F)} \quad (5.32)$$

and $G^A(E_F) - G^R(E_F) = 2\pi i g_F$. The expected result that the weight of the diffusion pole equals one, $A^{-1} = 1$, whenever the Ward identities are fulfilled follows directly from the demonstrated equality, $\partial \bar{\lambda} / \partial \omega |_{\omega=0} = 0$.

5.4 Mean-field theory of the Landau type

Although the asymptotic limit to infinite spatial dimensions greatly simplifies the original parquet equation (4.19), the resulting approximation defined by equations (5.15), (5.20) and (5.21) is still too complex for synoptic exploration of the diffusion pole weight A^{-1} in a system of a finite spatial dimensionality. To achieve a qualitative picture how A^{-1} depends on the disorder strength we implement several further simplifications. However,

before doing so we investigate low dimensions, $d \leq 2$, where some important conclusions can be made immediately.

We have seen that for the correlation function Φ^{AR} to display the diffusion pole, the same pole has to be in the ee -irreducible vertex $\bar{\Lambda}^{ee}$. The expression responsible for this non-analytic behavior reads

$$\frac{1}{1 - \bar{\gamma} \bar{\chi}(\mathbf{q})} \sim \frac{1}{-i\omega + Dq^2}. \quad (5.33)$$

In equation (5.15b), determining the quantity $\bar{\gamma}$, the diffusion pole (5.33) is to be integrated over momentum \mathbf{q} . This step represents no difficulty in dimensions $d \geq 3$. On the contrary, in the case of $d \leq 2$, the above pole is not integrable. Therefore, there can be no $\bar{\gamma}$ fulfilling equation (5.15b) in dimensions $d \leq 2$ if the vertex $\bar{\Lambda}^{ee}$ possesses the diffusion pole. Consequently, our mean-field approximation for two-particle vertices, formulae (5.15), predicts that the diffusive transport regime cannot take place in low dimensions, $d \leq 2$. This result is in agreement with other treatments which we referred to in Chapter 1.

In dimensions $d \geq 3$, the diffusive relaxation is generally possible. To arrive at numerical values of the diffusion pole parameters, the weight A^{-1} and the diffusion constant D , we utilize two simplifying steps. First, we relax the consistency between one- and two-particle vertex functions, the Ward identity (5.20). Instead of the correct selfenergy we use the Born selfenergy, expression (3.1b), or the CPA one, equation (3.4). Although this step might seem to be crude, it is not. Preliminary calculations employing the above given consistent selfenergy definition, formulae (5.20) and (5.21), do not show any significant differences when compared to the results achieved by using the Born or the CPA selfenergy only. The Born approximation, in particular, is chosen for the pleasant property that one can reach quite simple analytic formulae for all relevant quantities such as $G(z)$ and $\langle G^2(z) \rangle$ when the semi-elliptic band,

$$g^{(0)}(E) = \frac{2\pi}{w^2} \sqrt{w^2 - E^2}, \quad (5.34)$$

is considered for the lattice without disorder.⁵ The only parameter of this density of states is w , the band half-width. Although the density of electronic states (5.34) does not correspond to the hypercubic lattice in any spatial dimension, it represents a reasonable model choice in $d = 3$.

Second simplification that converts our rather complex theory into an easily manageable calculational scheme is a reduction of the formulae determining the two-particle functions. Instead of the whole geometric series, constituting the diffusion pole inside the sum over momentum \mathbf{q} , we retain only its first term,⁶

$$\bar{\gamma} = \gamma + \bar{\gamma} \frac{1}{N} \sum_{\mathbf{q}} \frac{\bar{\gamma}^2 \bar{\chi}^2(\mathbf{q})}{1 - \bar{\gamma} \bar{\chi}(\mathbf{q})} \quad \longrightarrow \quad \bar{\gamma} = \gamma + \frac{W^2}{8d} \bar{\gamma}^3 = \gamma + C_d W^2 \bar{\gamma}^3. \quad (5.35)$$

In this way we completely suppress the pole from the original equation (5.15b). It is thus clear that the reduction made in formula (5.35) is the more acceptable the higher is the

⁵Consult Appendix E for further details on this technical subject.

⁶To evaluate the sum $N^{-1} \sum_{\mathbf{q}} \chi^2(\mathbf{q})$ we used the convolution rule (5.10c) and the trivial identity $\chi(\mathbf{0}) = W/2$.

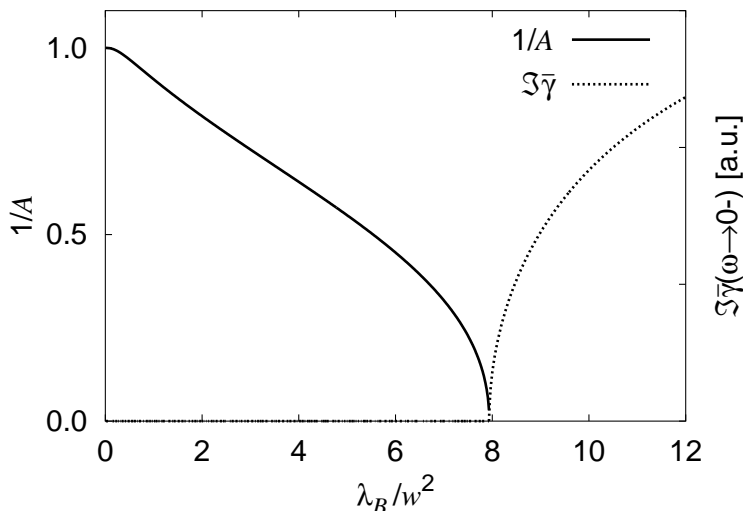


Figure 5.1: Weight of the diffusion pole A^{-1} and the order parameter in the localized phase $\Im\bar{\gamma}$ calculated from equation (5.35). We used a semi-elliptic energy band with the bandwidth $2w$, the self-consistent Born approximation for the selfenergy, and set $C_d = 0.1$. Fermi energy E_F lies in the center of the band.

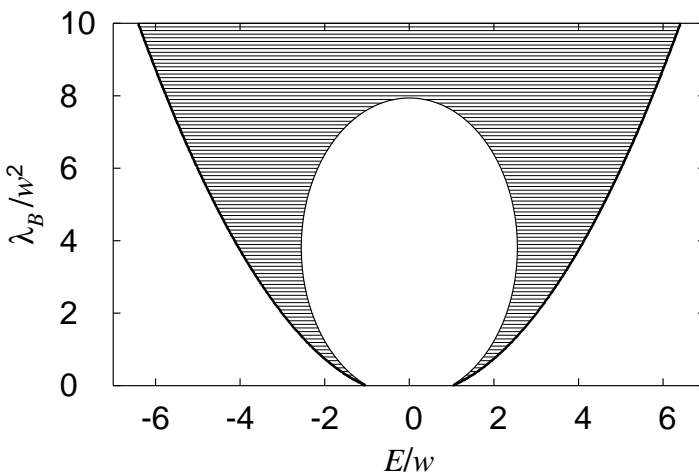
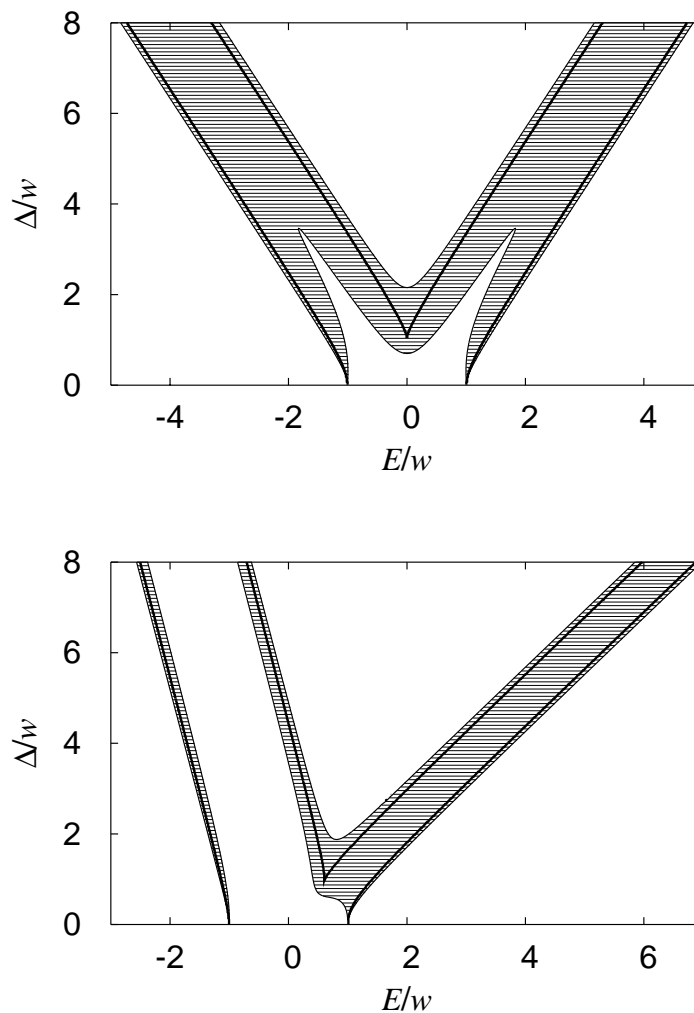


Figure 5.2: Phase diagram for the same setting as in Figure 5.1. The hatched area denotes localized states, $\Im\bar{\gamma} \neq 0$.

spatial dimensionality d . In the model calculations we performed, see Figures 5.1 – 5.3, the d -dependent constant C_d introduced in equation (5.35) does not represent its correct high-dimensional value $(8d)^{-1}$. It serves as a free parameter of our approximation scheme instead. It is quite reasonable to set C_d slightly larger than $(8d)^{-1}$ since the simplification performed in formula (5.35) surely underestimates the right-hand side of the original equation (5.15b).

The simplified cubic equation (5.35) resembles the Landau mean-field theory of (classical) phase transitions. It has generally three solutions for $\bar{\gamma}(E_F + i0, E_F - i0)$. For sufficiently small disorder strengths, $\gamma < \gamma_c$, all three solutions are real. A perturbative solution is of order γ , while two non-perturbative solutions are of order $\pm WC_d^{1/2}$. The perturbative solution increases and the module of the non-perturbative ones decreases with increasing disorder strength. At a critical randomness $3C_d W^2 \bar{\gamma}^2 = 1$, or equivalently $\gamma_c = 2(27C_d W^2)^{-1/2}$, the two positive solutions merge and move into the complex plane for $\gamma > \gamma_c$. Disappearance of positive solutions for $\bar{\gamma}(E_F + i0, E_F - i0)$ leads to suppression of the diffusion pole and simultaneously to vanishing of the diffusion constant. Quantity $\Im\bar{\gamma}(E_F + i0, E_F - i0)$, emerging beyond the critical point in the localized phase ($\gamma > \gamma_c$), plays the role of an order parameter for the Anderson metal-insulator

Figure 5.3: Band and mobility edges in energy-disorder plane for a binary alloy. Thick line is the band edge, region of localized states is hatched. Potential difference between distinct atoms is Δ . The upper pane shows the symmetric case with concentration of both alloy components $c = 0.5$. The diagram in the lower pane corresponds to an asymmetric alloy with concentration of the minor component $c = 0.2$. It is clear that the tendencies towards localization are enhanced in the impurity band. To calculate these figures we used a semi-elliptic band with the bandwidth $2w$ and the CPA selfenergy. The parameter C_d was set to $C_d = 1.8$. The extension of the area where $\Im\bar{\gamma} \neq 0$ outside the band is due to incomplete consistency between one- and two-particle functions.



transition, see Figure 5.1. The corresponding symmetry breaking “field” that controls the sign of $\Im\bar{\gamma}(E_F + i0, E_F - i0)$ is frequency ω .

Typical phase diagrams for localized-extended states calculated from formula (5.35) are plotted in Figures 5.2 and 5.3. In the former case, the selfenergy is calculated using the Born approximation. The results presented in the later figure are more realistic as they correspond to the binary alloy model, equation (1.7), with the CPA value for the selfenergy. Both figures demonstrate that the localization tendencies are most pronounced close to the band edges and in the impurity band, which agrees with the phenomenological picture introduced in Chapter 1.

Chapter summary

In this chapter we have achieved the most important results of the thesis. The parquet scheme for two-particle vertex functions, formulated in Chapter 4, was solved in the asymptotic limit to high spatial dimensions, $d \rightarrow \infty$. An explicit solution is allowed by the fact that the momentum dependencies of one- and two-particle Green functions are largely simplified in this limit. This solution, when applied in finite dimensions, plays the role of a mean-field approximation for transport properties of disordered systems. It displays two distinct phases — at weak and moderate disorder strengths it is the diffusive regime that goes over to the non-diffusive mode when the disorder gets strong enough. The critical disorder strength γ_c , at which the transition between these two phases takes place, is largest if the Fermi energy E_F lies in the center of the energy band and lowers when E_F moves towards the band edges. These properties nicely agree with the phenomenologically motivated scenario for transport phenomena in three and more spatial dimensions (Chapter 1). The metal-insulator transition we found is continuous. Our results hence support by direct calculation the nowadays widely accepted opinion that the Mott's concept of the minimal metallic conductivity σ_{\min} (Figure 1.3) is incorrect.

The calculational complexity of the mean-field approximation scheme proposed in this chapter is not much larger than the complexity of the coherent-potential approximation, which makes it a promising tool for future realistic (ab-initio) calculations.

6

Physics of suppression of diffusion

The mean-field theory for two-particle vertex functions, constructed in the preceding chapter, was shown to display a transition from the diffusive (metallic) to non-diffusive (insulating) transport regime. No details of the non-diffusive phase were discussed yet, we only learned that the diffusive solution is not possible in the whole range of disorder parameters. The label “non-diffusive regime” was used without any deeper understanding what physics takes place in the regions of the parameter space where the mean-field equation (5.35) does not provide for a solution possessing the diffusion pole. This final chapter of the thesis fills the just emphasized gap. Namely, it sheds some light on the mechanism of the metal-insulator transition as predicted by our mean-field approximation.

In order to reach the physical insight into the results of Chapter 5 we return back to the diffusive density relaxation studied in Section 2.4. The corresponding relaxation function ϕ is given as $\phi = \Phi^{AR}/(2\pi)$ where the electron-hole correlation function Φ^{AR} , formula (5.27), is to be inserted. Doing so we come to the time-momentum representation of the function ϕ in a form

$$\phi(t, \mathbf{q}) = \int_{-\infty}^{\infty} \frac{d\omega}{2\pi} e^{-i\omega t} \frac{g_F/A}{-i\omega + Dq^2} = -\frac{1}{A} \left(\frac{\partial n}{\partial \mu} \right) e^{-Dq^2 t}. \quad (6.1)$$

The density of states g_F was rewritten with the aid of the identity $g_F = (\partial n / \partial \mu)$ that holds at zero temperature, $T = 0$ K. The form of the derivative with respect to the chemical potential μ is more convenient at this moment. Fourier components of a density variation relax according to formula (2.32) that in the present case reads

$$\delta n_{\text{relax}}(t, \mathbf{q}) = e\varphi(\mathbf{q})\phi(t, \mathbf{q}) = -e\varphi(\mathbf{q}) \frac{1}{A} \left(\frac{\partial n}{\partial \mu} \right) e^{-Dq^2 t}. \quad (6.2)$$

This conclusion is somewhat controversial since equation (6.2) describes the relaxation of only a fraction of the whole non-equilibrium density variation $\delta n(0, \mathbf{q}) = \delta\mu (\partial n / \partial \mu) = -e\varphi(\mathbf{q}) (\partial n / \partial \mu)$. It is one of the objectives of this chapter to answer the question where we lost the rest of particles. The arguments collected in the following sections support a picture that there co-exist two types of electron eigenstates at the Fermi energy E_F . The part $A^{-1}g_F$ of them are extended through the whole sample and the other states, number of which is $(1 - A^{-1})g_F$, are localized in some finite subvolume. Electrons sitting in the

later states are immobile, and hence cannot contribute to the density relaxation (6.2). For the same reason, the localized electrons do not respond to the weak external field that was used to prepare the initial density variation $\delta n(0, \mathbf{q})$, cf. Section 2.4. This observation resolves the above controversy concerning the particle loss, since the correct zero-time variation should read $\delta n(0, \mathbf{q}) = -e\varphi(\mathbf{q})A^{-1}(\partial n/\partial\mu)$.

Before we turn our attention to details of the sketched physical interpretation, we first demonstrate that our inability to fully comply with Ward identities, which is the reason for the weight A^{-1} being less than one, is not due to improper approximations. We argue that such an inconsistency is rather general in its nature.

6.1 Ward identities vs. analyticity of the selfenergy

In this section we demonstrate that demanding validity of the Ward identity (2.57) leads to unphysical non-analytic behavior of the selfenergy when the diffusive phase is assumed. The situation gets even worse in the localized regime where the Ward identity (2.57) inevitably disallows to define the selfenergy at all. We start with the analysis of the metallic phase.

6.1.1 Diffusive phase

At first we summarize fundamental properties the theory should have to be acceptable. They are:

- (i) A diffusive behavior in the weak disorder limit (in dimensions $d \geq 3$). The correlation function Φ^{AR} should have the small frequency and small momentum asymptotics of the form

$$\Phi^{AR}(\omega, \mathbf{q}) \sim \frac{1}{-i\omega + Dq^2} \quad (6.3)$$

in this limit.

- (ii) Analyticity and causality of one-particle Green functions that are expressed in Kramers-Kronig relations.
- (iii) Electron-hole symmetry of two-particle vertices, expressed by equations (4.13) and (4.17), that is a manifestation of reversibility of the microdynamics. In other words, this symmetry originates in the invariance of equations of motion with respect to time reversal.
- (iv) Particle number conservation which gives rise to Ward identities (2.21) and (2.57) that link one- and two-particle functions.

All these four points are well justified and it would seem that there is no doubt about their fulfilling in any successful description of disordered solids. However, we are going to show that the listed properties are actually contradictory and cannot be imposed all in the same time, at least as far as we use the formalism of configurationally averaged Green functions.

We define a function Ω_E that is in the limit $\omega \rightarrow 0$ directly related to the derivative of the retarded selfenergy with respect to its energy parameter,

$$\Omega_E(\omega) = \frac{1}{N} \sum_{\mathbf{k}} \frac{\Sigma^R(E - \omega, \mathbf{k}) - \Sigma^R(E + \omega, \mathbf{k})}{2\omega} \xrightarrow{\omega \rightarrow 0} -\frac{1}{N} \sum_{\mathbf{k}} \frac{\partial \Sigma^R(E, \mathbf{k})}{\partial E}. \quad (6.4)$$

According to requirement (ii) this function has to be well behaved (apart from several points, such as E being just the band edge). On the other hand, some two-particle functions have to be non-analytic in order to catch up physics properly, item (i). The selfenergy is bound to two-particle functions via Ward identities and therefore a question arises whether or not traces of the diffusion pole are transferred into one-particle functions.

If we add and remove the selfenergy $\Sigma^A(E)$ on the right-hand side of definition (6.4), the two formed differences, $\Sigma^R(E - \omega) - \Sigma^A(E)$ and $\Sigma^A(E) - \Sigma^R(E + \omega)$, can be rewritten with the aid of the Vollhardt-Wölfle identity (2.57) in terms of the electron-hole irreducible vertex Λ^{eh} ,

$$\Omega_E(\omega) = \frac{1}{2\omega} \frac{1}{N^2} \sum_{\mathbf{k}\mathbf{k}'} \left\{ \Lambda_{\mathbf{k}\mathbf{k}'}^{eh,AR}(E, E + \omega; \mathbf{0}) [G^A(E, \mathbf{k}') - G^R(E + \omega, \mathbf{k}')] \right. \\ \left. - \Lambda_{\mathbf{k}\mathbf{k}'}^{eh,AR}(E, E - \omega; \mathbf{0}) [G^A(E, \mathbf{k}') - G^R(E - \omega, \mathbf{k}')] \right\}. \quad (6.5)$$

Inserting $G^R(E, \mathbf{k}') - G^R(E, \mathbf{k}') = 0$ into both square brackets and rearranging the resulting expression yields

$$\Omega_E(\omega) = \frac{1}{2\omega} \frac{1}{N^2} \sum_{\mathbf{k}\mathbf{k}'} \left\{ 2i \left[\Lambda_{\mathbf{k}\mathbf{k}'}^{eh,AR}(E, E + \omega; \mathbf{0}) - \Lambda_{\mathbf{k}\mathbf{k}'}^{eh,AR}(E, E - \omega; \mathbf{0}) \right] \Im G^A(E, \mathbf{k}') \right. \\ \left. + \Lambda_{\mathbf{k}\mathbf{k}'}^{eh,AR}(E, E + \omega; \mathbf{0}) [G^R(E, \mathbf{k}') - G^R(E + \omega, \mathbf{k}')] \right. \\ \left. - \Lambda_{\mathbf{k}\mathbf{k}'}^{eh,AR}(E, E - \omega; \mathbf{0}) [G^R(E, \mathbf{k}') - G^R(E - \omega, \mathbf{k}')] \right\}. \quad (6.6)$$

This formula is convenient for studying a transfer of non-analyticity from two- to one-particle functions. So far we do not know the behavior of the two-particle vertices as the requirement (i) concerns only the correlation functions $\Phi \sim \sum_{\mathbf{k}\mathbf{k}'} \Gamma_{\mathbf{k}\mathbf{k}'}(\mathbf{q})$. The path from Φ to Γ is not straightforward as the equation to be solved has an integral character. Fortunately, we can proceed as follows. Because the involved momentum integrations run over a limited set, i. e. over the first Brillouin zone, a pole in the correlation function Φ enforces a pole in the integrand Γ . The high-dimensional asymptotics outlined in Section 5.1 indicates that the vertex Γ displays the same diffusion pole as Φ does,

$$\Gamma_{\mathbf{k}\mathbf{k}'}^{AR}(E, E + \omega; \mathbf{q}) \sim \frac{1}{-i\omega + Dq^2}. \quad (6.7)$$

Moreover, it was shown that this pole comes from the vertex Λ^{ee} if the full vertex Γ is decomposed into irreducible vertices according to the parquet equation $\Gamma = \Lambda^{eh} + \Lambda^{ee} - I$,¹ formula (4.11). The fact that the diffusion pole can be traced down to the electron-electron irreducible vertex,

$$\Lambda_{\mathbf{k}\mathbf{k}'}^{ee,AR}(E, E + \omega; \mathbf{q}) \sim \frac{1}{-i\omega + Dq^2}, \quad (6.8a)$$

does not mean that the electron-hole irreducible vertex Λ^{eh} , which we need to insert into expression (6.6), is regular. Due to the time-reversal symmetry, property labelled (iii) in

¹Note that in this paragraph we do not distinguish between vertices with and without bar. These two differ only in local terms that do not change the discussed analytic properties.

the list at the beginning of this section, the vertex Λ^{eh} contains the Cooper pole,

$$\Lambda_{\mathbf{k}\mathbf{k}'}^{eh,AR}(E, E + \omega; \mathbf{q}) \sim \frac{1}{-i\omega + D(\mathbf{k} + \mathbf{k}' + \mathbf{q})^2}. \quad (6.8b)$$

At this moment we are ready to evaluate the function Ω_E from formula (6.6). The leading singular part of Ω_E is given by the first term on the right-hand side of equation (6.6) that behaves as

$$\frac{1}{\omega^2 + D^2(\mathbf{k} + \mathbf{k}')^4} \Im G^A(E, \mathbf{k}'). \quad (6.9)$$

The other two contributions are irrelevant compared to the previous one as their non-analyticity is weaker,

$$-\Lambda_{\mathbf{k}\mathbf{k}'}^{eh,AR}(E, E \pm \omega; \mathbf{0}) \frac{\partial G^R(E, \mathbf{k}')}{\partial E} \sim \frac{1}{\pm i\omega + D(\mathbf{k} + \mathbf{k}')^2}. \quad (6.10)$$

Critical for our investigation of function Ω_E is the integral of the leading term (6.9) over a vicinity of the pole at $\mathbf{k}' = -\mathbf{k}$. In d spatial dimensions it explicitly reads

$$\int d^d k d^d k' \frac{1}{\omega^2 + D^2(\mathbf{k} + \mathbf{k}')^4} \Im G^A(E, \mathbf{k}') \sim \int_0^M \kappa^{d-1} d\kappa \frac{1}{\omega^2 + D^2\kappa^4} \quad (6.11)$$

where we introduced a cut-off M characterizing the extent of the integration region. The simplification was done via an obvious change in the integration variables, $\mathbf{k}, \mathbf{k}' \rightarrow \mathbf{k}', \boldsymbol{\kappa} = \mathbf{k} + \mathbf{k}'$. As a next step we substitute $\kappa = x\sqrt{|\omega|/D}$ that leads to the following expression,

$$\frac{1}{\omega^2} \left(\frac{|\omega|}{D} \right)^{d/2} \int_0^{M\sqrt{D/|\omega|}} x^{d-1} dx \frac{1}{1+x^4}. \quad (6.12)$$

For our purposes it is sufficient to restrict the further investigation only to small frequencies ω . Under such circumstances the upper limit of the integral approaches infinity. The limit $\omega \rightarrow 0$ leaves the integral to be a finite number in dimensions $d \leq 3$. In $d = 4$ the integral logarithmically diverges as a function of ω and in higher dimensions the divergency is even stronger.² To find out the leading singular behavior of function Ω_E in dimensions $d \geq 5$, the above strategy has to be slightly modified. We differentiate the integral in expression (6.11) n times with respect to ω^2 . This yields

$$\frac{(-1)^n n!}{\omega^{2(n+1)}} \left(\frac{|\omega|}{D} \right)^{d/2} \int_0^{M\sqrt{D/|\omega|}} x^{d-1} dx \frac{1}{(1+x^4)^{n+1}}. \quad (6.13)$$

Now the integral converges in dimensions $d < 4n + 4$ and logarithmically diverges when $d = 4n + 4 = 4l$. Therefore, to characterize the singularity in function Ω_E we need to differentiate at least $n = d/4 - 1$ times. At the end, these n artificial derivatives has to be removed by a backward n -multiple integration. After collecting the above findings

²Note that this observation does not imply the whole expression (6.12) to be the more singular the higher the dimensionality. On the contrary, the opposite is true.

into a single formula we end up with the singular part of the testing function Ω_E being of the form

$$\Omega_E^{\text{sing}}(\omega) \sim K_d \left(\frac{Dk_F^2}{\omega} \right)^2 \left(\frac{|\omega|}{Dk_F^2} \right)^{d/2} \times \begin{cases} 1 & \text{for } d \neq 4l, \\ \ln \frac{Dk_F^2}{|\omega|} & \text{for } d = 4l. \end{cases} \quad (6.14)$$

The only purpose for introducing the Fermi momentum k_F into this formula is making the multiplicative constant K_d dimensionless.

The behavior of Ω_E is so that it has a point of non-analyticity at $\omega = 0$ for *every* energy parameter E . When the spatial dimensionality d is increased, the singular behavior is shifted to higher and higher derivatives with respect to E and disappears eventually in the limit $d = \infty$. If function Ω_E is not analytic, the selfenergy cannot be analytic either, cf. formula (6.4). Moreover, in dimensions $d = 1$ and $d = 2$ the non-analyticity of Ω_E is so strong that the selfenergy cannot even be defined since from equations (6.4) and (6.14) follows that $\Sigma \sim \lim_{\omega \rightarrow 0} \omega^{-1/2}$ and $\Sigma \sim \lim_{\omega \rightarrow 0} \ln \omega$ in these dimensions, respectively. In this way we showed that our starting assumptions — diffusive behavior at large scales, reversibility of the electron microdynamics and particle number conservation are in contradiction with analyticity of Green functions, i. e. with causality. As a consequence, we are forced to abandon one of the above natural properties when describing electron transport in disordered systems. But which one?

The construction given in the preceding chapter inherently led to a breakdown of conservation laws. However, more feasible would seem to give up time-reversibility of the equations of motion as the diffusion equation,

$$\left(\frac{\partial}{\partial t} - D\Delta \right) \delta n(t, \mathbf{r}) = 0, \quad (2.30)$$

which we want to (partly) recover, is itself not invariant under time-reversal. If we do so, the electron-hole irreducible vertex Λ^{eh} is allowed to be singularity-free and the above discovered inconsistency disappears. An example of a theory that follows such constraints is the coherent-potential approximation described in Section 3.1 and Appendix B. It provides diffusive relaxation (Section 3.1), fulfills Ward identities (Appendix B), while still has correct analytical properties, [66]. On the other hand, the CPA contains no sign of electron localization as it provides purely Drude-like transport. The phenomenon of weak localization (Section 3.2) demonstrates that for inclusion of localization tendencies the so-called Cooper pole in the vertex Λ^{eh} is crucial. Therefore, the only way we can proceed is a violation of Ward identities. To sacrifice causality is impossible, since it would turn all Green functions meaningless.

6.1.2 Localized phase

So far we somewhat avoided the localized regime. At the beginning of this chapter we started to argue that localized electron eigenstates are not accessible within our approach and we are going to further examine this observation in the next section. At this point we add a short but important note that the theory of Vollhardt and Wölfle (Section 3.3) also shows an inconsistency analogous to that described in the above paragraph.

The localized phase is signaled by the replacement of the diffusion constant D with $D(\omega) = -i\omega\xi^2$, which converts the diffusion pole in the electron-hole irreducible vertex Λ^{eh} , formula (6.8b), to

$$\Lambda_{\mathbf{k}\mathbf{k}'}^{eh,AR}(E, E + \omega; \mathbf{q}) \sim \frac{1}{-i\omega} \frac{1}{1 + \xi^2(\mathbf{k} + \mathbf{k}' + \mathbf{q})^2}. \quad (6.15)$$

We insert this expression into the Vollhardt-Wölfle identity (2.57) with momentum \mathbf{q} set to zero,

$$\Sigma^A(E, \mathbf{k}) - \Sigma^R(E + \omega, \mathbf{k}) = \frac{1}{N} \sum_{\mathbf{k}'} \Lambda_{\mathbf{k}\mathbf{k}'}^{eh,AR}(E, E + \omega; \mathbf{0}) [G^A(E, \mathbf{k}') - G^R(E + \omega, \mathbf{k}')]. \quad (6.16)$$

Doing so and performing the limit $\omega \rightarrow 0$ we arrive at an expression for the imaginary part of the advanced selfenergy,

$$\Im \Sigma^A(E, \mathbf{k}) \sim \lim_{\omega \rightarrow 0} \frac{1}{-i\omega} \frac{1}{N} \sum_{\mathbf{k}'} \frac{\Im G^A(E, \mathbf{k}')}{1 + \xi^2(\mathbf{k} + \mathbf{k}')^2}. \quad (6.17)$$

Since the sum over momentum \mathbf{k}' is nonzero, the Ward identity (2.57) requires the self-energy Σ^A to diverge *everywhere* inside the band. Such a behavior is clearly unphysical. Besides that, it is strongly incompatible with the Born selfenergy that Vollhardt and Wölfle use within their theory.

To conclude the results of the last two paragraphs, numbered 6.1.1 and 6.1.2 — we have demonstrated that the Ward identities cannot be fully fulfilled if disordered systems are described with the aid of configurationally averaged Green functions. If we require the Ward identities to be completely satisfied, we loose either the ability to approach the disorder-driven metal-insulator transition or the analytical properties of the selfenergy and hence of all Green functions. These findings are quite surprising. As far as we know, no such inconsistencies have ever been reported in the literature. Even a recent paper on Ward identities [67] is free of any observations similar to ours, which we believe is due to rather naive assumptions regarding how the configurational averaging acts.

6.2 Too distinct electron eigenstates

Up to now we presented more or less technical reasons why we cannot avoid giving up the conservation laws. Now we illuminate this unexpected conclusion by more physical means. We should keep in mind that it is not the real behavior, i. e. visible in experiment, which we are going to discuss. There, obviously, the particle number must be conserved. The question we want to address is rather how the real physical system projects onto the quantum-field-theoretical description we are using. The key observations are that localized electron eigenstates can hardly be approached perturbatively starting from Bloch waves and that configurational averaging changes physics more than usually expected.

6.2.1 One particular configuration of disorder

In the first step we analyze how electrons move in one given sample. Such a task is too difficult to be managed by analytical means due to the lack of apparent symmetries,

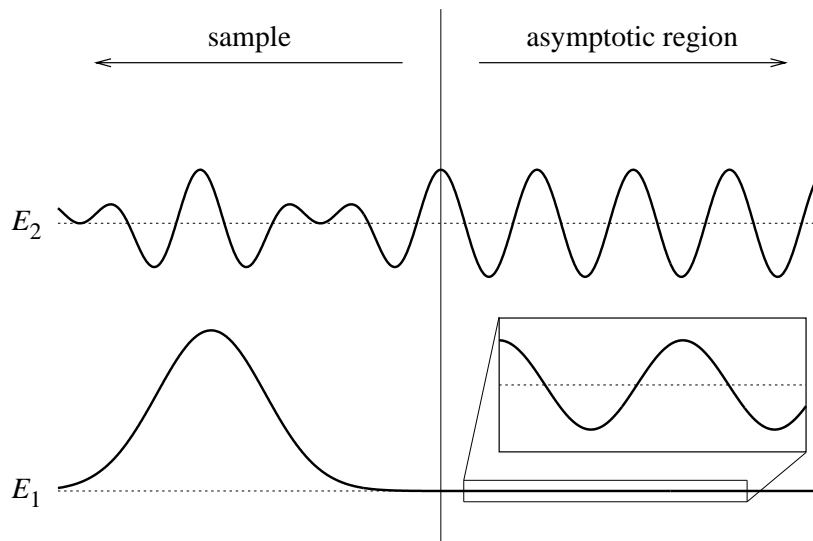


Figure 6.1: A simple draft showing how diffusive and “localized” states leak out of a finite sample. With the increasing system size the amplitude of asymptotic oscillations of “localized” states approaches zero.

and thus numerical simulations are the only option. However, if we seek only qualitative answers then just intuitive considerations are sufficient. Let us assume that the disorder is strong enough so that besides extended states also localized ones exist, for example close to the band edges. These two types of states are unlikely to co-exist at a given energy, since any small change in the random potential would cause admixtures of extended states with a localized state, and would thus delocalize it. Figure 6.1 shows how these two types of electron eigenstates look like in the case of a finite size sample. Note that the “localized” states are not literally localized as they are not strictly confined inside the sample and extend to the outer regions as well. This leaks get smaller with increasing the volume of the studied system and eventually vanish in the thermodynamic limit. Therefore, it is only the case of infinite volume when we can precisely distinguish between diffusive and localized wavefunctions.

Now it is time to recall the very basis of the description of disordered systems via Green functions that was explained in Chapter 2 and namely in Section 2.2 where the configurational averaging was introduced. There we proceeded along the following steps — take a clean crystal, eigenstates of which are Bloch waves, *perturbatively* include the random part of the Hamiltonian and finally perform the averaging over all disorder configurations term by term in the perturbation expansion. Notice that even for a single configuration, i. e. before configurational averaging, we are far from any exact solution. We can deal only with scattering experiments, in which a wave packet is prepared infinitely far from the investigated sample and then scattered on the random potential. At the end, the resulting waves are collected, again in the asymptotic region.

The reasoning given above implies that when localized states exist, they occupy some energy intervals (parts of bands) where no diffusive states can appear. In the same time, the localized states do not extend up to the asymptotic regions, and therefore no

scattered wave packets can have energies falling into such intervals. It is evident that the method of description we chose is not capable to catch all the physics that takes place in disordered electronic systems. Actually, we are able to capture only diffusion (scattering from asymptotics to asymptotics) whereas we cannot properly describe the localized states.

Another way to get convinced that the localized states are elusive is to look at norms of wavefunctions in the thermodynamic limit. A very natural assumption is that exact localized wavefunctions have similar properties as Wannier states $|n\rangle$, $\langle n'|n\rangle = \delta_{n',n}$, and that the diffusive states somewhat resemble the Bloch waves,

$$|\mathbf{k}\rangle = \frac{1}{\sqrt{N}} \sum_n e^{i\mathbf{k}\cdot\mathbf{R}_n} |n\rangle. \quad (6.18)$$

The norm of vectors $|\mathbf{k}\rangle$ is easily evaluated and reads

$$\langle \mathbf{k}'|\mathbf{k}\rangle = \frac{1}{N} \sum_n e^{i(\mathbf{k}-\mathbf{k}')\cdot\mathbf{R}_n} = \delta_{\mathbf{k}',\mathbf{k}}. \quad (6.19)$$

The above two formulae apply to a finite volume with N being the number of lattice sites. There is no problem with going over to $N \rightarrow \infty$ in equation (6.19), since the norm is 1 independently on the sample size. However, we cannot work directly with the Bloch wavefunctions in the limit $N \rightarrow \infty$ as $\langle n|\mathbf{k}\rangle \rightarrow 0$. Every calculation should thus be done in a finite volume with the eventual thermodynamic limit being the very last step. Unfortunately, such a procedure is too complicated and the limit $N \rightarrow \infty$ has to be performed much sooner so that the calculation becomes manageable.

If we want the Bloch states to preserve their physical meaning to the thermodynamic limit, the normalization factor $N^{-1/2}$ has to be replaced with $(a/2\pi)^{d/2}$,

$$|\mathbf{k}\rangle = \left(\frac{a}{2\pi}\right)^{d/2} \sum_n e^{i\mathbf{k}\cdot\mathbf{R}_n} |n\rangle, \quad (6.20)$$

when a d -dimensional hypercubic lattice with the lattice constant a is considered. The state vectors $|\mathbf{k}\rangle$ are no longer normalized to unity, but to the Dirac δ -function instead,³

$$\langle \mathbf{k}'|\mathbf{k}\rangle = \left(\frac{a}{2\pi}\right)^d \sum_n e^{i(\mathbf{k}-\mathbf{k}')\cdot\mathbf{R}_n} \xrightarrow{N\rightarrow\infty} \delta(\mathbf{k}-\mathbf{k}'). \quad (6.22)$$

These renormalization steps are accompanied with an essential change of the physical content of the corresponding wavefunctions. The localized states still describe a single particle confined to a finite subvolume, whereas the vectors $|\mathbf{k}\rangle$ are interpreted as particle *fluxes*. It is not surprising that we can work either with these fluxes or with localized

³Precisely, formula (6.22) should read

$$\left(\frac{a}{2\pi}\right)^d \sum_n e^{i(\mathbf{k}-\mathbf{k}')\cdot\mathbf{R}_n} \xrightarrow{N\rightarrow\infty} \sum_m \delta(\mathbf{k}-\mathbf{k}'+\mathbf{K}_m), \quad (6.21)$$

where \mathbf{K}_m are vectors of reciprocal lattice, [68]. However, only one of the δ -functions on the right-hand side falls into the first Brillouin zone.

states, but hardly with both simultaneously due to their different normalization. We thus come to the origin of the title of this section — the study of diffusion in strongly disordered solids involves electron eigenstates that are too different to be described simultaneously.

The representation space of a given disorder configuration can be characterized via a decomposition of unity operator

$$\hat{1} = \sum_{\boldsymbol{\kappa}}^{N_{\text{ext}}} |\boldsymbol{\kappa}\rangle\langle\boldsymbol{\kappa}| + \sum_{\nu}^{N_{\text{loc}}} |\nu\rangle\langle\nu|, \quad (6.23)$$

where $|\boldsymbol{\kappa}\rangle$ and $|\nu\rangle$ are exact diffusive and localized eigenfunctions of the corresponding Hamiltonian, respectively. The total number of eigenstates equals to the number of lattice sites, $N_{\text{ext}} + N_{\text{loc}} = N$. As we already noted several times, the only basis we can effectively work in is that of the Bloch waves $|\mathbf{k}\rangle$. If we try to rewrite equation (6.23) using this convenient basis we immediately run into trouble, because such a basis is not complete with respect to the physical system under investigation. The localized states $|\nu\rangle$ are in the thermodynamic limit orthogonal to the Hilbert space spanned over the set $\{|\mathbf{k}\rangle\}$, since $\langle\nu|\mathbf{k}\rangle/\langle\mathbf{k}|\mathbf{k}\rangle = O(N^{-1})$. The only states we are left with are those that are delocalized, as $\langle\boldsymbol{\kappa}|\mathbf{k}\rangle/\langle\mathbf{k}|\mathbf{k}\rangle = O(1)$. We may therefore expect that after going through all necessary calculations⁴ we end up with the configuration-dependent electron-hole correlation function having a form

$$\Phi^{AR}(\omega, \mathbf{q}) = \begin{cases} \frac{2\pi g_F}{-i\omega + Dq^2} & \text{for } E_F \text{ in the region of extended states,} \\ 0 & \text{otherwise.} \end{cases} \quad (6.24)$$

The anticipated zero in the regions of localized states is clearly unphysical and originates directly from the incompleteness of our basis set. However, the presented approach that builds on the Bloch states cannot be expected to provide anything more meaningful. If we were able to incorporate localized states into the description of disordered solids, the correlation function Φ^{AR} in the localized phase would read (cf. Section 3.3)

$$\Phi^{AR}(\omega, \mathbf{q}) = \frac{1}{-i\omega} \frac{2\pi g_F}{1 + (\xi q)^2}. \quad (6.25)$$

Such a form of the diffusion pole corresponds to infinitely slow diffusive relaxation. The assumption that formula (6.25) holds inside localized regions is not in contradiction with the conclusions of Section 6.1. There it was found that a pole of the form (6.25) does not fit into the (sub)space of Bloch waves where the configurationally averaged Green functions reside. The present considerations indicate the same — the Hilbert space spanned over the Bloch basis is insufficient for the description of the localized phase and hence needs to be extended in order to properly include the localized electron eigenstates.

6.2.2 Averaging over impurity configurations

The only available method how to achieve analytical results is to perform the configurational averaging term by term in the perturbation expansions for Green functions. This is

⁴Presently, there is no known scheme how to actually sum the non-averaged perturbation expansion above the Bloch states. But let us for a while assume that it is possible.

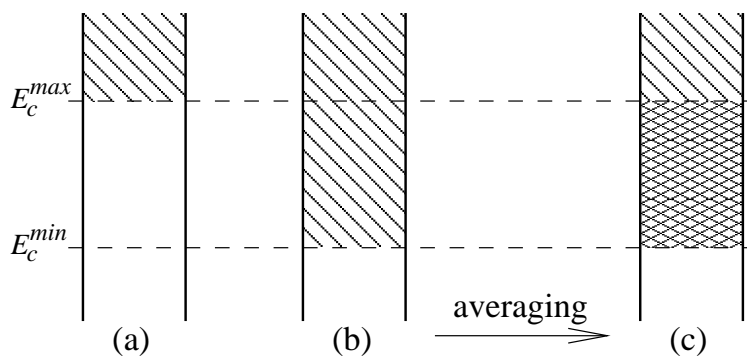


Figure 6.2: Configurational averaging causes mixing of extended and localized states if the mobility edge E_c is configurationally dependent. The parts (a) and (b) represent particular configurations of scattering centers, part (c) depicts configurational average. Dashed regions correspond to localized states. In the doubly dashed energy interval eigenstates of both types are present.

the path we followed in the preceding chapters. Once the averaging is done, all quantities are translationally invariant and the basis formed of Bloch waves becomes a very natural choice.

Continuation of the analysis started in the above paragraph may yield two different results. One possibility is that the averaging over configurations does not change the physics at all, i. e. that the expression for the averaged correlation function Φ^{AR} remains the same as formula (6.24). This would be the case if the boundary between extended and localized states, the mobility edge E_c , were not configurationally dependent. The other option is that the mobility edge substantially moves as the positions of scatterers change. At this point we are not aware of any general argument that could decide which of these two concepts is true. Nevertheless, we can find out which one fits our mean-field theory constructed in Chapter 5. We immediately see that it is not the idea of fixed mobility edge as formulae (6.24) and (6.25) do not match the findings of Chapter 5.

How does the expression for the correlation function Φ^{AR} change if the mobility edge E_c is not a constant with respect to disorder configurations? A graphical insight is provided by Figure 6.2. It is clear that after averaging certain energy regions appear, where extended and localized states co-exist. In terms of transport properties it means that if the Fermi energy E_F lies in such a “mixed” energy interval, not all states contribute to the diffusion process. This observation inherently leads to the introduction of a weight of the diffusion pole that measures the fraction of available diffusive states. If this weight is denoted as A^{-1} we can expect the averaged correlation function Φ^{AR} to have a form of a linear combination of formulae (6.24) and (6.25),

$$\Phi^{AR}(\omega + i0, \mathbf{q}) = \frac{1}{A} \frac{2\pi g_F}{-i\omega + Dq^2} + \left(1 - \frac{1}{A}\right) \frac{1}{-i\omega} \frac{2\pi g_F}{1 + (q\xi)^2}. \quad (6.26)$$

Comparing this expression to equation (5.27) achieved in Chapter 5 we see that our mean-field theory for two-particle vertex functions recovers only the diffusive part of the phenomenological formula (6.26). This is due to the above explained impossibility to fit localized states into the Hilbert space of Bloch waves when the thermodynamic limit is considered. The fact that the physics we try to describe is richer than the available state space demonstrates itself as a violation of the particle number conservation law.

Chapter summary

This chapter was devoted to the physical interpretation of some surprising aspects of the mean-field theory for two-particle vertices proposed in Chapter 5. We have demonstrated that the inability to fully comply with Ward identities, i. e. with conservation laws, does not originate in any improper approximations. Rather, it is a fundamental property of the description of disordered systems that uses configurationally averaged Green functions.

It was argued that within this translationally invariant formalism only extended (diffusive) states are accessible. As a consequence, the calculated evolution of the weight of the diffusion pole A^{-1} , starting from one in the weak disorder limit and terminating in zero at the metal-insulator transition (Figure 5.1), can be understood as a manifestation of co-existence of extended and localized states at the Fermi energy E_F . In other words, the position of the mobility edge E_c substantially depends on the configuration of scattering centers even in the thermodynamic limit.

A mean-field approximation for two-particle Green functions was derived within the Anderson model of non-interacting electrons moving on an impure lattice. This approximation was motivated and justified by the asymptotic limit to high spatial dimensions. The determination of the approximate two-particle Green functions amounts to solving just a single algebraic equation for a momentum independent quantity $\bar{\gamma}(E_F + i0, E_F - i0)$. For a weak disorder this quantity is real and positive, and the motion of electrons has the diffusive character. When a certain critical disorder strength is exceeded, a nonzero imaginary part $\Im\bar{\gamma}(E_F + i0, E_F - i0)$ emerges. In such a case the electron diffusion is no longer possible. The function $\Im\bar{\gamma}(E_F + i0, E_F - i0)$ plays the role of an order parameter in the transition from diffusive to non-diffusive phase. Achieved results are in agreement with the scenario that is expected to be followed in three and more spatial dimensions — for a weak disorder the electronic eigenstates are extended throughout the whole sample, whereas for a strong enough disorder all eigenstates become localized in some finite subvolume. In the presented thesis, a consistent and controllable mean-field-like theory of the disorder-driven metal-insulator transition was thereby achieved.

In the course of development of our theory we discovered a rather surprising fact that we are not able to fully comply with conservation laws represented by Ward identities. A further analysis showed that such an inconsistency is not an artifact of our approximations but is of a considerably deeper origin. In Chapter 6 we argued that the utilized formalism of configurationally averaged Green functions, which seems to be the only practicable way to tackle the disordered-electron problem by analytical means, is inherently incomplete. The averaging over disorder configurations produces an artificial translationally invariant electronic system, the Hilbert space of which is the one spanned over the Bloch-wave basis. The problems with conservation laws arise from the fact that such a Hilbert space cannot comprehend all the physical phenomena concerning electrons on disordered lattices, since the localized states are orthogonal to this Bloch-wave space in the thermodynamic limit.

A

Relation between density response and conductivity

As already discussed, the simple derivation of the generalized Einstein relation

$$\sigma(\omega, \mathbf{q}) = \frac{-ie^2\omega}{q^2}\chi(\omega, \mathbf{q}) \quad (2.56)$$

given in Section 2.6 can hardly be considered exact. Here we provide a more reliable reasoning based on the Vollhardt-Wölfle identity

$$\Sigma(z_1, \mathbf{k} + \mathbf{q}) - \Sigma(z_2, \mathbf{k}) = \frac{1}{N} \sum_{\mathbf{k}'} \Lambda_{\mathbf{k}\mathbf{k}'}(z_1, z_2; \mathbf{q}) [G(z_1, \mathbf{k}' + \mathbf{q}) - G(z_2, \mathbf{k}')] . \quad (2.57)$$

We start with the Bethe-Salpeter equation that in momentum representation reads

$$G_{\mathbf{k}\mathbf{k}'}^{(2)}(z_1, z_2; \mathbf{q}) = G(z_1, \mathbf{k} + \mathbf{q})G(z_2, \mathbf{k}) \times \left[\delta(\mathbf{k} - \mathbf{k}') + \frac{1}{N} \sum_{\mathbf{k}''} \Lambda_{\mathbf{k}\mathbf{k}''}(z_1, z_2; \mathbf{q}) G_{\mathbf{k}''\mathbf{k}'}^{(2)}(z_1, z_2; \mathbf{q}) \right] . \quad (2.18)$$

The product of the one-electron propagators on the right-hand side of this formula can be decomposed into

$$G(z_1, \mathbf{k} + \mathbf{q})G(z_2, \mathbf{k}) = -\frac{\Delta_{\mathbf{q}}G(z_1, z_2; \mathbf{k})}{\Delta z - \Delta_{\mathbf{q}}\Sigma(z_1, z_2; \mathbf{k}) - \Delta_{\mathbf{q}}\epsilon(\mathbf{k})} , \quad (A.1)$$

where we denoted $\Delta z = z_2 - z_1$ and

$$\Delta_{\mathbf{q}}\epsilon(\mathbf{k}) = \epsilon(\mathbf{k} + \mathbf{q}) - \epsilon(\mathbf{k}) , \quad (A.2a)$$

$$\Delta_{\mathbf{q}}G(z_1, z_2; \mathbf{k}) = G(z_1, \mathbf{k} + \mathbf{q}) - G(z_2, \mathbf{k}) , \quad (A.2b)$$

$$\Delta_{\mathbf{q}}\Sigma(z_1, z_2; \mathbf{k}) = \Sigma(z_1, \mathbf{k} + \mathbf{q}) - \Sigma(z_2, \mathbf{k}) . \quad (A.2c)$$

Multiplication of both sides of the Bethe-Salpeter equation (2.18) by the denominator from formula (A.1) and utilization of the Ward identity (2.57) yields a “difference” equa-

tion of motion

$$\begin{aligned}
[\Delta_{\mathbf{q}}\epsilon(\mathbf{k}) - \Delta z] G_{\mathbf{k}\mathbf{k}'}^{(2)}(z_1, z_2; \mathbf{q}) &= \Delta_{\mathbf{q}} G(z_1, z_2; \mathbf{k}) \delta(\mathbf{k} - \mathbf{k}') \\
&+ \frac{1}{N} \sum_{\mathbf{k}''} \Lambda_{\mathbf{k}\mathbf{k}''}(z_1, z_2; \mathbf{q}) \left[\Delta_{\mathbf{q}} G(z_1, z_2; \mathbf{k}) G_{\mathbf{k}''\mathbf{k}'}^{(2)}(z_1, z_2; \mathbf{q}) \right. \\
&\quad \left. - G_{\mathbf{k}\mathbf{k}'}^{(2)}(z_1, z_2; \mathbf{q}) \Delta_{\mathbf{q}} G(z_1, z_2; \mathbf{k}'') \right]. \quad (\text{A.3})
\end{aligned}$$

To simplify the notation we define four correlation functions describing density-density, density-current and current-current correlations

$$\Phi(z_1, z_2; \mathbf{q}) = \frac{1}{N^2} \sum_{\mathbf{k}\mathbf{k}'} G_{\mathbf{k}\mathbf{k}'}^{(2)}(z_1, z_2; \mathbf{q}), \quad (\text{A.4a})$$

$$\Phi_{\epsilon}(z_1, z_2; \mathbf{q}) = \frac{1}{N^2} \sum_{\mathbf{k}\mathbf{k}'} \Delta_{\mathbf{q}}\epsilon(\mathbf{k}) G_{\mathbf{k}\mathbf{k}'}^{(2)}(z_1, z_2; \mathbf{q}), \quad (\text{A.4b})$$

$$\bar{\Phi}_{\epsilon}(z_1, z_2; \mathbf{q}) = \frac{1}{N^2} \sum_{\mathbf{k}\mathbf{k}'} G_{\mathbf{k}\mathbf{k}'}^{(2)}(z_1, z_2; \mathbf{q}) \Delta_{\mathbf{q}}\epsilon(\mathbf{k}'), \quad (\text{A.4c})$$

$$\Phi_{\epsilon\epsilon}(z_1, z_2; \mathbf{q}) = \frac{1}{N^2} \sum_{\mathbf{k}\mathbf{k}'} \Delta_{\mathbf{q}}\epsilon(\mathbf{k}) G_{\mathbf{k}\mathbf{k}'}^{(2)}(z_1, z_2; \mathbf{q}) \Delta_{\mathbf{q}}\epsilon(\mathbf{k}'). \quad (\text{A.4d})$$

Summing up formula (A.3) over momenta \mathbf{k} and \mathbf{k}' we arrive at a continuity equation relating the density-density and the density-current correlation functions,

$$\Phi_{\epsilon}(z_1, z_2; \mathbf{q}) - \Delta z \Phi(z_1, z_2; \mathbf{q}) = \frac{1}{N} \sum_{\mathbf{k}} \Delta_{\mathbf{q}} G(z_1, z_2; \mathbf{k}). \quad (\text{A.5a})$$

The terms with the two-particle irreducible vertex Λ standing in equation (A.3) cancel each other provided this vertex is symmetric, i. e., $\Lambda_{\mathbf{k}\mathbf{k}'} = \Lambda_{\mathbf{k}'\mathbf{k}}$.

Another continuity equation can be derived by multiplying expression (A.3) with the energy difference $\Delta_{\mathbf{q}}\epsilon(\mathbf{k})$ and then performing the summation over the fermionic momenta \mathbf{k} and \mathbf{k}' . Doing so we obtain an equation relating the current-current and the density-current correlation functions,

$$\Phi_{\epsilon\epsilon}(z_1, z_2; \mathbf{q}) - \Delta z \bar{\Phi}_{\epsilon}(z_1, z_2; \mathbf{q}) = \frac{1}{N} \sum_{\mathbf{k}} \Delta_{\mathbf{q}} G(z_1, z_2; \mathbf{k}) \Delta_{\mathbf{q}}\epsilon(\mathbf{k}). \quad (\text{A.5b})$$

Combination of the above two continuity equations, formulae (A.5a) and (A.5b), yield a relation between the current-current and the density-density correlation functions,

$$\Phi_{\epsilon\epsilon}(z_1, z_2; \mathbf{q}) - (\Delta z)^2 \Phi(z_1, z_2; \mathbf{q}) = \frac{1}{N} \sum_{\mathbf{k}} \Delta_{\mathbf{q}} G(z_1, z_2; \mathbf{k}) [\Delta z + \Delta_{\mathbf{q}}\epsilon(\mathbf{k})]. \quad (\text{A.5c})$$

This formula replaces the operator continuity equation (2.53) from the original reasoning leading to the generalized Einstein relation (2.56), Section 2.6.

Now we apply the obtained results, equations (A.5), to response functions. To do so we define a generalization of the electrical conductivity

$$\begin{aligned}
\sigma_{\epsilon\epsilon}(\omega, \mathbf{q}) &= -e^2 \int_{-\infty}^{\infty} \frac{dE}{2\pi\omega} \left\{ [f(E + \omega) - f(E)] \Phi_{\epsilon\epsilon}^{AR}(E, E + \omega; \mathbf{q}) \right. \\
&\quad + f(E) \Phi_{\epsilon\epsilon}^{RR}(E, E + \omega; \mathbf{q}) - f(E + \omega) \Phi_{\epsilon\epsilon}^{AA}(E, E + \omega; \mathbf{q}) \\
&\quad \left. - f(E) [\Phi_{\epsilon\epsilon}^{RR}(E, E; \mathbf{q}) - \Phi_{\epsilon\epsilon}^{AA}(E, E; \mathbf{q})] \right\}. \quad (\text{A.6})
\end{aligned}$$

The continuity equation (A.5c) then straightforwardly provides the desired equation relating the conductivity $\sigma_{\epsilon\epsilon}$ and the density response χ ,

$$\begin{aligned} \sigma_{\epsilon\epsilon}(\omega, \mathbf{q}) + ie^2\omega\chi(\omega, \mathbf{q}) &= \frac{e^2}{\omega} \int_{-\infty}^{\infty} \frac{dE}{2\pi} f(E) [\Phi_{\epsilon\epsilon}^{RR}(E, E; \mathbf{q}) - \Phi_{\epsilon\epsilon}^{AA}(E, E; \mathbf{q})] \\ &\quad - \frac{ie^2}{\omega} \int_{-\infty}^{\infty} \frac{dE}{\pi} f(E) \frac{1}{N} \sum_{\mathbf{k}} \Delta_{\mathbf{q}\epsilon}(\mathbf{k}) [\Im G^R(E, \mathbf{k} + \mathbf{q}) - \Im G^R(E, \mathbf{k})] = 0. \end{aligned} \quad (\text{A.7})$$

Vanishing of the right-hand side of formula (A.7) can be explicitly manifested if the continuity equation (A.5c) is applied to the correlation functions $\Phi_{\epsilon\epsilon}^{RR}$ and $\Phi_{\epsilon\epsilon}^{AA}$. Doing so, the two terms on the right-hand side of equation (A.7) are easily shown to add to zero.

The remaining step is to elucidate how the generalized conductivity $\sigma_{\epsilon\epsilon}$ relates to the physical one. Such a connection can generally be found only in the limit $\mathbf{q} \rightarrow \mathbf{0}$. In such a case the energy difference $\Delta_{\mathbf{q}\epsilon}(\mathbf{k})$, defined by formula (A.2a), can be written in the form

$$\Delta_{\mathbf{q}\epsilon}(\mathbf{k}) = \frac{1}{2} \mathbf{q} \cdot [\mathbf{v}(\mathbf{k}) + \mathbf{v}(\mathbf{k} + \mathbf{q})] + O(q^3). \quad (\text{A.8})$$

As a consequence, the correlation function $\Phi_{\epsilon\epsilon}$ is given by $\Phi_{\epsilon\epsilon} = \sum_{\alpha\beta} q_{\alpha}q_{\beta}\Phi_{\alpha\beta}$,¹ where $\Phi_{\alpha\beta}$ stands for the physical current-current correlation function (compare with the earlier definition (2.46)),

$$\Phi_{\alpha\beta}(z_1, z_2; \mathbf{q}) = \frac{1}{N^2} \sum_{\mathbf{k}\mathbf{k}'} [v_{\alpha}(\mathbf{k}) + v_{\alpha}(\mathbf{k} + \mathbf{q})] [v_{\beta}(\mathbf{k}') + v_{\beta}(\mathbf{k}' + \mathbf{q})] G_{\mathbf{k}\mathbf{k}'}^{(2)}(z_1, z_2; \mathbf{q}). \quad (\text{A.9})$$

Assuming an isotropic lattice, formula (A.7) finally goes over to identity (2.56) that we aimed to prove. Note again that its validity is restricted only to the hydrodynamic limit, $\mathbf{q} \rightarrow \mathbf{0}$.

The same result might also be obtained using a different procedure based on the Velický identity (2.21). Such an approach, together with the one presented here, can be found in [69].

¹Note that for the quadratic dispersion relation $\epsilon(\mathbf{k}) = k^2/2m$ this expression holds for any momenta \mathbf{q} .

B

CPA for two-particle functions

Here we present a particular method how to derive the two-particle irreducible vertex λ consistent with the coherent-potential approximation for the selfenergy Σ , defined from the Soven equation

$$\left\langle \frac{1}{1 + (\Sigma(z) - V)G(z)} \right\rangle_{\text{av.}} = 1. \quad (3.4)$$

We follow the guidelines for the construction of conserving approximations given by Baym and Kadanoff in References 46 and 70.

The key step is to introduce an unphysical external field U so that derivatives of the corresponding one-particle Green function with respect to this field give elements of the two-particle Green function. We confine our discussion to the local quantity $G_{ii,ii}^{(2)}(z_1, z_2) = \langle \mathcal{G}_{ii}(z_1)\mathcal{G}_{ii}(z_2) \rangle_{\text{av.}}$ as it is sufficient for our purposes. The generalized Green function that provides the desired mixing of energy variables z_1 and z_2 is

$$\mathbb{G}^{-1} = \begin{pmatrix} \mathcal{G}_{ii}^{-1}(z_1) & -U \\ -U & \mathcal{G}_{ii}^{-1}(z_2) \end{pmatrix}. \quad (B.1)$$

From now on, all Green function elements, configuration dependent as well as averaged, are local. We can thus safely omit the subscripts ii in the rest of this appendix. Besides that, we drop also the subscript “av.” standing at the angular brackets, which denote the configurational averaging, since it cannot lead to any kind of confusion either.

From the equation $\mathbb{G}^{-1}\mathbb{G} = \mathbb{I}$ we find individual elements of the resolvent (B.1). They read

$$\mathbb{G}_{11} = \frac{\mathcal{G}^{-1}(z_2)}{\mathcal{G}^{-1}(z_1)\mathcal{G}^{-1}(z_2) - U^2} \quad \text{and} \quad \mathbb{G}_{12} = \mathbb{G}_{21} = \frac{U}{\mathcal{G}^{-1}(z_1)\mathcal{G}^{-1}(z_2) - U^2}. \quad (B.2)$$

The two-particle Green function we want to study is the derivative of the off-diagonal element with respect to the field U ,

$$\left\langle \frac{\delta \mathbb{G}_{12}}{\delta U} \Big|_{U=0} \right\rangle = \langle \mathcal{G}(z_1)\mathcal{G}(z_2) \rangle. \quad (B.3)$$

The other two derivatives give zero at the point $U = 0$,

$$\left\langle \frac{\delta \mathbb{G}_{11}}{\delta U} \Big|_{U=0} \right\rangle = \left\langle \frac{\delta \mathbb{G}_{22}}{\delta U} \Big|_{U=0} \right\rangle = 0. \quad (B.4)$$

In the above two formulae, (B.3) and (B.4), we performed the derivative first and only then we did the configurational averaging. In the following we reverse the order of these operations assuming that they commute. As far as the selfenergy is a local quantity, which it is in the CPA, the averaged Green function (B.1) can be written in the form

$$\langle \mathbb{G} \rangle^{-1} = \begin{pmatrix} G^{-1}(z_1) & -U - \Sigma_{12} \\ -U - \Sigma_{12} & G^{-1}(z_2) \end{pmatrix}. \quad (\text{B.5})$$

The derivative with respect to the coupling field U is found with the aid of the identity $\langle \mathbb{G} \rangle^{-1} \langle \mathbb{G} \rangle = \mathbb{I}$. We have

$$\begin{aligned} \left. \frac{\delta \langle \mathbb{G} \rangle}{\delta U} \right|_{U=0} &= - \langle \mathbb{G} \rangle \left. \frac{\delta \langle \mathbb{G} \rangle^{-1}}{\delta U} \langle \mathbb{G} \rangle \right|_{U=0} \\ &= \begin{pmatrix} G(z_1) \frac{\delta G^{-1}(z_1)}{\delta U} G(z_1) & G(z_1) \left(1 + \frac{\delta \Sigma_{12}}{\delta U} \right) G(z_2) \\ G(z_2) \left(1 + \frac{\delta \Sigma_{12}}{\delta U} \right) G(z_1) & G(z_2) \frac{\delta G^{-1}(z_2)}{\delta U} G(z_2) \end{pmatrix}, \end{aligned} \quad (\text{B.6})$$

where the derivatives on the right-hand side are taken at the point $U = 0$. The same applies to all such derivatives in the following formulae even if not explicitly noted. Comparing expressions (B.3) and (B.6) we obtain an equation

$$\begin{aligned} \langle \mathcal{G}(z_1) \mathcal{G}(z_2) \rangle &= G(z_1) G(z_2) + G(z_1) G(z_2) \frac{\delta \Sigma_{12}}{\delta U} \\ &= G(z_1) G(z_2) + G(z_1) G(z_2) \left(\frac{\delta \Sigma_{12}}{\delta \langle \mathbb{G}_{12} \rangle} \frac{\delta \langle \mathbb{G}_{12} \rangle}{\delta U} \right. \\ &\quad \left. + \frac{\delta \Sigma_{12}}{\delta \langle \mathbb{G}_{11} \rangle} \frac{\delta \langle \mathbb{G}_{11} \rangle}{\delta U} + \frac{\delta \Sigma_{12}}{\delta \langle \mathbb{G}_{22} \rangle} \frac{\delta \langle \mathbb{G}_{22} \rangle}{\delta U} \right). \end{aligned} \quad (\text{B.7})$$

The second equality assumes that the selfenergy Σ depends on the field U only through the Green function \mathbb{G} , i. e., it has a functional form $\Sigma = \Sigma[\mathbb{G}]$. Such an assumption is compatible with the Soven equation (3.4). Inserting derivatives (B.3) and (B.4) into formula (B.7) we easily come to the Bethe-Salpeter equation

$$\langle \mathcal{G}(z_1) \mathcal{G}(z_2) \rangle = G(z_1) G(z_2) + G(z_1) G(z_2) \frac{\delta \Sigma_{12}}{\delta \langle \mathbb{G}_{12} \rangle} \langle \mathcal{G}(z_1) \mathcal{G}(z_2) \rangle, \quad (\text{B.8})$$

where we can identify the two-particle irreducible vertex λ as a functional derivative of the selfenergy Σ with respect to the generalized Green function \mathbb{G} ,

$$\lambda(z_1, z_2) = \left. \frac{\delta \Sigma_{12}}{\delta \langle \mathbb{G}_{12} \rangle} \right|_{U=0}. \quad (\text{B.9})$$

This formula can be evaluated with the aid of the Soven equation (3.4), extension of which to the presence of the coupling field U is quite straightforward and reads

$$\langle \mathbb{A}^{-1} \rangle = \mathbb{I}, \quad \text{where} \quad \mathbb{A} = \mathbb{I} + \begin{pmatrix} \Sigma(z_1) - V & \Sigma_{12} \\ \Sigma_{12} & \Sigma(z_2) - V \end{pmatrix} \mathbb{G}. \quad (\text{B.10})$$

Now we perform the derivative of this equation with respect to $\langle \mathbb{G}_{12} \rangle$ and then express $\delta \mathbb{A}^{-1} / \delta \langle \mathbb{G}_{12} \rangle$ in terms of $\delta \mathbb{A} / \delta \langle \mathbb{G}_{12} \rangle$ using the same procedure that was utilized to arrive at equation (B.6). In this way we find formulae

$$\left. \frac{\delta \langle \mathbb{A}^{-1} \rangle}{\delta \langle \mathbb{G}_{12} \rangle} \right|_{U=0} = \left\langle \frac{\delta \mathbb{A}^{-1}}{\delta \langle \mathbb{G}_{12} \rangle} \right\rangle \Big|_{U=0} = - \left\langle \mathbb{A}^{-1} \frac{\delta \mathbb{A}}{\delta \langle \mathbb{G}_{12} \rangle} \mathbb{A}^{-1} \right\rangle \Big|_{U=0} = 0 \quad (\text{B.11})$$

and

$$\left. \frac{\delta \mathbb{A}}{\delta \langle \mathbb{G}_{12} \rangle} \right|_{U=0} = \begin{pmatrix} \frac{\delta \Sigma(z_1)}{\delta \langle \mathbb{G}_{12} \rangle} G(z_1) & \frac{\delta \Sigma_{12}}{\delta \langle \mathbb{G}_{12} \rangle} G(z_2) + \Sigma(z_1) - V \\ \frac{\delta \Sigma_{12}}{\delta \langle \mathbb{G}_{12} \rangle} G(z_2) + \Sigma(z_2) - V & \frac{\delta \Sigma(z_2)}{\delta \langle \mathbb{G}_{12} \rangle} G(z_2) \end{pmatrix}. \quad (\text{B.12})$$

Inserting derivative (B.12) into formula (B.11) provides four equations for the derivatives $\delta \Sigma / \delta \langle \mathbb{G} \rangle$. The two diagonal equations are not of our interest as they are not linked to the irreducible vertex λ , formula (B.9). On the other hand, the off-diagonal equations involve this vertex. Writing them explicitly we have

$$\left\langle \frac{1}{1 + (\Sigma(z_1) - V)G(z_1)} \left(\frac{\delta \Sigma_{12}}{\delta \langle \mathbb{G}_{12} \rangle} G(z_2) + \Sigma(z_1) - V \right) \times \frac{1}{1 + (\Sigma(z_2) - V)G(z_2)} \right\rangle = 0, \quad (\text{B.13a})$$

$$\left\langle \frac{1}{1 + (\Sigma(z_2) - V)G(z_2)} \left(\frac{\delta \Sigma_{12}}{\delta \langle \mathbb{G}_{12} \rangle} G(z_1) + \Sigma(z_2) - V \right) \times \frac{1}{1 + (\Sigma(z_1) - V)G(z_1)} \right\rangle = 0. \quad (\text{B.13b})$$

To derive these formulae we used the fact that the matrices \mathbb{A} and \mathbb{A}^{-1} are diagonal at the point $U = 0$. After some algebra, equation (B.13a) transforms to a form

$$\begin{aligned} \frac{\delta \Sigma_{12}}{\delta \langle \mathbb{G}_{12} \rangle} G(z_2) \left\langle \frac{1}{1 + (\Sigma(z_1) - V)G(z_1)} \frac{1}{1 + (\Sigma(z_2) - V)G(z_2)} \right\rangle = \\ \frac{1}{G(z_1)} \left[\left\langle \frac{1}{1 + (\Sigma(z_1) - V)G(z_1)} \frac{1}{1 + (\Sigma(z_2) - V)G(z_2)} \right\rangle - \right. \\ \left. \underbrace{\left\langle \frac{1}{1 + (\Sigma(z_2) - V)G(z_2)} \right\rangle}_{= 1, \text{ cf. (3.4)}} \right] \end{aligned} \quad (\text{B.14})$$

that directly leads to the desired expression for the two-particle irreducible vertex $\lambda = \delta \Sigma_{12} / \delta \langle \mathbb{G}_{12} \rangle$,

$$\lambda(z_1, z_2) = \frac{1}{G(z_1)G(z_2)} \left[1 - \left\langle \frac{1}{1 + (\Sigma(z_1) - V)G(z_1)} \frac{1}{1 + (\Sigma(z_2) - V)G(z_2)} \right\rangle^{-1} \right]. \quad (\text{B.15})$$

Finally we utilize the property that both equations (B.13) provide the same solution for the vertex λ . This symmetry allows to formulate a Ward identity. In order to do so we rewrite equations (B.13) to the following form,

$$(\lambda(z_1, z_2)G(z_2) + \Sigma(z_1)) \left\langle \frac{1}{1 + (\Sigma(z_1) - V)G(z_1)} \frac{1}{1 + (\Sigma(z_2) - V)G(z_2)} \right\rangle = \left\langle \frac{V}{1 + (\Sigma(z_1) - V)G(z_1)} \frac{1}{1 + (\Sigma(z_2) - V)G(z_2)} \right\rangle, \quad (\text{B.16a})$$

$$(\lambda(z_1, z_2)G(z_1) + \Sigma(z_2)) \left\langle \frac{1}{1 + (\Sigma(z_1) - V)G(z_1)} \frac{1}{1 + (\Sigma(z_2) - V)G(z_2)} \right\rangle = \left\langle \frac{V}{1 + (\Sigma(z_1) - V)G(z_1)} \frac{1}{1 + (\Sigma(z_2) - V)G(z_2)} \right\rangle. \quad (\text{B.16b})$$

Comparing the right-hand sides of these formulae we end up with a simple equality involving one- and two-particle irreducible vertices,

$$\Sigma(z_1) - \Sigma(z_2) = \lambda(z_1, z_2) [G(z_1) - G(z_2)], \quad (\text{B.17})$$

that is just the Vollhardt-Wölfle identity (2.57) in the momentum independent case.

C

Convolutions in high spatial dimensions

The limit to high spatial dimensions is used in Chapter 5 to substantially reduce momentum dependencies of one- and two-particle functions. With the help of such simplifications the parquet equations become soluble. In this appendix we present a derivation of the asymptotic representation of the off-diagonal (non-local) elements of elementary one- and two-particle functions,

$$\bar{G}_1(\mathbf{k}_1) = G_1(\mathbf{k}_1) - \chi_1 \doteq t \langle G^2(z_1) \rangle x(\mathbf{k}_1) \quad (5.2)$$

and

$$\bar{\chi}_{12} = \frac{1}{N} \sum_{\mathbf{k}} \bar{G}_1(\mathbf{k} + \mathbf{q}_1) \bar{G}_2(\mathbf{k} + \mathbf{q}_2) \doteq \frac{1}{2} t^2 \langle G^2(z_1) \rangle \langle G^2(z_2) \rangle X(\mathbf{q}_1 - \mathbf{q}_2) \quad (5.5)$$

In these expressions, two new functions of fermionic and bosonic momentum were introduced, $x(\mathbf{k}) = d^{-1/2} \sum_{\nu=1}^d \cos k_\nu$ and $X(\mathbf{q}) = d^{-1} \sum_{\nu=1}^d \cos q_\nu$. The local element of the one-particle Green function is denoted $\chi_1 = L^{-d} \sum_{\mathbf{k}} G_1(\mathbf{k})$ throughout this appendix. To simplify the notation, the energy arguments are indicated via subscripts of the respective functions.

For performing calculations in the high-dimensional limit of the hypercubic lattice we adopt methods similar to those of Reference 71. In this approach, the one-particle resolvents are written in the form of an exponential

$$G(z, \mathbf{k}) = \frac{1}{z - \Sigma(z) - \epsilon(\mathbf{k})} = \begin{cases} -\int_0^\infty d\lambda e^{i\lambda[z - \Sigma(z) - \epsilon(\mathbf{k})]} & \text{if } \Im z > 0, \\ \int_{-\infty}^0 d\lambda e^{i\lambda[z - \Sigma(z) - \epsilon(\mathbf{k})]} & \text{if } \Im z < 0. \end{cases} \quad (C.1)$$

The energy dispersion relation corresponding to the scaled Hamiltonian (5.1) reads $\epsilon(\mathbf{k}) = -td^{-1/2} \sum_{\nu=1}^d \cos k_\nu = -tx(\mathbf{k})$ where we set the lattice constant $a = 1$. The selfenergy Σ used in the exponential representation (C.1) is local and d -independent, i. e., it is the selfenergy from the $d = \infty$ limit (CPA). It is easily demonstrated that corrections to the CPA value do not influence the leading order of the expansion of G in powers of d^{-1} . The

reason is that the non-local selfenergy contributions have the high-dimensional asymptotics $\sim d^{-3/2}$ as follows from the diagrammatic analysis, [62, 65]. Because we are interested in just the leading order of the d^{-1} expansion, we can safely continue with the local (CPA) selfenergy only.

At first we evaluate the convolution involving two one-electron resolvents,

$$\begin{aligned}\chi_{12} &= \frac{1}{N} \sum_{\mathbf{k}} G_1(\mathbf{k} + \mathbf{q}_1) G_2(\mathbf{k} + \mathbf{q}_2) \\ &= \frac{1}{N} \sum_{\mathbf{k}} \int d^2\lambda e^{i\lambda_1\zeta_1 + i\lambda_2\zeta_2} \\ &\quad \times \prod_{\nu=1}^d \exp\left(i\lambda_1 \frac{t}{\sqrt{d}} \cos k_{\nu} \cos q_{1,\nu} - i\lambda_1 \frac{t}{\sqrt{d}} \sin k_{\nu} \sin q_{1,\nu} \right. \\ &\quad \left. + i\lambda_2 \frac{t}{\sqrt{d}} \cos k_{\nu} \cos q_{2,\nu} - i\lambda_2 \frac{t}{\sqrt{d}} \sin k_{\nu} \sin q_{2,\nu} \right).\end{aligned}\quad (\text{C.2})$$

The integration limits for variables λ as well as the overall sign are not explicitly written. They depend on signs of imaginary parts of the energies z and can be readily reconstructed at any point of the following derivation. The new quantity ζ abbreviates the difference $z - \Sigma(z)$. The exponentials of cosines and sines in expression (C.2) are expanded up to second order, i. e. up to d^{-1} . Replacing the sums over momentum components with integrals, $N^{-1/d} \sum_{k_{\nu}} \rightarrow (2\pi)^{-1} \int_{-\pi}^{\pi} dk_{\nu}$, and using the elementary formulae,

$$\int_{-\pi}^{\pi} \frac{dk_{\nu}}{2\pi} \cos^2 k_{\nu} = \int_{-\pi}^{\pi} \frac{dk_{\nu}}{2\pi} \sin^2 k_{\nu} = \frac{1}{2} \quad \text{and} \quad \int_{-\pi}^{\pi} \frac{dk_{\nu}}{2\pi} \cos k_{\nu} \sin k_{\nu} = 0, \quad (\text{C.3})$$

leads to a representation

$$\chi_{12} = \int d^2\lambda e^{i\lambda_1\zeta_1 + i\lambda_2\zeta_2} \exp\left[-\frac{t^2}{4}(\lambda_1^2 + \lambda_2^2) - \lambda_1\lambda_2 \frac{t^2}{2} X(\mathbf{q}_1 - \mathbf{q}_2) \right]. \quad (\text{C.4})$$

The exponential was restored with the aid of the well-known formula

$$\prod_{\nu=1}^d \left(1 + \frac{f_{\nu}}{d} \right) \xrightarrow{d \rightarrow \infty} \exp\left(\frac{1}{d} \sum_{\nu=1}^d f_{\nu} \right). \quad (\text{C.5})$$

To extract the non-local contribution $\bar{\chi}_{12}$ we have to subtract the product of the local Green function elements from the full ‘‘bubble’’ χ_{12} . These local elements, evaluated with the same precision as expression (C.4), read

$$\chi_{1,2} = \int d\lambda e^{i\lambda\zeta_{1,2}} \exp\left[-\frac{t^2}{4}\lambda^2 \right]. \quad (\text{C.6})$$

Consequently, the convolution $\bar{\chi}_{12}$ has a form

$$\bar{\chi}_{12} = \chi_{12} - \chi_1\chi_2 \doteq - \int d^2\lambda e^{i\lambda_1\zeta_1 + i\lambda_2\zeta_2} \exp\left[-\frac{t^2}{4}(\lambda_1^2 + \lambda_2^2) \right] \lambda_1\lambda_2 \frac{t^2}{2} X(\mathbf{q}_1 - \mathbf{q}_2) \quad (\text{C.7})$$

where we retained only the first non-vanishing term of the expansion in powers of the momentum-dependent function X . It means that all contributions with $X^n(\mathbf{q}_1 - \mathbf{q}_2)$, $n > 1$, were neglected. Finally, the integrals in expression (C.7) can be rewritten using the following equalities,

$$\int d\lambda \lambda e^{i\lambda\zeta_1} \exp\left[-\frac{t^2}{4}\lambda^2\right] = -i\frac{\partial\chi_1}{\partial\zeta_1} = i\frac{1}{N} \sum_{\mathbf{k}} \frac{1}{[\zeta_1 - \epsilon(\mathbf{k})]^2} = i\langle G^2(z_1) \rangle. \quad (\text{C.8})$$

In this way we recover the asymptotic expression (5.5) announced at the beginning of this appendix.

At this moment it is useful to summarize the key steps that led to the approximate formula (C.7). These simplifications are

- expansion in powers of d^{-1} and dropping all terms except the leading one, which is of order $O(1)$,
- and subsequent retaining of only the slowest non-vanishing mode of the momentum dependence.

In the rest of the appendix we focus on justification of the asymptotic expression for the off-diagonal propagator \bar{G} , equation (5.2). Such a Green function obviously generates our approximation of the non-local “bubble”, formula (5.5). However, a question arises, how the effective propagator (5.2) performs for higher-order convolutions. The quantity built up of n one-particle Green functions in an analogous way as the two-particle “bubble” (C.2) reads

$$\begin{aligned} \chi_{12\dots n} &= \frac{1}{N} \sum_{\mathbf{k}} G_1(\mathbf{k} + \mathbf{q}_1) G_2(\mathbf{k} + \mathbf{q}_2) \dots G_n(\mathbf{k} + \mathbf{q}_n) \\ &= \int d^n\lambda \exp\left[i \sum_{i=1}^n \lambda_i \zeta_i - \frac{t^2}{4} \sum_{i=1}^n \lambda_i^2 - \frac{t^2}{2} \sum_{\substack{i,j=1 \\ i<j}}^n \lambda_i \lambda_j X(\mathbf{q}_i - \mathbf{q}_j) \right]. \end{aligned} \quad (\text{C.9})$$

This is a generalization of formula (C.4), i. e., it is just the leading-order term of the d^{-1} expansion. We use expression (C.9) to evaluate the non-local convolution $\bar{\chi}_{1234}$. The subtraction of local terms becomes more and more tedious with the increasing number of one-particle Green functions involved. Within the approximation rules listed above we have

$$\begin{aligned} \bar{\chi}_{1234} &= \chi_{1234} - 3\chi_1\chi_2\chi_3\chi_4 - \chi_1\chi_{234} - \chi_2\chi_{134} - \chi_3\chi_{124} - \chi_4\chi_{123} \\ &\quad + \chi_1\chi_2\chi_{34} + \chi_1\chi_3\chi_{24} + \chi_1\chi_4\chi_{23} + \chi_2\chi_3\chi_{14} + \chi_2\chi_4\chi_{13} + \chi_3\chi_4\chi_{12} \\ &\doteq \frac{t^4}{4} \prod_{i=1}^4 \langle G^2(z_i) \rangle [X(\mathbf{q}_1 - \mathbf{q}_2)X(\mathbf{q}_3 - \mathbf{q}_4) + X(\mathbf{q}_1 - \mathbf{q}_3)X(\mathbf{q}_2 - \mathbf{q}_4) \\ &\quad + X(\mathbf{q}_1 - \mathbf{q}_4)X(\mathbf{q}_2 - \mathbf{q}_3)]. \end{aligned} \quad (\text{C.10})$$

To reach the first non-vanishing term we had to expand the exponential in expression (C.9) up to X^2 . Generally, to evaluate a convolution of $2n$ propagators the expansion in momentum variables needs to be performed up to terms of the order X^n .

Formula (C.10) has a form of the sum of all complete pair-wise contractions on four nodes that allows for the following simple notation that resembles the Wick theorem from the quantum field theory,

$$\begin{aligned}
& \frac{1}{N} \sum_{\mathbf{k}} \bar{G}_1(\mathbf{k} + \mathbf{q}_1) \bar{G}_2(\mathbf{k} + \mathbf{q}_2) \bar{G}_3(\mathbf{k} + \mathbf{q}_3) \bar{G}_4(\mathbf{k} + \mathbf{q}_4) \\
& \doteq \overbrace{\bar{G}_1(\mathbf{q}_1) \bar{G}_2(\mathbf{q}_2)} \overbrace{\bar{G}_3(\mathbf{q}_3) \bar{G}_4(\mathbf{q}_4)} + \overbrace{\bar{G}_1(\mathbf{q}_1) \bar{G}_2(\mathbf{q}_2) \bar{G}_3(\mathbf{q}_3) \bar{G}_4(\mathbf{q}_4)} \\
& \quad + \overbrace{\bar{G}_1(\mathbf{q}_1) \bar{G}_2(\mathbf{q}_2) \bar{G}_3(\mathbf{q}_3) \bar{G}_4(\mathbf{q}_4)}. \quad (\text{C.11})
\end{aligned}$$

Every indicated elementary contraction between points i and j brings in the factor $W_{ij} X(\mathbf{q}_i - \mathbf{q}_j)/2$ with W_{ij} abbreviating the combination $t^2 \langle G^2(z_i) \rangle \langle G^2(z_j) \rangle$.

Now we take a look what we get if four effective off-diagonal Green functions (5.2) are convoluted. The overall factor $W_{12}W_{34}$ is obvious and the momentum dependent part can be evaluated as follows,

$$\begin{aligned}
& \frac{1}{N} \sum_{\mathbf{k}} x(\mathbf{k} + \mathbf{q}_1) x(\mathbf{k} + \mathbf{q}_2) x(\mathbf{k} + \mathbf{q}_3) x(\mathbf{k} + \mathbf{q}_4) \\
& = \frac{1}{N^{2/d} d^2} \sum_{\substack{\mu, \nu \\ \mu \neq \nu}} \sum_{k_\mu, k_\nu} [\cos(k_\mu + q_{1,\mu}) \cos(k_\mu + q_{2,\mu}) \cos(k_\nu + q_{3,\nu}) \cos(k_\nu + q_{4,\nu}) \\
& \quad + 2 \text{ other pairings}] \\
& \quad + \frac{1}{N^{1/d} d^2} \sum_{\nu} \sum_{k_\nu} \cos(k_\nu + q_{1,\nu}) \cos(k_\nu + q_{2,\nu}) \cos(k_\nu + q_{3,\nu}) \cos(k_\nu + q_{4,\nu}) \\
& = \frac{1}{4d^2} \sum_{\substack{\mu, \nu \\ \mu \neq \nu}} [\cos(q_{1,\mu} - q_{2,\mu}) \cos(q_{3,\nu} - q_{4,\nu}) + 2 \text{ other pairings}] \\
& \quad + \frac{1}{8d} [X(-\mathbf{q}_1 - \mathbf{q}_2 + \mathbf{q}_3 + \mathbf{q}_4) \\
& \quad \quad + X(\mathbf{q}_1 - \mathbf{q}_2 + \mathbf{q}_3 - \mathbf{q}_4) + X(-\mathbf{q}_1 + \mathbf{q}_2 + \mathbf{q}_3 - \mathbf{q}_4)] \\
& = \frac{1}{4} [X(\mathbf{q}_1 - \mathbf{q}_2) X(\mathbf{q}_3 - \mathbf{q}_4) \\
& \quad \quad + X(\mathbf{q}_1 - \mathbf{q}_3) X(\mathbf{q}_2 - \mathbf{q}_4) + X(\mathbf{q}_1 - \mathbf{q}_4) X(\mathbf{q}_2 - \mathbf{q}_3)] \\
& \quad + \frac{1}{8d} [X(-\mathbf{q}_1 - \mathbf{q}_2 + \mathbf{q}_3 + \mathbf{q}_4) \\
& \quad \quad + X(\mathbf{q}_1 - \mathbf{q}_2 + \mathbf{q}_3 - \mathbf{q}_4) + X(-\mathbf{q}_1 + \mathbf{q}_2 + \mathbf{q}_3 - \mathbf{q}_4)]. \quad (\text{C.12})
\end{aligned}$$

The first equality employs the fact that only products of an even number of cosines with common integration variable survive the momentum integration. In the last step, the summand with $\mu = \nu$ is added to the sum over μ, ν and removed again at an other part of the expression. We see that formulae (C.10) and (C.12) differ only in the $O(d^{-1})$ -term that makes them equal with respect to our approximation defined above. The same applies to any convolution of $2n$ one-particle propagators. On the other hand, momentum sums of the odd number of Green functions behave quite differently. For example, the

correct high-dimensional asymptotics of the function $\bar{\chi}_{123}$ reads

$$\begin{aligned}\bar{\chi}_{123} &= \chi_{123} + 2\chi_1\chi_2\chi_3 - \chi_1\chi_{23} - \chi_2\chi_{13} - \chi_3\chi_{12} \\ &\doteq -i\frac{t^4}{4}\prod_{i=1}^3\langle G^2(z_i)\rangle [X(\mathbf{q}_1 - \mathbf{q}_2)X(\mathbf{q}_1 - \mathbf{q}_3) + X(\mathbf{q}_1 - \mathbf{q}_2)X(\mathbf{q}_2 - \mathbf{q}_3) \\ &\quad + X(\mathbf{q}_1 - \mathbf{q}_3)X(\mathbf{q}_2 - \mathbf{q}_3)],\end{aligned}\tag{C.13}$$

whereas the evaluation using the effective one-particle Green function (5.2) gives an incorrect value, $\bar{\chi}_{123} = 0$. Such a discrepancy is not, however, crucial for our considerations. The reason is that we aim at applying the method of high-dimensional evaluation of convolutions, explained in this appendix, only to two-particle functions. These are build up of diagrams involving only even numbers of one-particle Green functions.

D

Self-consistent asymptotic solution for two-particle vertices in the strict limit $d = \infty$

At the end of Chapter 5 we examined predictions of our self-consistent theory for two-particle vertex functions, defined by equations

$$\bar{\Lambda}_{\mathbf{k}\mathbf{k}'}^{ee}(\mathbf{q}) = \gamma + \bar{\gamma} \frac{\bar{\gamma} \bar{\chi}(\mathbf{q})}{1 - \bar{\gamma} \bar{\chi}(\mathbf{q})} \quad \text{and} \quad \bar{\gamma} = \gamma + \bar{\gamma} \frac{1}{N} \sum_{\mathbf{q}} \frac{\bar{\gamma}^2 \bar{\chi}^2(\mathbf{q})}{1 - \bar{\gamma} \bar{\chi}(\mathbf{q})}, \quad (5.15a,b)$$

in physically most interesting dimensions, $d = 1, 2, 3$. Here we apply this theory to the infinite-dimensional hypercubic lattice, $d = \infty$, and compare the obtained results with the conclusions of Section 5.1 where this spatial dimensionality was studied by purely perturbative means.

In the limit $d \rightarrow \infty$, the momentum summation in equation (5.15b) can be evaluated by using the Gaussian rules formulated in Appendix C,

$$f_d = \frac{1}{N} \sum_{\mathbf{q}} \frac{\bar{\gamma}^2 \bar{\chi}^2(\mathbf{q})}{1 - \bar{\gamma} \bar{\chi}(\mathbf{q})} = \sum_{m=2}^{\infty} \frac{1}{N} \sum_{\mathbf{q}} \bar{\gamma}^m \bar{\chi}^m(\mathbf{q}) = \sum_{n=1}^d \frac{(2n)!}{2^n n!} \frac{1}{d^n} \left(\frac{W^2 \bar{\gamma}^2}{8} \right)^n. \quad (D.1)$$

The factor $(2n)!/(2^n n!)$ is the number of all possible pairwise contractions in the product of $m = 2n$ “bubbles” $\bar{\chi}$ (odd products do not contribute). The upper bound for the number of contractions, being d , comes from the fact that in d dimensions the sum $\sum_{\mathbf{q}}$ can decompose to maximally d independent summations. The contributions from products of more than $2d$ bubbles $\bar{\chi}$ are inaccessible within the Gaussian convolution rules and were dropped. They are of higher asymptotic orders than the leading one studied here.

The value in question is now the limit $\lim_{d \rightarrow \infty} f_d$. If we express all factorials in equation (D.1) via the Stirling formula we get

$$f_d \sim \sum_{n=1}^d \left(\frac{n}{d} Q \right)^n \quad (D.2)$$

where we introduced a parameter $Q = W^2 \bar{\gamma}^2 / (4e)$ to provide better transparency of subsequent expressions. The application of the Stirling formula causes that the low order terms of the sum f_d are not treated very accurately. Fortunately, they do not play any significant role. The last term of the sum (D.2) reads Q^d which indicates that the

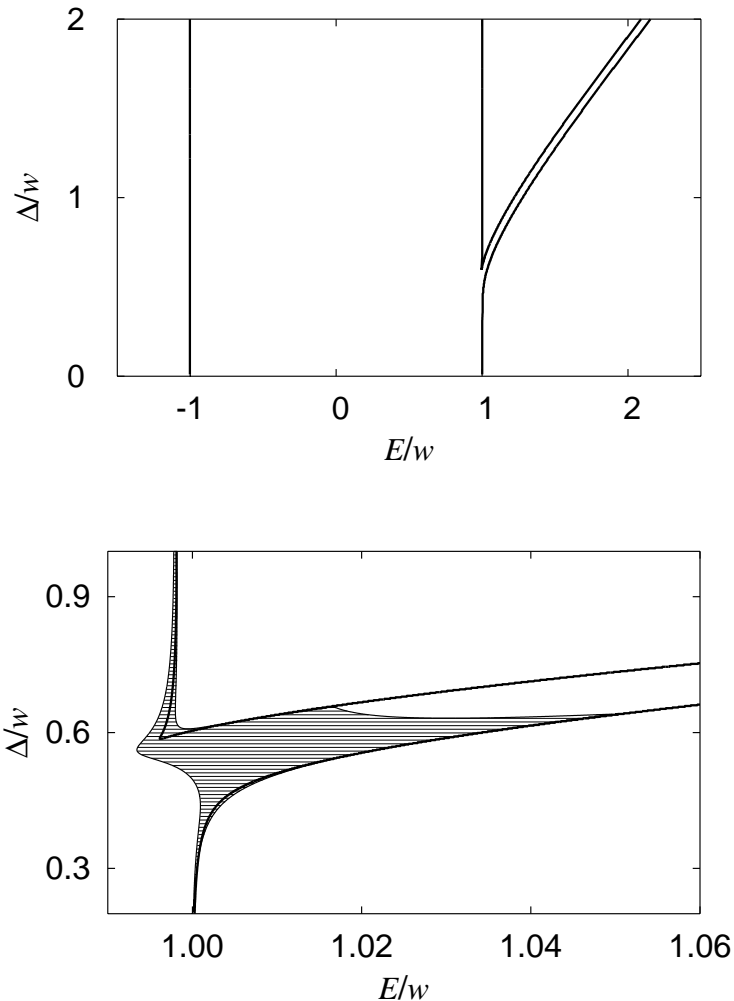


Figure D.1: Band and mobility edges in the energy-disorder plane for a binary alloy with concentration of the minor component $c = 0.001$. Potential difference between distinct atoms is Δ . Lower pane shows a detail of the satellite band with a region of localized states, $\gamma > \gamma_c$, hatched. The extension of the non-diffusive region outside the energy band is an artifact of the approximation and does not imply the presence of any states there.

series $\lim_{d \rightarrow \infty} f_d$ does not converge when $Q \geq 1$, i. e. when $\bar{\gamma} \geq \gamma_c = 2\sqrt{e}/W$. To investigate the opposite case, $Q < 1$, is slightly more involved. We proceed as follows.

The closer the dimensionality d approaches infinity the better is the sum in equation (D.2) approximated by an integral,

$$f_d \sim \sum_{n=1}^d \frac{1}{d} \left(\frac{n}{d} Q\right)^{d \frac{n}{d}} \sim d \int_{1/d}^1 dy e^{yd \ln(yQ)} = f_d^{(1)} + f_d^{(2)}. \quad (\text{D.3})$$

For convenience we split this integral into two parts, $f_d^{(1)}$ and $f_d^{(2)}$, corresponding to integration intervals $(d^{-1}, d^{-1/2})$ and $(d^{-1/2}, 1)$, respectively. At first we analyze the contribution $f_d^{(2)}$. The exponent in the integrand is convex. Therefore, its replacement with a linear function, $\xi(y) = y \ln(Q)$, can only enlarge the result. Performing the remaining integration we arrive at

$$f_d^{(2)} \leq d \int_{d^{-1/2}}^1 dy e^{yd \ln(Q)} = \frac{Q^d - Q^{\sqrt{d}}}{\ln(Q)} \xrightarrow{d \rightarrow \infty} 0. \quad (\text{D.4})$$

The second integral, $f_d^{(1)}$, does not contribute either. To demonstrate this statement

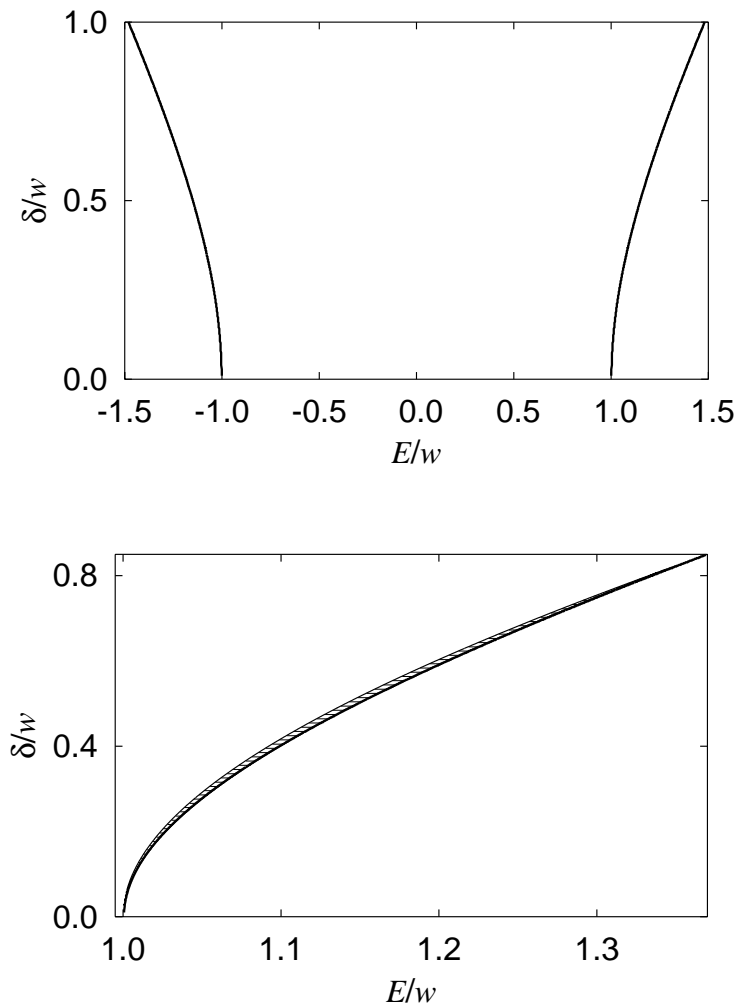


Figure D.2: Band and mobility edges for the so-called box disorder. Lower pane zooms to a narrow area of localized states at the (right) band-edge.

we use convexity again, this time for the integrand as a whole. The estimate utilizing the trapezoidal integration rule is obviously an upper limit for the exact value of the integral $f_d^{(1)}$. As this simple estimate goes to zero in the limit $d \rightarrow \infty$,

$$f_d^{(1)} \leq \frac{1}{2} \left[\frac{Q}{\sqrt{d}} + Q \left(\frac{Q}{\sqrt{d}} \right)^{\sqrt{d}-1} \right] \xrightarrow{d \rightarrow \infty} 0, \quad (\text{D.5})$$

the exact value of the integral $f_d^{(1)}$ goes to zero as well. In this way we come to a conclusion that the sum f_d behaves as

$$\lim_{d \rightarrow \infty} f_d = \begin{cases} 0 & \text{if } Q < 1 \Leftrightarrow \bar{\gamma} < \gamma_c, \\ \infty & \text{if } Q \geq 1 \Leftrightarrow \bar{\gamma} \geq \gamma_c. \end{cases} \quad (\text{D.6})$$

With the aid of this result it is straightforward to write down the solution of the self-consistent equation (5.15b) in infinite spatial dimensions,

$$\bar{\gamma} = \begin{cases} \gamma & \text{if } \gamma < \gamma_c, \\ \text{no (real) solution} & \text{if } \gamma \geq \gamma_c. \end{cases} \quad (\text{D.7})$$

We see that below the critical value γ_c the perturbative analysis of Section 5.1 exactly applies, whereas above this limit a qualitatively different solution emerges that does not allow for diffusion.¹ This means that the coherent-potential approximation *is not* an exact solution of the disordered electron problem on the infinite-dimensional lattice in the whole range of disorder parameters. Of course, we have not demonstrated yet that the critical magnitude γ_c of the vertex γ can be reached in realistic models. Figures D.1 and D.2 show that it can, indeed, although the non-diffusive regions are rather tiny.

The presented numerical calculations were performed with the unperturbed, i. e. without disorder, density of states having the semi-elliptic form

$$g^{(0)}(E) = \frac{2\pi}{w^2} \sqrt{w^2 - E^2} \quad (5.34)$$

with w being the band half-width. Such a density of states is chosen because it allows for analytical expressions for the local element of the one-particle Green function $G(z)$ as well as for the quantity $\langle G^2(z) \rangle$. Although the density of states (5.34) does not correspond to the infinite-dimensional hypercubic lattice we are working with, it has a motivation in high-dimensional considerations as it belongs to an infinite-dimensional Bethe lattice [72]. In the same time, the semi-elliptic density of states provides a reasonable model choice in three dimensions, which we made use of in Section 5.4. Figures D.1 and D.2 are calculated for a binary disorder (1.7) and a box disorder (1.5), respectively. The non-diffusive regions are found in either case.

¹The link between non-existence of real $\bar{\gamma}$ and impossibility of diffusive behavior is established in Sections 5.3 and 5.4.

E

Born approximation in the semi-elliptic band

In Section 5.3 we presented a sample evaluation of the diffusion pole weight A^{-1} as a function of the disorder strength, Figure 5.1. The calculation was performed using the self-consistent Born approximation for one- and two-particle irreducible vertices Σ and \bar{I} . Although there are better approximation schemes available, such as the CPA, the Born values are chosen for considerable simplicity of all relevant formulae. When, additionally, a semi-elliptic form of the unperturbed density of states $g^{(0)}$ is utilized,

$$g^{(0)}(E) = \frac{2\pi}{w^2} \sqrt{w^2 - E^2}, \quad (5.34)$$

we can evaluate the weight A^{-1} analytically. Particularly important is the ability to avoid the numerical evaluation of the derivative $\partial\bar{\lambda}/\partial\omega$ standing in definition (5.26).

The one-particle Green function generating the density of states (5.34) is

$$G^{(0)}(z) = \frac{2}{w^2} \left(z - \sqrt{z^2 - w^2} \right), \quad (E.1)$$

with the aid of which the full averaged Green function G can be written as $G(z) = G^{(0)}(z - \Sigma(z))$. This form with just a simple shift in the energy variable is allowed, since only a single band is taken into consideration. Equation (3.1b) defining the Born selfenergy in the present case reads

$$\Sigma^R(E) = \lambda_B G^{(0)}(E + i0 - \Sigma^R(E)). \quad (E.2)$$

An explicit expression for the retarded selfenergy Σ^R is easily found to be

$$\Sigma^R(E) = \begin{cases} \frac{2\lambda_B}{w^2 + 4\lambda_B} \left(E - i\sqrt{w^2 + 4\lambda_B - E^2} \right) & \text{for } |E| < E_e, \\ \frac{2\lambda_B}{w^2 + 4\lambda_B} \left(E - \frac{E}{|E|} \sqrt{E^2 - w^2 - 4\lambda_B} \right) & \text{for } |E| \geq E_e, \end{cases} \quad (E.3)$$

where we denoted band edges via $\pm E_e$, $E_e = \sqrt{w^2 + 4\lambda_B}$.¹

¹It is appropriate to note that even the CPA provides analytically writable expressions for the selfenergy in the semi-elliptic band (5.34), see e. g. Reference 45 for details. However, these are substantially more involved than the Born solution (E.3). Moreover, it is unnecessary to enter such complications when our goal is to learn just a qualitative behavior of the weight of the diffusion pole A^{-1} .

Further, we turn our attention to two-particle functions evaluated in the vicinity of the band center, $E = 0$, where the real part of the selfenergy vanishes, $\Re\Sigma^R(0) = 0$. More precisely, we choose the two complex energies to be $z_1 = \pm i0$ and $z_2 = \omega \mp i0$. The energy difference ω acts as a small parameter in the following expressions where we keep only terms up to order $O(\omega)$. Such an expansion is sufficient as it is only the derivative $\partial\bar{\lambda}/\partial\omega$ that we want to arrive at in the end, cf. equation (5.26). In order to find the full local two-particle vertex γ_B we start with the product

$$G^A(0)G^R(\omega) = \frac{4}{w^2 + 4\lambda_B} \left[1 + \frac{i}{\sqrt{w^2 + 4\lambda_B}} \omega \right] + o(\omega) \quad (\text{E.4})$$

that we insert into the local Bethe-Salpeter equation analogous to formula (B.8). This procedure yields an expression

$$\gamma_B(\omega) = \frac{\lambda_B(w^2 + 4\lambda_B)}{w^2} \left[1 + \frac{4i\lambda_B}{w^2\sqrt{w^2 + 4\lambda_B}} \omega \right] + o(\omega). \quad (\text{E.5})$$

Besides the vertex γ_B we need to determine the factor W emerging in the Gaussian contractions (5.10). Its evaluation amounts to finding an expression for $\langle G^2(z) \rangle$. In order to access this quantity we first differentiate equation (E.1) with respect to z ,

$$\left\langle [G^{(0)}(z)]^2 \right\rangle = -\frac{\partial G^{(0)}(z)}{\partial z} = -\frac{2}{w^2} \left[1 - \frac{z}{\sqrt{z^2 - w^2}} \right], \quad (\text{E.6})$$

and then perform the energy shift $z \rightarrow z - \Sigma(z)$,

$$\langle G^2(z) \rangle = \left\langle [G^{(0)}(z - \Sigma(z))]^2 \right\rangle. \quad (\text{E.7})$$

The two values of $\langle G^2(z) \rangle$ that constitute the desired factor W , which is defined as

$$W(\omega) = t^2 \left\langle [G^A(0)]^2 \right\rangle \left\langle [G^R(\omega)]^2 \right\rangle, \quad (\text{E.8})$$

consequently read

$$\left\langle [G^A(0)]^2 \right\rangle = -\frac{2}{w^2 + 2\lambda_B}, \quad (\text{E.9a})$$

$$\left\langle [G^R(\omega)]^2 \right\rangle = -\frac{2}{w^2 + 2\lambda_B} \left[1 + \frac{i\sqrt{w^2 + 4\lambda_B}}{w^2 + 2\lambda_B} \omega \right] + o(\omega). \quad (\text{E.9b})$$

Finally we have to establish a relation between the hopping amplitude t and the unperturbed half-bandwidth w . To do so we recall the dispersion relation corresponding to Hamiltonian (5.1). In d spatial dimensions we can immediately conclude that

$$\epsilon(\mathbf{k}) = -\frac{t}{\sqrt{d}} \sum_{\nu=1}^d \cos k_\nu = -t_d \sum_{\nu=1}^d \cos k_\nu \quad \Rightarrow \quad w_d = t_d d = t\sqrt{d}. \quad (\text{E.10})$$

For three-dimensional systems we thus have $t = w/\sqrt{3}$, by virtue of which we come to an expression

$$W(\omega) = \frac{4w^2}{3(w^2 + 2\lambda_B)^2} \left[1 + \frac{i\sqrt{w^2 + 4\lambda_B}}{w^2 + 2\lambda_B} \omega \right] + o(\omega). \quad (\text{E.11})$$

We have collected all the inputs needed for the Landau-like equation (5.35) that determines the two-particle vertices. Further steps towards the weight of the diffusion pole A^{-1} will be indicated only verbally, since the corresponding explicit expressions are rather complicated. Equation (5.35) is cubic in the unknown vertex $\bar{\gamma}$, hence its (three) roots can be written down with the aid of the Cardan's formulae. The physical solution is such that its weak scattering limit matches low orders of the perturbation expansion in powers of the disorder strength. Having selected the correct root we can successively insert the appropriate expression for $\bar{\gamma}$ into formulae (5.19) and (5.26). Doing so we finally achieve the desired analytic expression for the weight A^{-1} .

- [1] N. W. Ashcroft and N. D. Mermin. *Solid state physics* (Holt, Rinehart and Winston, 1976).
- [2] P. W. Anderson. *Absence of diffusion in certain random lattices*. Phys. Rev. **109**, 1492 (1958).
- [3] P. Erdős and R. C. Herndon. *Theories of electrons in one-dimensional disordered systems*. Adv. in Phys. **31**, 65 (1982).
- [4] E. Abrahams, P. W. Anderson, D. C. Licciardello, and T. V. Ramakrishnan. *Scaling theory of localization: Absence of quantum diffusion in two dimensions*. Phys. Rev. Lett. **42**, 673 (1979).
- [5] D. Vollhardt and P. Wölfle. *Self-consistent theory of Anderson localization*. In W. Hanke and Y. V. Kopayev, eds., *Electronic Phase Transitions* (Elsevier Science Publishers B.V., Amsterdam, 1992).
- [6] S. V. Kravchenko, G. V. Kravchenko, J. E. Furneaux, V. M. Pudalov, and M. D'Iorio. *Possible metal-insulator transition at $B = 0$ in two dimensions*. Phys. Rev. B **50**, 8039 (1994).
- [7] A. Prinz, V. M. Pudalov, G. Brunthaler, and G. Bauer. *Metal-insulator transition in Si-MOS structures*. Superlattices and Microstructures **27**, 301 (2000).
- [8] P. W. Anderson, E. Abrahams, and T. V. Ramakrishnan. *Possible explanation of nonlinear conductivity in thin-film metal wires*. Phys. Rev. Lett. **43**, 718 (1979).
- [9] G. J. Dolan and D. D. Osheroff. *Nonmetallic conduction in thin metal films at low temperatures*. Phys. Rev. Lett. **43**, 721 (1979).
- [10] D. J. Bishop, D. C. Tsui, and R. C. Dynes. *Nonmetallic conduction in electron inversion layers at low temperatures*. Phys. Rev. Lett. **44**, 1153 (1980).
- [11] B. L. Altshuler, A. G. Aronov, and P. A. Lee. *Interaction effects in disordered Fermi systems in two dimensions*. Phys. Rev. Lett. **44**, 1288 (1980).
- [12] B. L. Altshuler, D. Khmel'nitzkii, A. I. Larkin, and P. L. Lee. *Magnetoresistance and Hall effect in a disordered two-dimensional electron gas*. Phys. Rev. B **22**, 5142 (1980).

- [13] Y. Kawaguchi and S. Kawaji. *Negative magnetoresistance in silicon (100) MOS inversion layers*. J. Phys. Soc. Japan **48**, 699 (1980).
- [14] G. Bergmann. *Weak localization in thin films: A time-of-flight experiment with conduction electrons*. Phys. Rep. **107**, 1 (1984).
- [15] J. Fröhlich and T. Spencer. *Absence of diffusion in the Anderson tight binding model for large disorder or low energy*. Commun. Math. Phys. **88**, 151 (1983).
- [16] И. М. Лифшиц. С. А. Гредескул. Л. А. Пастур. *Введение в теорию неупорядоченных систем* (Наука, Москва, 1982).
- [17] R. J. Elliott, J. A. Krumhansl, and P. L. Leath. *The theory and properties of randomly disordered crystals and related physical systems*. Rev. Mod. Phys. **46**, 465 (1974).
- [18] P. Dean. *The vibrational properties of disordered systems: Numerical studies*. Rev. Mod. Phys. **44**, 127 (1972).
- [19] R. J. Bell. *The dynamics of disordered lattices*. Rep. Prog. Phys. **35**, 1315 (1972).
- [20] P. Soven. *Coherent-potential model of substitutional disordered alloys*. Phys. Rev. **156**, 809 (1967).
- [21] B. Velický. *Theory of electronic transport in disordered binary alloys: Coherent-potential approximation*. Phys. Rev. **184**, 614 (1969).
- [22] P. A. Lee and T. V. Ramakrishnan. *Disordered electronic systems*. Rev. Mod. Phys. **57**, 287 (1985).
- [23] N. F. Mott. *Metal-insulator transitions* (Taylor & Francis, London, 1974).
- [24] F. J. Wegner. *Electrons in disordered systems. Scaling near the mobility edge*. Z. Phys. B **25**, 327 (1976).
- [25] F. Wegner. *The mobility edge problem: Continuous symmetry and a conjecture*. Z. Phys. B **35**, 207 (1979).
- [26] L. Schäfer and F. Wegner. *Disordered system with n orbitals per site: Lagrange formulation, hyperbolic symmetry, and Goldstone modes*. Z. Phys. B **38**, 113 (1980).
- [27] K. B. Efetov. *Supersymmetry and theory of disordered metals*. Adv. in Phys. **32**, 53 (1983).
- [28] S. Hikami. *Anderson localization in a nonlinear- σ -model representation*. Phys. Rev. B **24**, 2671 (1981).
- [29] W. Bernreuther and F. J. Wegner. *Four-loop-order β function for two-dimensional nonlinear sigma models*. Phys. Rev. Lett. **57**, 1383 (1986).
- [30] B. Kramer and A. MacKinnon. *Localization: theory and experiment*. Rep. Prog. Phys. **56**, 1469 (1993).

-
- [31] K. Slevin and T. Ohtsuki. *Corrections to scaling at the Anderson transition*. Phys. Rev. Lett. **82**, 382 (1999).
- [32] T. F. Rosenbaum, K. Andres, G. A. Thomas, and R. N. Bhatt. *Sharp metal-insulator transition in a random solid*. Phys. Rev. Lett. **45**, 1723 (1980).
- [33] S. Katsumoto, F. Komori, N. Sano, and S. Kobayashi. *Fine tuning of metal-insulator transition in $Al_{0.3}Ga_{0.7}As$ using persistent photoconductivity*. J. Phys. Soc. Japan **56**, 2259 (1987).
- [34] K. M. Itoh, M. Watanabe, Y. Ootuka, E. E. Haller, and T. Ohtsuki. *Complete scaling analysis of the metal-insulator transition in $Ge:Ga$: Effects of doping-compensation and magnetic field*. J. Phys. Soc. Japan **73**, 173 (2004).
- [35] R. Kubo. *Statistical-mechanical theory of irreversible processes I. General theory and simple applications to magnetic and conduction problems*. J. Phys. Soc. Japan **12**, 570 (1957).
- [36] J. Rammer. *Quantum transport theory* (Perseus books, Reading, Massachusetts, 1998).
- [37] G. D. Mahan. *Many-particle physics* (Plenum, New York, 2000).
- [38] R. Kubo, M. Yokota, and S. Nakajima. *Statistical-mechanical theory of irreversible processes II. Response to thermal disturbance*. J. Phys. Soc. Japan **12**, 1203 (1957).
- [39] R. Kubo, M. Toda, and N. Hashitsume. *Statistical Physics II — Nonequilibrium Statistical Mechanics* (Springer-Verlag, Berlin, 1995).
- [40] D. Belitz and T. R. Kirkpatrick. *The Anderson-Mott transition*. Rev. Mod. Phys. **66**, 261 (1994).
- [41] V. Janiš and D. Vollhardt. *Conductivity of disordered electrons: Mean-field approximation containing vertex corrections*. Phys. Rev. B **63**, 125112 (2001).
- [42] D. Vollhardt and P. Wölfle. *Diagrammatic, self-consistent treatment of the Anderson localization problem in $d \leq 2$ dimensions*. Phys. Rev. B **22**, 4666 (1980).
- [43] С. В. Малеев, Б. П. Топерверг. *Поправки к диффузии и проводимости в поле случайно расположенных силовых центров*. ЖЭТФ **69**, 1440 (1975). [S. V. Maleev and B. P. Toperverg, Sov. Phys. JETP **42**, 734 (1975)].
- [44] R. Vlaming and D. Vollhardt. *Controlled mean-field theory for disordered electronic systems: Single-particle properties*. Phys. Rev. B **45**, 4637 (1992).
- [45] B. Velický, S. Kirkpatrick, and H. Ehrenreich. *Single-site approximations in the electronic theory of simple binary alloys*. Phys. Rev. **175**, 747 (1968).
- [46] G. Baym and L. P. Kadanoff. *Conservation laws and correlation functions*. Phys. Rev. **124**, 287 (1961).

- [47] J. Kolorenč, L. Smrčka, and P. Středa. *Inter-layer Hall effect in double quantum wells subject to in-plane magnetic fields*. Phys. Rev. B **66**, 085301 (2002).
- [48] J. S. Langer and T. Neal. *Breakdown of the concentration expansion for the impurity resistivity of metals*. Phys. Rev. Lett. **16**, 984 (1966).
- [49] G. Bergmann. *Physical interpretation of weak localization: A time-of-flight experiment with conduction electrons*. Phys. Rev. B **28**, 2914 (1983).
- [50] А. И. Ларкин. Д. Е. Хмельницкий. *Андерсоновская локализация и аномальное магнетосопротивление при низких температурах*. УФН **136**, 536 (1982). [A. I. Larkin and D. E. Khmel'nitskii, Sov. Phys. Usp. **25**, 185 (1982)].
- [51] D. E. Khmel'nitskii. *Localization and coherent scattering of electrons*. Physica B & C **126**, 235 (1984).
- [52] S. Chakravarty and A. Schmid. *Weak localization: The quasiclassical theory of electrons in a random potential*. Phys. Rep. **140**, 193 (1986).
- [53] D. Vollhardt and P. Wölfle. *Anderson localization in $d \leq 2$ dimensions: A self-consistent diagrammatic theory*. Phys. Rev. Lett. **45**, 842 (1980).
- [54] D. Vollhardt and P. Wölfle. *Scaling equations from a self-consistent theory of Anderson localization*. Phys. Rev. Lett. **48**, 699 (1982).
- [55] K. Ter-Martirosyan. *Equation for vertex part corresponding to fermion-fermion scattering*. Phys. Rev. **111**, 948 (1958).
- [56] R. W. Haymaker and R. Blankenbecler. *Variational principles for crossing-symmetric off-shell equations*. Phys. Rev. **171**, 1581 (1968).
- [57] A. D. Jackson, A. Lande, and R. A. Smith. *Variational and perturbation theories made planar*. Phys. Rep. **86**, 55 (1982).
- [58] N. E. Bickers and S. R. White. *Conserving approximations for strongly fluctuating electron systems. II. Numerical results and parquet extension*. Phys. Rev. B **43**, 8044 (1991).
- [59] V. Janiš. *Parquet approach to nonlocal vertex functions and electrical conductivity of disordered systems*. Phys. Rev. B **64**, 115115 (2001).
- [60] J. Kolorenč and V. Janiš. *Towards mean-field theory of Anderson localization*. In *Proceedings of Weak of Doctoral Students 2003*, pp. 550–555 (Charles University in Prague, Faculty of Mathematics and Physics, 2003).
- [61] R. Brout. *Statistical mechanical theory of ferromagnetism. High density behavior*. Phys. Rev. **118**, 1009 (1960).
- [62] W. Metzner and D. Vollhardt. *Correlated lattice fermions in $d = \infty$ dimensions*. Phys. Rev. Lett. **62**, 324 (1989).

-
- [63] A. Georges, G. Kotliar, W. Krauth, and M. J. Rozenberg. *Dynamical mean-field theory of strongly correlated fermion systems and the limit of infinite dimensions*. Rev. Mod. Phys. **68**, 13 (1996).
- [64] G. Kotliar and D. Vollhardt. *Strongly correlated materials: Insights from dynamical mean-field theory*. Physics Today **57**, 53 (2004).
- [65] V. Janiš. *Asymptotic limit of high spatial dimensions and thermodynamic consistence of mean-field theories*. Phys. Rev. Lett. **83**, 2781 (1999).
- [66] E. Müller-Hartmann. *Analyticity of the coherent potential approximation*. Solid State Commun. **12**, 1269 (1973).
- [67] R. Ramazashvili. *Ward identities for disordered metals and superconductors*. Phys. Rev. B **66**, 220503 (2002).
- [68] В. С. Владимиров. *Уравнения математической физики* (Наука, Москва, 1981).
- [69] V. Janiš, J. Kolorenč, and V. Špička. *Density and current response functions in strongly disordered electron systems: Diffusion, electrical conductivity and Einstein relation*. Eur. Phys. J. B **35**, 77 (2003).
- [70] G. Baym. *Self-consistent approximations in many-body systems*. Phys. Rev. **127**, 1391 (1962).
- [71] E. Müller-Hartmann. *Correlated fermions on a lattice in high dimensions*. Z. Phys. B **74**, 507 (1989).
- [72] E. N. Economou. *Green's Functions in Quantum Physics* (Springer-Verlag, Berlin, 1979).